2011

Calcium Dynamics Of Glial Cells And Genetic Influences On Behavior Of The Nematode Caenorhabditis Elegans

Randy Franklin Stout
University of Alabama at Birmingham

CALCIUM DYNAMICS OF GLIAL CELLS AND GENETIC INFLUENCES ON BEHAVIOR OF THE NEMATODE *CAENORHABDITIS ELEGANS*

by

RANDY FRANKLIN STOUT JR.

VLADIMIR PARPURA, COMMITTEE CHAIR
MICHAEL MILLER
LUCAS POZZO-MILLER
HARALD SONTHEIMER
BRADLEY YODER

A DISSERTATION

Submitted to the graduate faculty of The University of Alabama at Birmingham,
in partial fulfillment of the requirements for the degree of
Doctorate of Philosophy

BIRMINGHAM, ALABAMA

2011

CALCIUM DYNAMICS OF GLIAL CELLS AND GENETIC INFLUENCES ON BEHAVIOR OF THE NEMATODE *CAENORHABDITIS ELEGANS*

RANDY FRANKLIN STOUT JR.

NEUROBIOLOGY

ABSTRACT

A major challenge in neuroscience is understanding how the different neural cell types work together to process information and produce a behavioral output. Glial cells of the human brain have long been thought to act as support for the fundamental cell to cell communication at the core of cognition: neuronal synaptic communication. Research over the past several decades measuring glial activity and experimentally controlling glial cells in rodent model systems has shown that the two macroglia sub-types of glial cells (astrocytes and oligodendrocytes) have active roles in establishment, maintenance, and modulation of synaptic communication in the mammalian brain. Much of this research has utilized cell-type specific promoters to identify and genetically manipulate mammalian glial cells to better understand their role in intercellular communication in the brain. My research is aimed at examining the glia of *C. elegans*: a model organism chosen for a reductionist approach to research on how gene products and gene regulation work in development and function of a simple nervous system. I chose to focus on a subset of glia in this nematode, the sheath glia of the cephalic sensilla, due to cellular characteristics unique to this invertebrate and their morphological similarity to mammalian astrocytes and oligodendrocytes. I hypothesized that as the most evolutionarily ancient proto-astrocytes with some oligodendrocytes characteristics, these glia of *C. elegans* would exhibit a hallmark of mammalian glia: robust calcium dynamics

upon stimulation. To test this hypothesis, I determined experimental applications for the *hlh-17* gene promoter that would avoid confounding effects on behavior and used it to examine cultured *C. elegans* glia for the first time. I then adapted a genetically encoded calcium sensor to show that cultured glial cephalic sheath cells respond to membrane depolarization with increases in cytoplasmic calcium. I show that voltage-gated calcium channels underlie this response, indicating that glia of *C. elegans* have taken on a functional profile less like that known for mature mammalian glial cells but with some remaining commonalities. This establishes *C. elegans* as a model organism that can be used to study glia in a simple nervous system through contrast and comparison with macroglia of mammalian model organisms with similarities possibly representing ancient roles of glia and differences possibly representing roles taken on to meet demands imposed by a more complex nervous system.

Key words: glia, *Caenorhabditis elegans*, model organism, astrocyte, oligodendrocyte

DEDICATION

To Jessica Stout for always being there for me and making my life happy.

ACKNOWLEDGMENTS

I would like to thank my wife Jessica Stout whose support over the past five years has been unwavering. I only hope to be able to be deserving of the amount of faith and kindness she showed toward me during my graduate studies.

I would also like to thank my brother Warren who has been a steadfast friend to me for my entire life.

I thank my parents Randy Sr. and Teresa for their support. I also thank my grandparents Les and Verlee for all their encouragement in biological research.

I would like to particularly thank Vladimir Grubišić for both his friendship and camaraderie in and out of the lab setting.

I thank all of the other lab members whom I've worked with over the years who showed great warmth and friendship: William Lee, Dr. R. Reyes, Dr. D. Rubio, Dr. R. Gomez, Dr. E. Malarkey, Manoj Gottipati, Wendy Hung, Dr. C. Pontrello, Kyle Osborne and Robert Grammer.

I thank the staff and faculty of the UAB Neurobiology Department for welcoming a student transferring from another institution with such generosity and acceptance. I

would also like to than Dr. Anthony Norman of the University of California Riverside for taking a chance on an unconventional graduate student prospect and giving excellent initial guidance.

I thank the members of my initial graduate research committee at the University of California, Riverside: Dr. Doug Altschuler, Dr. Leah Haimo, Dr. Richard Cardullo and of course, Dr. Morris Maduro.

I would like to thank Dr. J. David Sweatt for helping me expand my research interests and for providing such an excellent environment in which to do graduate research. Dr. Morris Maduro and Gina Broitman-Maduro extended a level of effort to assist my development as a researcher, and of acceptance in allowing me to take up space and material in their lab for which I cannot thank them enough. The time that Morris spent teaching me how to perform high-quality research provided an invaluable resource to my graduate work.

I thank my committee members: Dr. Michael Miller, Dr. Lucas Pozzo-Miller, Dr. Harald Sontheimer, and Dr. Bradley Yoder who have all contributed to my research and to whom I look to as an example of success in scientific research.

Lastly, but certainly not least, I want to thank my mentor Dr. Vladimir Parpura who pushed himself to allow me to learn what it takes to be a scientist. I have been a member of many teams, organizations, and work groups but I have never had a leader who showed such strength as to never allow himself to take the easy, compromised path in his role as a teacher and guide. I do not think that I even yet realize all the ways he has been teaching me to do what is necessary to be exceptional in my work, but I hope to use what I have learned so far to the best of my ability.

TABLE OF CONTENTS

Page

LIST OF TABLES

Table *Page*

A LOCOMOTION PHENOTYPE CAUSED BY TRANSGENIC OVER-REPRESENTATION OF A CAENORHABDITIS ELEGANS GLIAL PROMOTER

DISCUSSION

LIST OF FIGURES

Figure *Page*

A LOCOMOTION PHENOTYPE CAUSED BY TRANSGENIC OVER-REPRESENTATION OF A CAENORHABDITIS ELEGANS GLIAL PROMOTER

CALCIUM DYNAMICS IN CULTURED NEMATODE GLIAL CELLS

VOLTAGE-GATED CALCIUM CHANNEL TYPES IN CULTURED C. ELEGANS CEP SHEATH GLIAL CELLS

LIST OF ABBREVIATIONS

ADE	anterior deirid
ATP	adenosine triphosphate
Aldh1L1	10-formyltetrahydrofolate dehydrogenase
bHLH	basic helix-loop-helix
C. elegans	*Caenorhabditis elegans*
i[Ca^{2+}]	intracellular calcium concentration
$[Ca^{2+}]_{cyt}$	cytoplasmic calcium concentration
CEP	cephalic neuron
CEPsh	cephalic sheath
CGC	Caenorhabditis Genetics Center
CACNA1	voltage-dependent calcium channel alpha 1
DA	dopaminergic
DCC	deleted in colorectal cancer
DM1	myotonic dystrophy type 1
DNA	deoxyribonucleic acid
dF/Fo	change in fluorescence over baseline fluorescence
EM	electron microscopy
ER	endoplasmic reticulum
FMR1	fragile x mental retardation 1
FXS	fragile x syndrome

FXTAS	fragile-x associated tremor/ataxia syndrome
GFAP	glial fibrillary acidic protein
GFP	green fluorescent protein
GLAST	glutamate aspartate transporter
GLT1	glutamate transporter one
NemA	nemadipine-A
NG2	neuroglia proteoglycan 2
Olig2	oligodendrocyte transcription factor 2
OPC	oligodendrocyte precursor cell
Pdat-1	promoter for the dopamine transporter gene
PDE	posterior deirid
PDGFRα	platelet-derived growth factor receptor α
Phlh-17	promoter of the *hlh-17* gene

PLP	proteolipid protein
RFP	red fluorescent protein
RNA	ribonucleic acid
S100β	S100 calcium binding protein beta
t-*Pdat-1*	trans-*dat-1* promoter
t-*Phlh-17*	trans-*hlh-17* promoter
t-*Punc-54*	trans-*unc-54* promoter
VCP	ventral coiler phenotype
VGCC	voltage-gated calcium channel

INTRODUCTION

Current challenges in glial research

Neurons and glia are the two neural cell types. The view of what roles glia play in the human nervous system has changed more dramatically than that for neurons over the past thirty years of scientific research. While progress on the range of glial functions in the mammalian brain has been substantial and has greatly improved our understanding of how the brain functions as a whole, many fundamental questions remain. At the root of the process by which the nervous system forms and functions are genes and the regulation of their expression. One approach to understanding how the brain develops and functions is to gain knowledge of which genes are expressed in specific cell types of the brain, study how the protein products of those genes work within the brain, and how the expression of the genes are regulated. This scientific approach in combination with others such as electrophysiology, histology, and pharmacology has revealed that glial cells can be subdivided into three main types (astrocytes, oligodendrocytes/Schwann cells, and microglia) and that each cell type performs many important and specialized roles in the nervous system.

Research on functions of mammalian glia

Known functions that are performed by astrocytes include: i) As a sink to distribute potassium away from areas of high neuronal activity (Orkand et al. 1966; Kuffler 1967; Gardner-Medwin et al. 1981); ii) Metabolic support to neurons with specificity for areas of high neuronal activity (Pellerin and Magistretti 1994; Magistretti and Pellerin 1996; Rouach et al. 2008); iii) Receive and send signals in the form of chemical gliotransmitters [(Kettenmann et al. 1984; Parpura et al. 1994; Patneau et al. 1994; Steinhauser and Gallo 1996; Condorelli et al. 1999) for reviews see (Verkhratsky et al. 2009; Verkhratsky et al. 2011)]; iv) Communication with other astrocytes through gap junctions [(Brightman and Reese 1969; Gutnick et al. 1981; Yamamoto et al. 1990b; Yamamoto et al. 1990a) and reviewed in (Scemes et al. 2009)]; v) Control blood flow in the brain by signaling to the microvasculature as reviewed in (Gordon et al. 2009); and vi) Exhibit robust changes in $[Ca^{2+}]_{cyt}$ and inter-cellular calcium waves (Cornell-Bell et al. 1990).

Oligodendrocytes have been shown to perform a different but somewhat overlapping set of functions as those of astrocytes: i) Insulate axons to improve action potential conductance speed (Bunge et al. 1962); ii) Sense neuronal activity and respond with morphology changes that control the characteristics of action potentials (Patneau et al. 1994; Yamazaki and Kato 2007; Fields 2008).

While more glial functions are likely to be uncovered in the future, the impact of the roles listed above on nervous system function is not well understood. Major questions remain, including the obvious and hotly debated question of whether glial calcium dynamics regulate the activity of glia and neurons in development, learning, and

cognition [(Cornell-Bell et al. 1990) see and (Agulhon et al. 2008) for a review]. At present, there is intense debate over whether calcium dependent vesicular release of gliotransmitters and trophic factors have profound effects on synapse function (Santello and Volterra 2009), sleep (Halassa et al. 2009), long term potentiation and memory (Mothet et al. 2000; Mothet et al. 2005; Henneberger et al. 2010; Fossat et al. 2011), breathing (Gourine et al. 2010), and synaptic development and neuronal survival, or if glial calcium signaling has almost no effect on neuronal function [(Fiacco et al. 2007; Petravicz et al. 2008) and see (Kirchhoff 2010) for a commentary on the debate]. Much research is presently being directed at using genetic tools to measure and affect cellular activity specifically in the macro glia of rodent model organisms (Casper et al. 2007; Petravicz et al. 2008; Ortinski et al. 2010; Shigetomi et al. 2010; Figueiredo et al. 2011).

Uses of genetic tools in vertebrate glial research

A combination of approaches using all of the most effective and advanced tools that are available would be the rational approach to answering the questions about glial cell function; I focus on reductionist and genetic based tools here. Glial cell type specific promoters are essential to most studies that use mammalian model organisms. They are used as markers for specific glial cell types. These promoters drive the expression of genes encoding proteins that are found exclusively in glia, or at least exclusively glial cells within specific brain regions or developmental stages. The promoters for the genes encoding the GFAP, S100β, GLT1, GLAST, and Aldh1L1 proteins have been used to mark astrocytes (Brenner et al. 1994; Lehre et al. 1995; Vives et al. 2003; Regan et al. 2007; de Vivo et al. 2010; Yang et al. 2011). Promoters for myelin basic protein, and PLP

have been used to express transgenic reporter proteins in oligodendrocytes (Chen et al. 1998; Chen et al. 1999; Yoshida and Macklin 2005; Fitzner et al. 2006; Dhaunchak and Nave 2007). Promoters for genes encoding Olig2, NG2, PDGFRα have been used to express reporters in immature glia to determine cell type fates of glial progenitors. The use of these promoters highlights the fact that glia have a different pattern of gene regulation than neurons; these differences establish and maintain the differences in proteins and cellular contents between neurons and glia and result in the different forms and functions of these cells.

Research using C. elegans

The use of *C. elegans* as a model system was devised by Sydney Brenner in the early 1970's to allow for a reductionist research approach to understand how genes specify and maintain the nervous system and behavioral output. Sydney Brenner's 1974 publication describing his criteria for choosing this nematode and initial work on genetic influences on behavior was generally directed at identifying and mapping mutations that influence neuron development or function (Brenner 1974). This choice of model organism combined with genetic analysis has proven extremely successful. Numerous genes and gene regulatory systems have been identified in *C. elegans* based studies that have gone on to be recognized as critical components in the mammalian nervous system e.g. unc-13 (Munc13), unc-18 (Munc18), unc-40 (deleted in colorectal cancer, DCC), unc-5 (netrin receptor UNC5), and RNA interference (Brenner 1974; Hedgecock et al. 1990; Kolodziej 1997; Fire et al. 1998). My aim was to extend the use of *C. elegans* as a model organism to the study of glia.

The glia of C. elegans

Fifty-six cells were called "glia-like support cells" when the first electron microscopic analyses of the *C. elegans* nervous system were published. These fifty-six cells were called glia based on their clear association with the nervous system and lack of the pre-synaptic structure that the neurons of the worm were shown to possess (Ward et al. 1975; White et al. 1976; White et al. 1986; Hall and Russell 1991). Like nearly all other cells, *C. elegans* glia contain membrane compartments that traffic from the ER and sometimes fuse with the plasma membrane, but do not have areas where synaptic vesicles are concentrated together for release onto neurons within the nerve ring, which is considered the central nervous system are of the worm (Ward et al. 1975). Six cells of mesoderm origin (the GLR cells) were later removed from the list of worm glial cells by some researchers upon the completion of the *C. elegans* developmental cell fate map, further studies of the morphology of the nervous system, and when as more was learned about their gene expression profile (Sulston and Horvitz 1977; White et al. 1986; Krause et al. 1994). From this point forward when discussing *C. elegans* glia, I will be referring to the fifty ectodermal derived non-neuronal cells of the worm's nervous system. A zinc finger transcription factor (lin-26) was found to prevent non-neuronal fated cells, including the glia, from adopting a neuron-like morphology and gene expression profile (Labouesse et al. 1994; Labouesse et al. 1996; Chanal and Labouesse 1997). The glia of *C. elegans* are associated through proximity and developmental interaction with the sensory neurons. They form membrane tubes that surround single, or bundles of sensory neurons near the ciliated ends of dendritic extensions emanating from the neuronal cell

bodies near the nerve ring and extending to the anterior tip of the worm body (about 300 μm). This elongated ring-like structure caused them to be named sheath and socket cells, with each sheath cell having a corresponding socket cell. Since each normal adult hermaphrodite *C. elegans* has the same 959 cells in the same locations within the worm body, each cell was given a name. In general glia were named after the neurons that they encircle at the sensory tips at the anterior end of the worm. The ciliated sensory tip extends just beyond the anterior limit of the ring formed by the socket cell, with the sheath cells forming a second ring around the dendritic extension of the neurons and apposing the ring of the socket cell. Following the thin membrane extensions of all three cells toward the posterior direction, the cell bodies of the socket cells appear first then the sheath glia and neuron cell bodies are found where they reside near/in the nerve ring. The early EM studies on the nervous system showed that one subset of four glial sheath cells possessed morphological characteristic that are very different from neurons or other worm glia. These cells, named the cephalic sensilla sheath cells (CEPsh), extend thin sheet-like membrane extensions between and around the nerve ring and the ventral axon bundle which is roughly equivalent to the mammalian spinal cord. The four CEPsh cells were given individual names based on their location: CEPsh-ventral left, CEPshVL; CEPsh-ventral right, CEPshVR; CEPsh-dorsal left, CEPshDL; and CEPsh-dorsal right, CEPshDR. The dorsal and ventral CEPsh cell pairs have slightly different shapes in that the nuclei of the ventral cells are situated slightly (~20 μm) toward the posterior end of the worm and their membrane sheet extensions are elongated. The gene expression and developmental specification differs between the dorsal and ventral cells, also, as discussed below (Wadsworth et al. 1996; Yoshimura et al. 2008). The CEPsh cells also

send membrane processes into the nerve ring where they generally terminate at the same synaptic connections in each individual worm. Because I set out to use *C. elegans* to study the glial roles in nervous system function I chose to focus on the CEPsh cells because based on morphology, they could perform similar functions as those of astrocytes and/or oligodendrocytes. When I began my research on the CEPsh cells nothing was known about their function outside of what could be inferred based on studies on other sheath cells showing that glial genes are necessary for the development of the neuron and glial structures at the sensory process endings and that they may have a role in development (Wadsworth et al. 1996). While the functions of the CEPsh cells were unknown some information existed on their gene expression.

CEPsh glial cell gene expression

Outside of the basic housekeeping, structural, and metabolic genes expressed in most cell types, the CEPsh cells were found to express some specialized genes, a selection of which are discussed below. The expression of these genes in the CEPsh cells was identified through the use of gene knockout, immunohistochemistry, and promoter-reporter transgenic studies. The gene expression profile that has been uncovered for the CEPsh cells supports the glial cell type designation and makes them likely to be important for studies on glial function. As discussed above, all glia and along with other non-neuronal cells of ectodermal origin express the zinc-finger domain transcription factor LIN-26 (Labouesse et al. 1994; Labouesse et al. 1996; Chanal and Labouesse 1997). The ventral pair of CEPsh cells were found to express the netrin homolog UNC-6 in embryonic development through the use of transgenic expression of epitope tagged

UNC-6 under its own promoter (Wadsworth et al. 1996). Unc-6 in general, plays an important role in axon guidance in both mammals and *C. elegans.* Unc-6 expression in the ventral CEPsh cells was later shown to have a role in synapse development or axon guidance since UNC-6 transgenic rescue-expression is required in these glia specifically for the formation of a synapse important for control of locomotion (Colon-Ramos et al. 2007). Four gap junction protein coding genes are expressed in the CEPsh cells (four innexins: inx-3, 5, 11, and 13) (Altun et al. 2009). The discovery that the basic helix-loop-helix (bHLH) domain protein HLH-17 is expressed in the CEPsh cells and that its promoter, *Phlh-17,* drives fluorescent reporter proteins at high levels exclusively in the four CEPsh cells from the embryo through adulthood greatly facilitated research on these cells (McMiller and Johnson 2005). The *hlh-17* gene encodes a protein most closely related to the bHLH domain transcription factor Olig2 wich is involved with glial development (McMiller and Johnson 2005; Yoshimura et al. 2008). As shown by Yoshimura et. al. in 2008, the regulation of *hlh-17* expression is controlled by genes whose mammalian homologues control the expression of Olig2 and are important for glial development and glial direction of neuronal development (Lu et al. 2002; Muller et al. 2003; Cai et al. 2007; Yoshimura et al. 2008).

Transgenes carrying the *Phlh-17* are used extensively in the research presented in this dissertation and have previously been used by other researchers to mark the CEPsh cells in studies on the function of *unc-6*. It was also recently used to mark CEPsh glia for a microarray based study aimed at profiling the genes expressed in CEPsh cells along with other cell types marked by other promoters (Spencer et al. 2011). This study identified a large number of genes whose transcripts are specifically over-represented in

the CEPsh cells. I will discuss some of the identified genes below, although more information about the functions of the CEPsh cells will allow this information to be put into better context.

Since cell type specific promoters have proven very useful in mammalian model systems, I began using the *Phlh-17* to express red fluorescent protein markers in the CEPsh cells but discovered a behavior phenotype in some of the transgenic lines. To be able to use this promoter as a tool to study the CEPsh glia I performed experiments to characterize this phenotype and to understand how it affects behavior of the intact worm (Stout and Parpura, submitted 2011). Having determined the proper experimental uses for the *Phlh-17*, I went on to develop and test a transgenic worm strain that would allow me to study characteristics of calcium changes in the CEPsh cells.

A transgenic worm line for studying glial calcium fluctuations

The robust calcium fluctuations and intracellular waves of calcium elevation in cultured astrocytes was one of the first ways glia of mammals were recognized as having roles outside of mechanical support in the brain (Cornell-Bell et al. 1990). Based on our findings on the *Phlh-17* and practical considerations of the worm and the CEPsh cells (the pressurized cuticle and thin web-like structure of the glia make intact recording of electrical events infeasible with current techniques), we sought to develop a way to measure change in calcium levels in cultured *C. elegans* glia. An embryonic primary mixed-type cell culture system was developed and described by Christensen and colleagues in 2001(Christensen and Strange 2001; Christensen et al. 2002). They found that with correct conditions, dissociated embryonic cells could grow *in vitro*. Cell type

specific promoters were used to mark neurons in this mixed cell culture and subsequent analysis showed that cultured neurons specifically express many of the genes that the same neuron subtype would express in mature neurons of the intact worm (Christensen and Strange 2001; Bianchi and Driscoll 2006). This finding was replicated for the dopaminergic neurons (8 cells in hermaphrodite worms; 2 ADE, 2 PDE and 4 CEP neurons) when they were marked in culture using the promoter for the *dat-1* gene (*Pdat-1*) (Carvelli et al. 2004).When planning ways to monitor CEPsh cell calcium in culture, I chose the newly developed green-fluorescent genetically encoded calcium indicator GCaMP2.0 for its simplicity of use and because it had the highest baseline brightness and best dynamic range of available single fluorophore genetically encoded calcium indicators at that time (Tallini et al. 2006). GCaMP2.0 has been expressed in C. elegans neurons and muscle using cell type specific promoters see [(Kerr 2006; Tian et al. 2009) for a reviews]. The second section of this dissertation discusses the basic characteristics of the changes in $[Ca2+]_{cyt}$ that we found using the transgenic line and culture system that I developed (Stout and Parpura 2011b). Having established a system to detect changes in calcium levels of cultured glia, the next step toward the overall goal of a comparison between the functions of genes in mammalian and *C. elegans* glia was to test which, if any, stimuli that trigger calcium fluctuations in mammalian glia also affect cultured CEPsh cell calcium levels.

Voltage-gated calcium channels in the mammalian nervous system

Membrane depolarization is the mechanism that operates voltage-gated calcium channels at the presynaptic terminal during vesicular release and is important in backward propagation of signals in dendrites of neurons [see review and citations within

(Catterall 2011)]. Voltage- gated calcium channels are also important for all types of muscle contraction (Reuter 1976; Curtis and Catterall 1984). The expression and function of these channels in glia is less well known although they are more prominent in immature or undifferentiated glia such as oligodendrocytes precursor cells (OPCs) and astrocytes that have been passaged multiple times in culture (Yaguchi and Nishizaki 2010).This does not mean that VGCCs are not important for glial cell development and function. The development of OPCs into oligodendrocytes with formation of extensions of myelinating membrane processes and expression of myelin basic protein (MBP) are regulated by VGCCs (Yoo et al. 1999; Fulton et al. 2010). Exactly how this occurs in immature glia is not fully known at the time of writing but is thought to be accomplished though calcium signaling by second messengers in localized areas of the OPCs and through changes in gene expression (Gomez-Ospina et al. 2006; Fulton et al. 2010).

Before discussion of how VGCCs operate and how they could bring about the changes in immature glial cells discussed above, some background on what is known about these channels is warranted. The core of the channel consists of a single protein made up of a six transmembrane domain protein called the α_1 subunit, for a review see (Catterall 2011) and cited references. The α_1 subunit determines the VGCC channel type based on its influence on voltage gating properties. In mammals the high and low voltage activated channels form two general groups that are subdivided based on the channel open time and pharmacology. The types of VGCCs found in mammals include the low (less depolarized) voltage activated channels designated T-type channels due to the transient nature of the channel open time (Nowycky et al. 1985). The high (more depolarization- requiring) voltage activated L-type channels are blocked by nifedipine.

The N-type channels also require more membrane depolarization to open but are not blocked by nifedipine (Nowycky et al. 1985). Other high voltage activated channels include P/ Q, and R-types which have different brain region and intracellular localizations (Llinas and Yarom 1981; Tsien et al. 1988; Llinas et al. 1989; Mintz et al. 1992; Randall and Tsien 1995).

Accessory subunits are also part of VGCCs but their properties are not as well understood as those of the α_1 subunit. The $\alpha_2\delta$ subunits are translated as a single protein but separated into two peptides and then re-linked by a disulfide bond (Takahashi et al. 1987; Jay et al. 1991). The $\alpha_2\delta$ subunit modulates voltage gating, current flux, and trafficking of the α_1 subunit .The β subunit modifies trafficking and gating of the α_1 subunit. The γ subunit also associates with the channel and some isoforms such as stargazing regulate co-localization of the VGCCs with ionotropic glutamate receptors (Chen et al. 2000). Many questions about how the expression and trafficking of these channels is regulated in neurons and glia are left to be answered and *C. elegans* has already served as a model organism to study them in neurons (Saheki and Bargmann 2009).

Voltage-gated calcium channels of C. elegans

Examination of the sequenced genome of *C. elegans* shows only three genes with clear α_1 subunit homology (Bargmann 1998). Sequence comparisons, expression in *Xenopus* oocytes, and studies with genetically encoded calcium sensors in neurons and electrophysiological measurements in *C. elegans* muscle have demonstrated that EGL-19,

CCA-1, and UNC-2 correspond to L-type, T-type, and N,P/Q,R-type, respectively (Jeziorski et al. 2000). Using knockout, loss of function and gain of function alleles for the α_1 subunit encoding genes of the worm, the effects due to loss of one or multiple channels were determined for *C. elegans* body wall and pharynx muscle cells in a series of studies (Shtonda and Avery 2005; Steger et al. 2005; Liu et al. 2011). Neurons were also shown to express all three channel types to different degrees according to neuron subtype (Nickell et al. 2002; Frokjaer-Jensen et al. 2006; Bauer Huang et al. 2007). In general the three types of channels were found to have properties that mirrored those of other species. Loss of *unc-2* was shown to have either positive or negative effects on calcium flux through the L-type channel depending on the cell type (muscle or neuron). Because individual cells and there connections are known for most neurons of the worm, cell type specific promoters can be used to examine the effects of VGCC encoding gene mutations at the level of single neuron axons. Studies exploring the functions of VGCC accessory subunits in *C. elegans* sensory neurons have provided information that aided the interpretation of my own results. The $\alpha_2\delta$ encoding gene *unc-36* seems to be shared in a stoichiometric manner between two α_1 subunit proteins in a pair of sensory neurons (Bauer Huang et al. 2007). In a subsequent study of the functions of UNC-36, roles in trafficking of VGCC channels from the ER to the presynaptic terminal were found through analysis of mutant lines and GFP reporter fusion transgenic lines (Saheki and Bargmann 2009). Using the transgenic line I constructed in conjunction with the parameters I had defined, I first studied the effect of depolarizing the cultured CEPsh cells. The third CHAPTER of this dissertation describes tests and their results showing that cultured glia have multiple VGCCs types that are responsive to membrane voltage.

Other invertebrate model organisms

Establishment of *C. elegans* as a new model organism for the study of glial cells is needed because the aspects of this worm's biology create new or more direct ways to monitor and affect glial functions than can be accomplished in rodent model systems. However, there are other genetically tractable model organisms that need to be considered, namely *Drosophila melanogaster*. Based on morphology and cell location within the nervous system, the glia of the fruit fly seem to have characteristics that represent a kind of intermediate between the currently known characteristics of *C. elegans* and mammalian glia (Freeman and Doherty 2006). The total number of glia has expanded greatly compared to the worm in both the peripheral/sensory and central portions of the fly nervous system. The relationship between glia of different model organisms will be considered in more detail in the DISCUSSION section of this dissertation. The glia of C. elegans are more optically accessible for experiments with genetically encoded indicators but the pressurized cuticle represents a major obstacle to the use of indicator dyes and electrophysiological experiments. The small size of *C. elegans* neurons and glia (ranging from ~5-20 μm for the main cell body) can pose a problem but the limited number of components and determined cell and neural connectivity pattern allow for a combination of genetic and synapse specific analysis not possible in any other widely used model organism.

General scientific aims

The overarching aim of the research described in this dissertation is to answer the question of how the model organism *C. elegans* can be modified and manipulated to study glial cells. I used modified genetic sequences and produced transgenic lines to mark the CEPsh glia and study how they interact with specific subsets of neurons in intact worms and then continued on to study these glia *in vitro* to answer questions about their morphology and calcium handling in isolation form direct neuronal contact. This work produced information about what aspects of *C. elegans* were influenced by neurons and other cell types. While working with these genetic tools to study CEPsh glia I identified a behavioral change due to use of genetic elements associated with these glia. I performed experiments to answer the question of what the mechanistic basis of this phenotype is and then established the parameters of the behavioral phenotype to guide future experimental design for glial research using genetic tools in *C. elegans.* Having established genetic tools and procedures for *C. elegans* glial research, I began testing the hypothesis that the glia of *C. elegans* would respond to stimuli that might be present in the intact nervous system of the worm. Mammalian glia respond to various extracellular stimuli with increases in intracellular calcium. I hypothesized that the CEPsh glia would respond to experimentally increased external potassium concentration and the resulting depolarization of the cell membrane with changes in intracellular calcium levels that are mediated by one or more ion channels. I present the details of the testing, results, and suggest conclusion that may be drawn from this research throughout the rest of this manuscript.

A *CAENORHABDITIS ELEGANS* LOCOMOTION PHENOTYPE DUE TO TRANSGENIC OVER-REPRESENTATION OF THE GLIAL PROMOTER *HLH-17*

RANDY F STOUT JR., VLADIMIR PARPURA

Submitted to *PNAS,*

Format adapted for dissertation

CHAPTER 1

A *CAENORHABDITIS ELEGANS* LOCOMOTION PHENOTYPE DUE TO TRANSGENIC OVER-REPRESENTATION OF THE GLIAL PROMOTER *HLH-17*

Abstract

Cell type specific promoters are widely used in research to drive expression of various transgenes; little attention has been given to the effects that the trans-promoter itself could have on the phenotypes. We present evidence that a variably penetrant locomotion phenotype in transgenic *C. elegans* is caused by repeats of the glial trans-*hlh-17* promoter, but not by the transgene expression driven by the promoter. This finding is not only essential for research using this promoter in *C. elegans*, but will also be important for any transgenic cell type/animal. Furthermore, we suggest some implications for human disease research.

Introduction

Phenotypic effects of transgenes driving expression of various fluorescent reporters are common and have been attributed to over expression of a foreign protein within cells, the site of transgene integration, or transfection vector (Palmiter and Brinster 1986; Muruve et al. 1999; Sekar et al. 2007). However, possible effects of the trans-promoter have received little attention in spite of some indications that it may affect cellular processes, e.g., causing reactive astrocytosis (Ortinski et al. 2010). Several methods have been used to introduce transgenes into the popular model organism *C. elegans* to produce lines carrying heritable transgene arrays. The most widely used method involves injecting plasmid DNA directly into the gonad syncytium of adult worms (Mello et al. 1991; Mello and Fire 1995). This procedure produces an array of 300-500 repeats of the injected DNA construct with substantial rearrangements of the plasmid sequence. These complex repetitive sequences are transmitted, as extrachromosomal arrays, to offspring with little change between generations and between individuals within the same transgenic line, but with mosaicism across cells within worms and variable transmission to progeny. To avoid mosaicism, arrays can be integrated semi-randomly into the endogenous genomic DNA through several methods, including gamma irradiation. Once integrated, transgenic arrays are generally transmitted in a similar way as endogenous genes (Mello et al. 1991).

Highly repetitive transgene sequences in extrachromosomal or integrated form are epigenetically marked and localized to the periphery of the nucleus but not completely silenced (Towbin et al. 2011). Although cellular responses to foreign repetitive elements

are not well understood, transgenic arrays, containing cell specific promoters, are in widespread use as research tools.

The *hlh-17* promoter (*Phlh-17)* has been used as a marker for the cephalic sensilla sheath (CEPsh) glial cells (McMiller and Johnson 2005; Colon-Ramos et al. 2007; Yoshimura et al. 2008; Grove et al. 2009; Stout and Parpura 2011a). It drives strong expression of fluorescent reporter proteins in the four CEPsh glial cells in the head region of *C. elegans* from the embryo to the adult stage, and in some transgenic strains, weak transient expression in other cells (McMiller and Johnson 2005; Yoshimura et al. 2008). We initially identified a variably penetrant, but stereotypic abnormal behavioral phenotype in some worm lines carrying various transgenic constructs consisting of the trans-*Phlh-17* (t-*Phlh-17*) driving glial cell specific expression of a fluorescent protein. We identified overrepresentation of t-*Phlh-17*, but not of the downstream expression of a transgene, as the underlying cause of the locomotion behavior, which manifests as ventral coiler phenotype (VCP) during backwards movement. We describe tests and establish parameters that could be used in future studies to quantify and compare the proportion and severity of the VCP in order to assess whether this phenomenon would be compatible with each particular application in which transgenic *C. elegans* would be used.

Furthermore, additional information on the function of the t-*Phlh-17* as a transgenic tool should be informative in studies on *C. elegans* glial cells, since it has been a popular method to mark the CEPsh cells and could be used to alter their activity in future studies as has been done numerous times with the neurons through tissue specific promoter(s) in combination with the "genetic tool-box" available for the worm (Bacaj and Shaham 2007; Chelur and Chalfie 2007; Guo et al. 2009; Stirman et al. 2010). The

findings we present here could, therefore, be used to establish controls/guidelines when studying roles that CEPsh glial cells have in nervous system function and the behavior of *C. elegans*.

Table 1

Description of utilized C. elegans strains

Strain	Plasmid(s)	Integrated	Genotype	VCP
N2	none	NA	non-transgenic Bristol N2	N
VPR839	pRSG + pDP#MM016B	Y	N2, *irIs67[Phlh-17::GFP + unc-119(+)]*	N
VPR128	pRSXP2	Y	N2, *vprIs128 [Phlh-17::DsRedExpress2]*	Y
VPR127	pRSG	Y	N2, *vprIs127 [Phlh-17::GFP]*	Y
VPR156	pRSR2	Y	N2, *vprIs156 [Phlh-17::monomericDsRed]*	Y
VPR157	pRSG	Y	N2, *vprIs157 [Phlh-17::GFP array]*	Y
VPR121	pRSDAR	Y	N2*, vprIs121 [Pdat-1::monomericDsRed]*	N
VPR133	pRSHDA2	N	N2, *vprEx133 [Phlh-17‖Pdat-1::DsRedExpress2]*	Y
VPR160	pRSV2 + pU54mCh	N	N2, *vprEx160 [Phlh-17::none + Punc-54::mCherry]*	Y
VPR163	pU54mCh	N	N2, *vprEx163 [Punc-54::mCherry]*	N

Note: Plasmid description is available in Supplemental Materials and Methods. VCP, ventral coiler phenotype.

Results and Discussion

We identified abnormal locomotion in the form of the ventral coiler phenotype (VCP) when worms of two transgenic *C. elegans* lines, both carrying the genome integrated arrays, one *vprIs128* (*Phlh-17::DsRedExpress2*) and the other v*prIs156* (*Phlh-17::monomericDsRed*), and thus expressing the red fluorescent proteins (DsRedExpress2 or monomericDsRed, respectively) in CEPsh glial cells, undergo backward movement (see Table 1 and Supplement for descriptions of plasmids and strains). This behavior can occur spontaneously (Fig. 1A) or in response to mechanical stimulation to the anterior of the worm (Fig. 1 B; also see Supplemental movies 1 and 2). We quantified the proportion of times (out of 6 trials) that individual worms exhibited the VCP. VPR128 and VPR156 worms failed to crawl backwards with an average VCP proportion of 0.67$\pm$0.06 and 0.78$\pm$0.05, respectively. This was significantly higher than the proportion in N2 (Bristol strain) control worms (average VCP proportion= 0.00 $\pm$0.03) which displayed normal backward crawling (Fig.1 B). However, we did not observe the VCP in the VPR839 line which carries a transgenic construct containing the t-*Phlh-17* driving the expression of green fluorescence protein (GFP) (Fig.1 B).

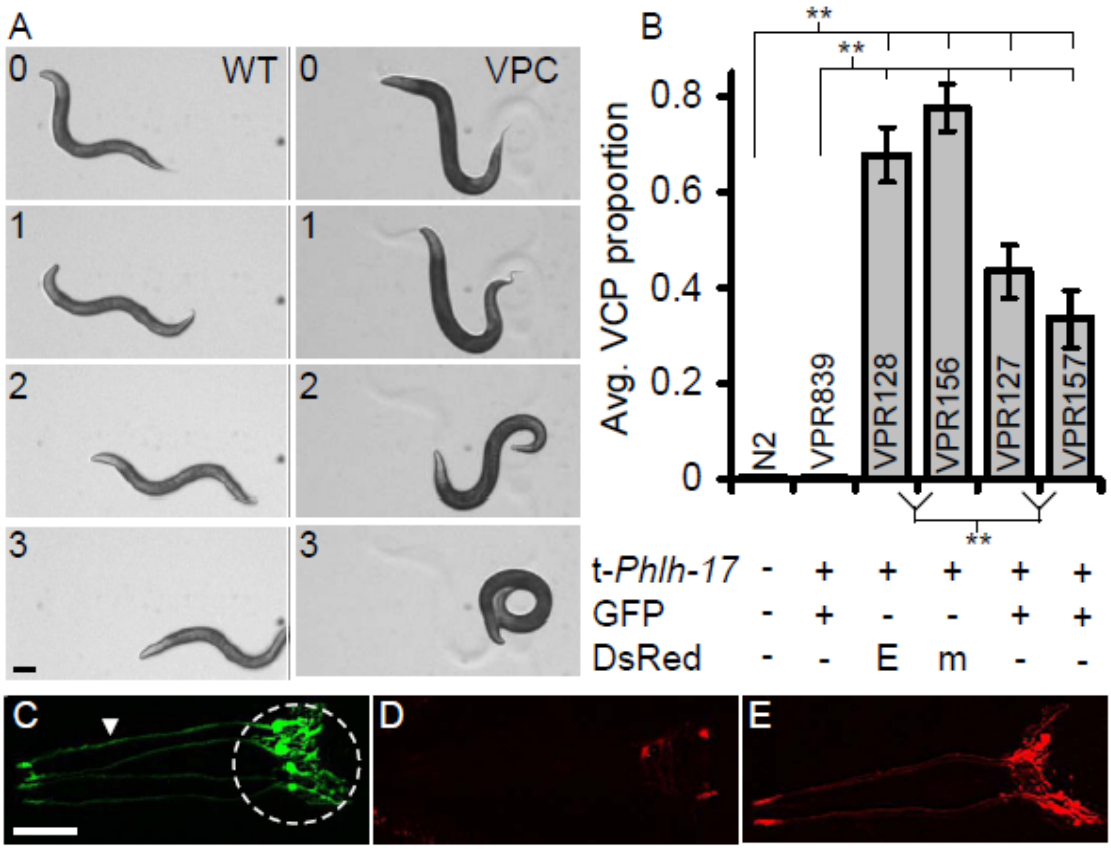

Figure 1. *A subset of lines carrying transgenic array containing the trans-hlh-17 promoter (t-Phlh-17) to drive expression of fluorescent proteins in the CEPsh cells display a ventral coiler phenotype (VCP) during backward movement.*

(A) Image series depicting normal spontaneous reverse movement (WT, left column) and spontaneous VCP in line VPR156 (VCP, right column). Worms shown crawling with right lateral side of the body on the agar surface. Numbers indicate time in seconds; scale bar= 100 µm. (B) Proportion of trials in which the touch-induced VCP was displayed by N2 (non-transgenic, Bristol strain) and t-*Phlh-17* transgenic (VPR839, VPR128, VPR156, VPR127, and VPR157) strains. The matrix below the graph indicates the composition of transgenes in each line (E, DsRedExpress2; m, monomericDsRed). Bars represent means ± sem; n=53 for all groups; ** indicates a significant difference at $p<0.01$, Kruskal-

Wallis one-way ANOVA (KWA) followed by Newman-Keuls multiple comparisons test (MCT). C-E) Transgenic worm lines expressing fluorescent proteins in the CEPsh glial cells driven by the t-*Phlh-17*. Confocal images show anterior, head, portion of worms. (C) VPR839 shows diffuse cytosolic GFP expression. Dashed circle indicates the CEPsh glial cell bodies and membrane extensions. The arrowhead indicates the thin processes emanating to the anterior sensory structures. (D) VPR128 shows clumped DsRed Express2 expression in cell bodies, (E) VPR156 shows diffuse monomericDsRed expression in bodies and processes of CEPsh glial cells. Scale bar= 20 μm.

Next we examined VPR839, VPR128 and VPR156 worms under fluorescence microscopy (Fig. 1 C-E, respectively). The t-*Phlh-17* in VPR839 worms drives expression of GFP in the four CEPsh glial cells within their bodies, membrane extensions engulfing the nerve ring, and also in a long anterior process possessed by each cell that closely interacts with the dendritic extension of a nearby CEP neuron (Fig. 1 C), as previously reported (McMiller and Johnson 2005; Yoshimura et al. 2008). The t-*Phlh-17* promoter in the VPR128 worms drives expression of DsRedExpress2 in the four CEPsh glial cells but with severe clumping of this reporter within sheet like extensions of CEPsh glial cells (Fig.1 D). VPR156 strain in which t-*Phlh-17* drives the expression of monomericDsRed showed essentially no clumping (Fig. 1 E). These findings implicated that the VCP is not dependent on protein clumping. However, since the gene encoding DsRed is very different in sequence from that of GFP, the data available from these lines might be taken as an indication that the VCP could be reporter protein specific.

Besides VPR839, we examined the two additional lines, VPR127 and VPR157, carrying integrated copies of the t-*Phlh-17::GFP* array in order to address this issue. These two lines showed essentially no protein clumping (Supplemental Fig. 1 A, B), while exhibiting the VCP with proportions that were significantly higher than those observed in N2 and VPR389 worms, albeit smaller than those of DsRed variant-expressing worms (Fig. 1B). The latter fact should not distract from the major finding: the presence of the VCP in worms expressing GFP and DsRed variants. In further support of this notion that the VCP is not fluorescent reporter protein specific, when we tested worm lines in which the t-*Phlh-17* drives the expression of GFP (Grove et al. 2009), mCherry (Colon-Ramos et al. 2007; Stout and Parpura 2011a) and/or GCaMP2.0 (Stout and Parpura 2011a), we found them displaying the VCP at various proportions (Supplemental Fig. 3). Furthermore, the variability in the VCP proportion recorded from different genome integrations of the same transgenic *Phlh-17::GFP* array points to level of protein expression and/or copy number of the t-*Phlh-17* itself as a possible cause for the VCP.

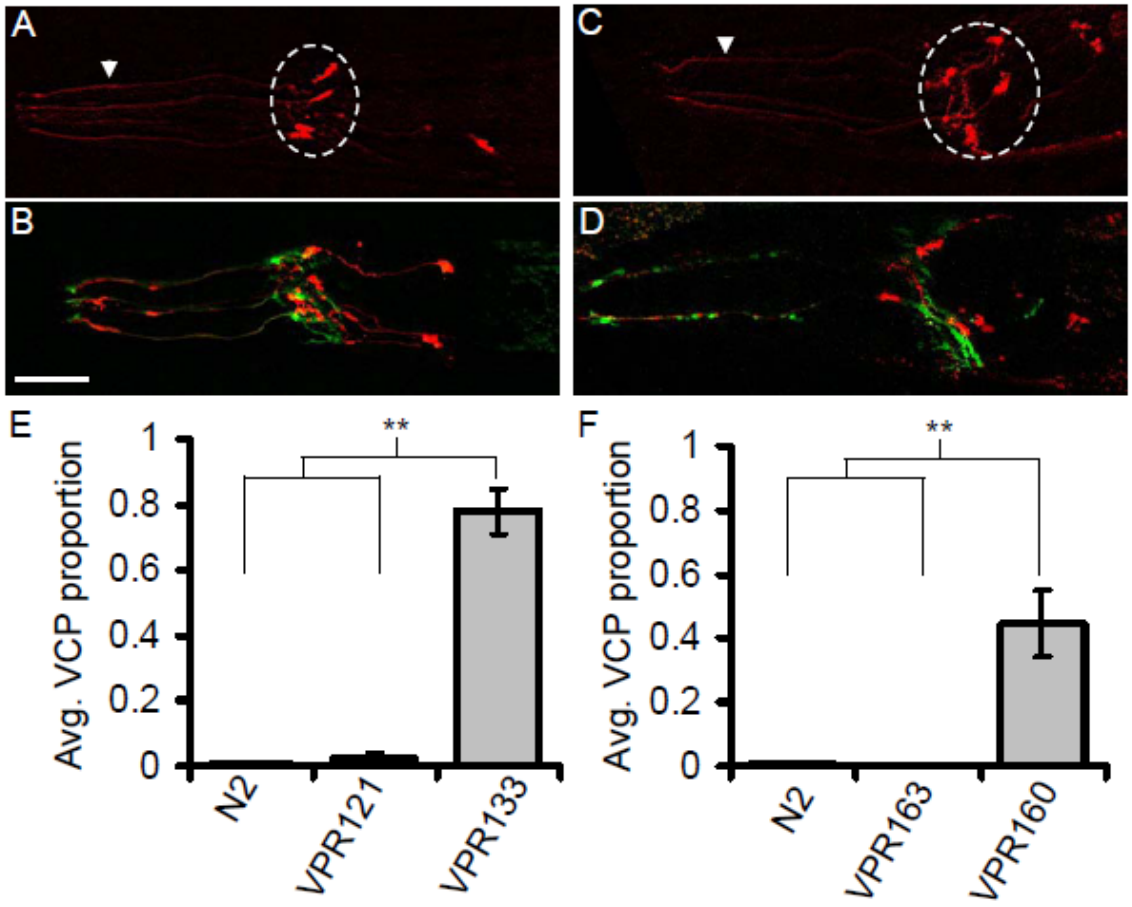

Figure 2. *The t-Phlh-17 produces the VCP without driving fluorescent protein expression.* (A) Line VPR121 expresses monomericDsRed in CEP neurons. (B) Neuronal expression of DsRed in line VPR121 can be easily distinguished from GFP expressing CEPsh cells in a cross between strains VPR121 and VPR839. (C) Strain VPR133 (*Phlh-17*‖*Pdat-1::DsRedExpress2*) expresses a DsRed variant in CEP neurons. (D) Neuronal expression of DsRed in line VPR133 can be readily distinguished from GFP expressing CEPsh cells in a cross between strains VPR133 and VPR839. Dashed-line ellipse indicates CEP neuron cell bodies; arrowheads indicate dendritic processes; confocal images, scale bar= 20µm. (E) Average proportion of trials in which the VCP was displayed by N2 (non-transgenic control; n= 53, data sourced from Fig. 1 B), VPR121 (n= 30), and VPR133 (n=21) worms. (F) Average proportion of trials in which the VCP was displayed by

strains N2 (as in E), VPR163 (*Punc-54::mCherry* alone; n= 21) and VPR160 (*Phlh-17::none + Punc-54::mCherry*; n= 21). Bars in E and F represent means ± sem. ** $p<0.01$, KWA followed by Dunn's MCT.

To test if over-expression of protein by the t-*Phlh-17* caused the VCP, we used transgenic construct that included the t-*Phlh-17* but lacked downstream protein expression. One such construct is made out of the same plasmid used to make line VPR128 but with the *dat-1* promoter (*Pdat-1*) inserted between the 3' end of the t-*Phlh-17* and the start of the DsRedExpress2 coding region. We made the transgenic line VPR133 using this construct. As a control we used the strain VPR121, that expresses monomericDsRed under the *dat-1* promoter in the CEP neurons (Fig. 2 A) whose bodies are near, and whose dendritic extensions closely interact with, CEPsh glial cells, that themselves lack the expression of DsRed, as previously reported (Nass et al. 2001; Nass et al. 2002). Similarly CEP neurons, but not CEPsh glial cells, expressed DsRed in VRP133 line as seen under fluorescent microscopy (Fig. 2 C); there was some ectopic expression in unidentified cells in some individual animals (data not shown). Expression of DsRed in CEP neurons of VPR121 and VPR133 worms can be readily distinguished from GFP expressing CEPsh cells in crosses between these strains with VPR839 (Fig. 2 B and D, respectively). The expression of DsRed under the *Pdat-1* alone in VP121 did not cause the VCP since worms of strain VPR121 show a similar proportion of the VCP as non-transgenic controls (Fig. 2 E). However, when the t-*Phlh-17* was included in the extrachromosomal arrays, but without t-*Phlh-17* driven protein expression, as in strain VPR133, we observed the VCP (Fig. 2, E) with an average proportion of 0.78±0.07

which is significantly higher than that recorded for worms of strain VPR121 (0.02±0.02; Fig 2E) or N2 (non-transgenic control, data sourced from Fig. 1 B). Thus, it appears that the t-*Phlh-17* itself is the cause of the VCP. Since VPR133 displays the VCP induced by extrachromosomal arrays, it also appears that genome integration is not necessary for t-*Phlh-17* to cause the VCP.

To further test if protein expression causes the VCP we made the transgenic line VPR160, using a similar construct to one used to make strain VPR839, but lacking the GFP coding sequence downstream of the t-*Phlh-17*. To report on success of transgenic line production and achieve their selection based on red fluorescence, we co-injected the *Punc-54::mCherry* to drive reporter expression in muscle cells (Supplemental Fig. 2) as previously described (Ruan et al. 2010). As a control we made the VPR163 line expressing only this red muscle marker, which did not cause the VCP (Fig. 2 F). However, there was a robust display of the VCP in the VPR160 strain (Fig. 2 F). Taken together, protein expression driven by the t-*Phlh-17* is not necessary for the VCP.

Having determined that t-*Phlh-17* itself is the cause of the VCP, we next tested if its copy number is relevant for the severity level of the phenotype. Since integrated transgene copy number is normally stable between generations and lacks mosaicism, we were able to increase and decrease the copy number through breeding. We also implemented a more sophisticated analysis of touch-induced back crawling, based on scoring with a counting number scale (1-10; 1, normal, while 10, full VCP), in order to assess the severity of the VCP (Supplemental Movies 3 & 4). To determine if decreasing copy number reduces phenotype severity, the VPR156 line, which has high VCP severity, was crossed to N2. The VCP required a double dose of the *vprIs156* array since, since

the cross, which is heterozygous for the array, lacked the VCP and behaviorally was indistinguishable from N2 (Fig. 3 A). Thus, the copy number of t-*Phlh-17* can modulate the extent of VCP display/severity.

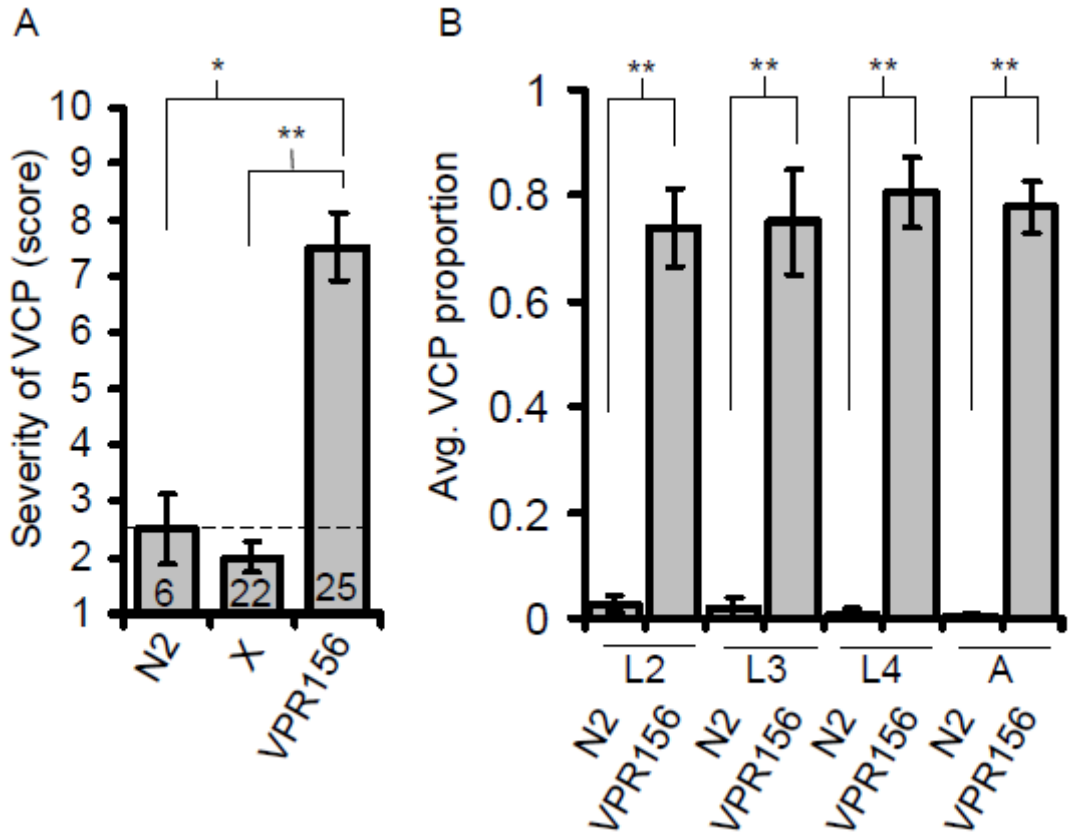

Figure 3. *The severity of the VCP depends on copy number of the trans-promoter, and is maintained from early larval stages through adulthood.*

A) Averaged VCP severity rating assigned to worms (parental N2 and VPR 156 lines, as well as their cross, X, heterozygous for transgenic array) based on a 1-10 counting number scale (1, normal backward crawling; 10, full VCP). Dashed line indicates baseline score for N2 (Supplemental Movie 3). Number of worms tested for each category is shown within each column. Groups were compared using KWA followed by Dunn's MCT; **p<0.01, * p<0.05. B) The VCP is maintained from early larval stages

through adulthood. Average proportion of trials in which the VCP was displayed by N2 and VPR156 lines at various life stages. L, larval stages 2-4; A, adult. Note that L1 worms were not tested due to their size. Data for adults is sourced from Fig. 1B (n=53); n=18 for both genotypes for all other life stages shown. Groups at each life stage were compared using Mann-Whitney U-test; ** $p<0.01$. Bars in A and B represent means $\pm$ sem.

In all experiments presented thus far we used adult worms. To assess whether the VCP might be developmentally regulated, we compared the VPR156 line showing severe VCP with non-transgenic N2 worms at various life stages (larval 2-4 and adult). The VCP was seen at all stages in VPR156, while N2 worms showed normal locomotion (Fig. 3B, Supplemental Movies 5 & 6). Thus, consistent with the known activity of t-*Phlh-17* throughout the development of worms from an oocyte to the adulthood (Colon-Ramos et al. 2007; Stout and Parpura 2011a), its increased copy number leads to a locomotion phenotype of worms at all developmental stages tested.

The results we present here show that a specific locomotion phenotype is caused by over-representation of the t-*Phlh-17*. In general this indicates that copy number of transgenic array is important in research utilizing the CEPsh cell specificity of the t-*Phlh-17* as a marker or as a tool to influence cellular activity. Introduction of multiple exogenous copies of the promoter also perturbs the activity of the t-*Phlh-17* itself (Supplemental Fig. 4). This is a common phenomenon seen in transgenic *C. elegans* lines when multiple transgenic reporters are driven from the same promoter and therefore may not seem surprising on first consideration but it indicates that some factor acting on the t-

Phlh-17 is in limited supply and the pool of such factors is depleted or sequestered when multiple copies of the t-*Phlh-17* are present. This also raises the possibility that dysfunction of the glial cells might underlie some aspects of the phenotype since the endogenous *Phlh-17* driven expression of the *hlh-17* gene is important for development of the CEPsh cells which is, in turn, a requirement for normal development of the rest of the nervous system (Hedgecock et al. 1990; Colon-Ramos et al. 2007; Yoshimura et al. 2008).

We propose two possible mechanisms as the cause of the VCP. As alluded to above, our results indicate that some DNA interacting factor might be affected by the multiple copies of the t-*Phlh-17*, with transcription factors important for neuronal or glial development as obvious candidates. An alternative mechanism for the VCP could be RNA toxicity induced by untranslated RNA transcripts produced by the multiple copies of the t-*Phlh-17*. Interestingly, there is some shared basis for phenotypes caused by RNA toxicity and those caused by non-coding sequence mediated transcription factor depletion/sequestration (Ebralidze et al. 2004). Since we observed the VCP in lines that had several different sequences downstream of the promoter (Fig. 1 & 2, Supplemental Fig. 2), this finding indicates that the VCP is not caused by a specific transcript but we could not rule out RNA toxicity as the cause of the VCP.

The transgenic arrays produced in *C. elegans* are complex and variable in sequence, order, and repeat number between individual lines produced from each injection but are nearly identical within transgenic worm lines in both extra-chromosomal and integrated forms (Mello et al. 1991). Even within lines containing identical or nearly identical transgenic sequences, expression of reporters is variable in the same cell

between individual worms and also between cells of the same tissue type within single animals, as reported previously (Hsieh et al. 1999). Elimination of extrachromosomal array-caused mosaic effects on transgene expression lowers but does not abolish this variability in lines carrying t-*Phlh-17* driven reporters. This variable expression has interesting parallels in transgenic mammals using glial and neuron specific transgenes (Lee et al. 1994; Feng et al. 2000). Although transgenic reporter protein expression is not required to generate the VCP, variability observed for reporters driven by the t-*Phlh-17* coincides with variability in VCP proportion and severity; this raises the possibility of a shared underlying cause. Because repetitive transgene sequences in *C. elegans* are specifically epigenetically modified and sequestered to the periphery of the nucleus, stochastic variability in epigenetic modifications and the three dimensional arrangement of chromatin might be an underlying cause of the variability in reporter expression in our work and in VCP penetrance. In support of this idea, stochastic changes in transcription factor levels in *C. elegans* have been shown to destabilize transcription factor regulatory networks with involvement of chromatin (Raj et al. 2010). This implicates an additional mechanism between the DNA of the promoter and the phenotype through sequestration of epigenetic machinery instead of, or in addition to, transcription factor sequestration. The identity of factors that are altered by the presence of t-*Phlh-17* repeats is not addressed in this study but is an exciting area for future research. Since copy number of transgene arrays (large ~ 300 vs. lower ~ 50) is handled differently by nuclear proteins (Towbin et al. 2011), DNA interacting factors involved in this differential transgene handling are excellent candidates for this vein of study.

The phenomenon of multiple copies of an untranslated sequence affecting behavior that we uncovered here is not only a variable to be controlled for in research on *C. elegans* glia, but could be taken into account when studying human disease and transcriptional regulatory networks. RNA sequestration of splicing and transcription factors has been implicated as a cause of human locomotion diseases associated with expansions of non-coding repeats such as myotonic dystrophy and fragile X-associated tremor/ataxia syndrome (Gardner-Medwin et al. 1981; Ebralidze et al. 2004). Upon expression of RNA associated with a mutation that causes human myotonic dystrophy type 1 (DM1), specific transcription factors were sequestered away from promoters where they would normally act in the genome, which resulted in perturbation of normal activity levels of those promoters (Ebralidze et al. 2004). *C. elegans* has been recently shown to be a good model of the RNA splicing caused aspects of DM1 (Wang et al. 2011). We suggest that results presented in this report show that *C. elegans* could also be used to selectively model effects of transcription factor depletion in human diseases caused by regulatory region expansion mutations without the obscuring effects of splicing factors. The unique aspects of transgenic line production, i.e., large multi-copy transgenes containing transcription factor binding sequences, make *C. elegans* a particularly important model for exploring human genetic diseases. We envision transgenic *C. elegans* lines with multiple copies of just the regions expanded in human diseases without production of transcripts with evaluation of resulting neural development and behavior phenotypes, facilitated by the wealth of cell specific markers, genetics, anatomic information and tools available for this organism.

Materials and Methods

Transgenic Construct Production

Plasmids and sequences are available upon request. The *hlh-17* promoter was copied from genomic DNA and inserted into a plasmid. Resulting pRSG was used to generate all subsequent plasmids containing the t-*Phlh-17*. The *Pdat-1::monomericDsRed* containing plasmid is a modification of pRB490 [*Pdat-1::GFP;* (Nass et al. 2002)], while previously published pU54mCh (Ruan et al. 2010) and pDP#MM016B (Maduro and Pilgrim 1995) where obtained from original sources. Descriptions and sources of all plasmids are available in Supplemental.

Transgenic Line Production, Selection and Crosses

Transgenic lines were constructed by germline transformation after microinjection (Mello and Fire 1995) of plasmids (75 ng/µL with the exception of the p*Phlh-17::none* at 100ng/µL, *pPunc-54::mCherry* at 30 ng/µL and *pPunc-54::mCherry* at 150ng/µL) into N2 worms. Transgenic lines were selected using a macro zoom microscope (MVX10, Olympus) equipped with transmitted-light (30 W Halogen) and wide-field fluorescence (100 W Xenon arc) illumination along with standard GFP, DsRed, and GFP/DsRed filter sets (Chroma Technology). The transgenic array was integrated by gamma irradiation. Worms were maintained at 20ºC on standard nematode growth medium/agar (NGM)

seeded with OP50 strain *E. coli* (Brenner et al. 1994). All integrated lines were backcrossed at least 2 times to N2 strain. Selecting for VCP severity testing and assigning a blind key (with number designation from a list of random four digit numbers), was a two-step procedure: i) prior to testing we picked individual hermaphrodite young adult worms, which were F1 generation of a single hermaphrodite, heterozygous for the *vpr156* array, and then ii) post testing individual worms were allowed to have self-fertilized offspring with the genotype of the F1 generation assessed based on F2 assortment and then matched back to the pretesting selection.

Behavior Testing

Behavior testing was carried out at 20ºC on growth plates using transmitted light images of a macro zoom microscope equipped with: i) a Gigaware® 2.0MP webcam (Ignition L.P.) mounted to an ocular (Miller and Roth 2009) and driven by Webcam Companion 3 software*;* and ii) a top port mounted CoolSNAP HQ^2 CCD camera (Photometrics) driven by Metamorph™ imaging software ver. 7.0 (Molecular Devices Inc.).

A) VCP Proportion. Each worm was tested in 6 trials, each trial containing sequential testing for forward and backward crawling. To assure viability of a worm, forward crawling was induced by touching the posterior quarter of the worm's body once using an eyebrow hair attached to a toothpick (Chelur and Chalfie 2007). Worms that were able to crawl forward were then tested on backwards crawling by touching the anterior quarter of the body repeatedly until the worm crawled backward for one body

length (Supplemental Movie 1) or one of the following criteria were met which constituted exhibition of the VCP for that trial (Supplemental Movie 2): i) the tail touched any part of the worms body, or ii) the worm initiated backward movement and the anterior continued moving while the tail remained frozen in an abnormal curved position (tail paralysis). The VCP proportion for each worm was calculated as the number of failures, out of 6 trials, to crawl backward. Each line was tested from at least 3 separate plates with at least 6 worms per plate.

B) *VCP severity*. Each selected worm was filmed and resulting videos were scored blind to genotype on a counting number scale ranging from 1 to 10 (1 being completely normal backwards crawling, while 10 being VCP: a tight curl of the tail immediately or "freezing" upon initiation of backward movement) for severity of the VCP (See Supplemental Movies 3 & 4). After scoring the individual worms were matched back to a key containing genotype.

Morphological Assessment of Transgenics

For morphological assessment of transgenics, individual worms were immobilized using sodium azide solution (20 mM), deposited onto a glass coverslip and imaged using a 20 x oil immersion objective (0.80 NA) of a FluoView FV 300 (Olympus) confocal laser scanning microscope controlled by FluoView 5.0 software. We used an Argon ion laser (10 mW at 488 nm) for excitation of GFP, and a HeNe ion laser (1 mW at 544 nm) for DsRed variants and mCherry excitation, while respective emission was collected at FITC (green channel) and TRITC (red channel) settings. The entire width of each worm was

imaged using serial sagital z-plane section image scans and the resultant image stacks were processed as maximum projection reconstructions using Metamorph™.

Acknowledgements

This work was supported by the National Science Foundation (CBET 0943343). We thank Jessica Romano for blind severity scoring of the VCP. We thank V. Grubišić for some assistance with imaging. We thank M. Maduro for comments on a previous version of the manuscript. We thank G. Broitman-Maduro for advice in production of some of the transgenic strains used in this research. We thank L. Pozzo-Miller and L. Wadiche for access to confocal microscope equipment. The Heflin Center Genomics Core at UAB provided sequencing for the DNA plasmids used in this work.

Supplemental Materials and Methods

Plasmid Construction

All plasmids made in the laboratory for transgenic VPR worm lines production in this study and their sequences are available upon request. The summary of all plasmids, including additional, previously published plasmids and available form original sources, used for transgenic worm production are summarized in Supplemental Table 1. All plasmids contained unc-54 3'untranslated region sequence (UTR) following the promoter or the gene, with the exception of pDP#MM016B. We list below plasmids with their transpromoter and transgene disclosed in brackets associated with the plasmid name.

pRSG [*Phlh-17::GFP*]. We copied *hlh-17* promoter [as originally described in (McMiller and Johnson 2005)], from genomic DNA using a set of primers (forward, *hlh-17 BamHI*: ggccaggatccgaacagcttagctatttcgt; and reverse, *hlh-17 Xmal*: ctttggccaatcccccgggtccatgactgg) which creates HindIII and XmaI restriction enzyme recognition sites on the 5' and 3' ends of a 2.5 kbp fragment 118 bps before the translation start site of the *hlh-17* gene (McMiller and Johnson 2005; Yoshimura et al. 2008). The promoter was inserted into *C. elegans* vector pPD95.69 (A. Fire, S. Xu, J. Ahm, and G. Seydoux, personal communication; courtesy of A. Fire, Stanford University, Palo Alto, CA). Since pPD95.69 contains *GFP* followed by the *unc-54_3'UTR*, by cutting pPD95.69 and the PCR product with BamHI and XmaI, followed by ligation, the resulting pRSG contains *Phlh-17::GFP*::unc-54_3'UTR. For simplicity, in subsequent

construct descriptions we omit referral to unc-54_3'UTR, unless necessary. All plasmids containing the *Phlh-17* used in reported work were modification of this plasmid.

pRSRXP2 [*Phlh-17::DsRedExpress2*]. PCR was performed using a set of primers (forward: aacacgatgataacccgggtatggccacaacc; and reverse: tagagtcgcggccgctacaggaacag) and pIRES2-DsRedExpress2 (Clontech, Mountain View, CA) as template. The PCR product containing *DsRedExpress2* was instead into a modified and previously published version of pRSG, pRSFX4 (Stout and Parpura 2011b), using digestion of product and vector with XmaI and NotI, followed by ligation. Thus, the resulting pRSRXP2 contains *Phlh-17* that drives expression of the DsRedExpress2 coding sequence.

pRSR2 [*Phlh-17::monomericDsRed*]. PCR was performed using a set of primers (forward: gccggatccccgggattggccaaggacc; and reverse: cgtacggccgactagtaggaaacag) and pRSDAR (construction described below) as template to amply a fragment containing monomericDsRed with the unc-54_3'UTR. The resulting PCR product and pRSG were trimmed/cut with XmaI and SpeI restriction enzymes (removing the *GFP* and *unc-54_3'UTR* from pRSG) and the trimmed *monomericDsRed::unc-54_3'UTR* fragment was inserted by ligation. The resulting pRSR2 contains *Phlh-17* that drives expression of *the monomericDsRed* coding sequence.

pRSDAR [*Pdat-1::monomericDsRed*]. The *GFP* in pRB490 [pPD95.73 backbone vector containing *Pdat-1::GFP;* kindly provided by R. Blakely, Vanderbilt University, Nashville, TN (Nass et al. 2002)] was replaced by *monomericDsRed* from pDsRed-Monomer-C1 (Clontech, Mountain View, CA) by cutting both plasmids with the

enzymes AgeI and EcoRI, followed by ligation. The resulting pRSDAR contains *Pdat-1* that drives expression of *the monomericDsRed* coding sequence.

pRSHDA2 [*Phlh-17*‖*Pdat-1:: DsRedExpress2*]. PCR was performed using a set of primers (forward, agcttaccggtatgaaatggaacttgaatcc; and reverse, taacatcaccatctaattcaacaagaattgggac) and pRB490 as template to copy the *Pdat-1*. The PCR product was trimmed with the enzyme AgeI, while pRSRXP2 was cut with XmaI. The resulting fragments were ligated and checked for proper orientation of the *Pdat-1* by sequencing. The resulting pRSHDA2 has *Phlh-17* positioned 5' of *Pdat-1,* with only later, downstream promoter capable of riving expression of *DsRedExpress2*.

pRSV2 [*Phlh-17::none*]. We made this plasmid as pRSG, but using pPD95.67 that had its *GFP* coding sequence removed. This removal was done is two steps: i) first, treating pPD95.67 with enzymes BamHI and SpeI which removed the *GFP* with *unc-54_3′ UTR* ; and ii) then missing *unc-54_3′ UTR* was re-instead after obtaining it by BamHI and SpeI restriction of pBY103 (kindly provided by M. Maduro, University of California, Riverside, CA (Maduro and Pilgrim 1995)]. The resulting pRSV2 contains only *Phlh-17* with downstream *unc-54_3′ UTR* , but lacking a transgene.

Transgenic Strains and Crosses

All transgenic VPR lines made in the laboratory for this study are available upon request. We summarize below additional worm lines used in this study for Supplemental data/figures and to generate some of the lines reported in Table 1. We list transgenic worm lines with their transgenic arrays reported in parentheses within which trans-

promotor/gene are in brackets. MS839 and UL1713 lines where made using worm strains rooted in N2 (non-transgenic, Bristol strain) background, while all other lines were made directly into N2 strain.

MS839 (*unc-119 (ed4) III, irIs67[Phlh-17::GFP + unc-119(+)*]). This line was produced by co-microinjection of plasmids pRSG and pDP#MM016B into *unc-119 (ed4)III* worms [kindly provided by M. Maduro; (Maduro and Pilgrim 1995)] and then screened for rescue of the *unc-119(+)* phenotype, followed by the transgene array integration with gamma irradiation.

VPR839 (*unc-119 (ed4) III, irIs67[Phlh-17::GFP + unc-119(+)*]). This line was produced by backcrossing MS839 line 4 times to N2 strain.

TV2394 (*wyEx915 [Phlh-17::mCherry + Punc-122::GFP], *[Punc-122::RFP]);* asterisks indicates unnamed array. This unpublished line was generously provided by D.A. Colón-Ramos (Yale University, New Haven, CT) which was produced as previously described (Colon-Ramos et al. 2007). Due to injection of pDACR (backbone vector pPD49.26) encoding *Phlh-17::mCherry,* CEPsh glial cells of this line express mCherry. Additionally, *Punc-122::GFP and Punc-122::RFP* drive expressing of these fluorescent proteins in coelomocytes [for reporter expression driven by *Punc-122* see (Loria et al. 2004); information of coelomocytes available at http://www.wormatlas.org/hermaphrodite/coelomocyte/Coelomoframeset.html].

VPR168 (*wyEx915 [Phlh-17::mCherry + Punc-122::GFP])* was generated by crossing TV2393 with N2 and followed by progeny selection. Worms containing *wyEx915 [Phlh-17::mCherry + Punc-122::GFP]* bu lacking *Punc-122::RFP* array were selected.

VPR 169 (*irIs67[Phlh-17::GFP + unc-119(+)], wyEx915 [Phlh-17::mCherry + Punc-122::GFP])*. We obtained this line by crossing VPR839 with VRP168. Due to coelomocytes location elsewhere, GFP fluorescence in the head region is solely originating from the CEPsh glial cells.

VPR108 (*vprIs108* [*Phlh-17::GCaMP2.0 + Phlh-17::mCherry*]). We previously produced this line (Stout and Parpura 2011a; Stout and Parpura 2011b) by co-microinjection of plasmids encoding *Phlh-17::GCaMP2.0* and *Phlh-17::mCherry*, with array integration using gamma irradiation, followed by backcrossing to N2 four times.

UL1713 *(unc-119(ed3) III, leEx1713[hlh-17::GFP + unc-119(+)]* was generously provided by the Caenorhabditis Genetics Center (University of Minnesota, Minneapolis, MN, http://www.cbs.umn.edu/CGC; funded by the NIH National Center for Research Resources) on behalf of A.J. Walhout's laboratory. This line was produced by particle bombardment as previously described (Grove et al. 2009). It should be noted that the *Phlh-17* used in this line, due to its 5' end truncation, is 2 kbp in length, as opposed to 2.5 kbp length used in all other plasmids/transgenics.

Morphological Assessment of Transgenics

Besides using confocal laser scanning microscopy, for morphological assessment of transgenic worms in a subset of experiments (Supplemental Fig. 1 & 2) we used an inverted microscope (IX71, Olympus) equipped with wide-field epifluorescence and differential interference contrast (DIC) illumination. Visualization of GFP was accomplished using a standard fluorescein isothiocyanate (FITC) filter set, while a

standard Texas Red filter set was used for imaging red fluorescent protein variants; both filter sets were from Chroma Technology Corp. Images were captured through a 40 x oil-immersion objective [UAPO40XOI3/340, Olympus; NA set at 1.35] using a CoolSNAP *HQ*^{2} CCCD camera driven by Metamorph™ imaging software ver. 7.0.

Supplemental Table 1

Summary of plasmids by name, background vector, their promoter and gene content, and location of gene expression in transgenic C. elegans cells

Plasmid	Background Vector	Promoter	Gene	Expression
pRSG	pPD95.69	*Phlh-17*	*GFP*	CEPsh glia
pRSRXP2	pPD95.69	*Phlh-17*	*DsRedExpress2*	CEPsh glia
pRSR2	pPD95.69	*Phlh-17*	*monomericDsRed*	CEPsh glia
pRSDAR	pPD95.73	*Pdat-1*	*mCherry*	CEP, ADE, PDE neurons
pRSHDA2	pPD95.69	*Phlh-17*‖*Pdat-1*	*DsRedExpress2*	CEP, ADE, PDE and other unidentified neurons
pRSV2	pPD95.69	*Phlh-17*	*none*	NA
pDP#MM016B *	pBluescript II KS(-)	*unc-119p*	*unc-119*	most neurons
pU54mCh *	pPD30.38	*Punc-54*	*mCherry*	muscle cells

Abbreviations: CEP, cephalic sensilla; CEPsh, CEP sheath ADE, Anterior DEirids; PDE, Posterior DEirids;

* previously published: pDP#MM016B [kindly provided by M. Maduro (Maduro and Pilgrim 1995)]; pU54mCh [kindly provided by G.A. Caldwell, University of Alabama, Tuscaloosa, AL (Ruan et al. 2010)]

Supplemental Figures

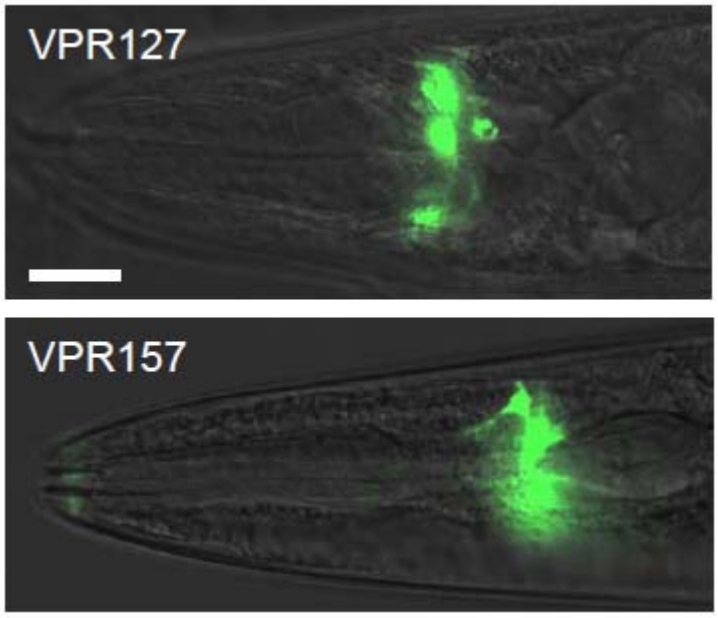

Supplemental Figure 1. Expression pattern of GFP in VPR127 and VPR157 worms. Images are wide field fluorescence images of GFP overlaid with differential interference contrast (DIC).

Only the anterior, head, portion of each worm is shown. Basic cell morphology of CEPsh glial cells with their bodies and the thin sheet-like extensions can be observed based on the expression GFP fluorescence driven by the t-*Phlh-17*. Both lines showed essentially no protein clumping and no apparent mosaicism in GFP expression consistent with their integrated arrays. Scale bar, 20 μm.

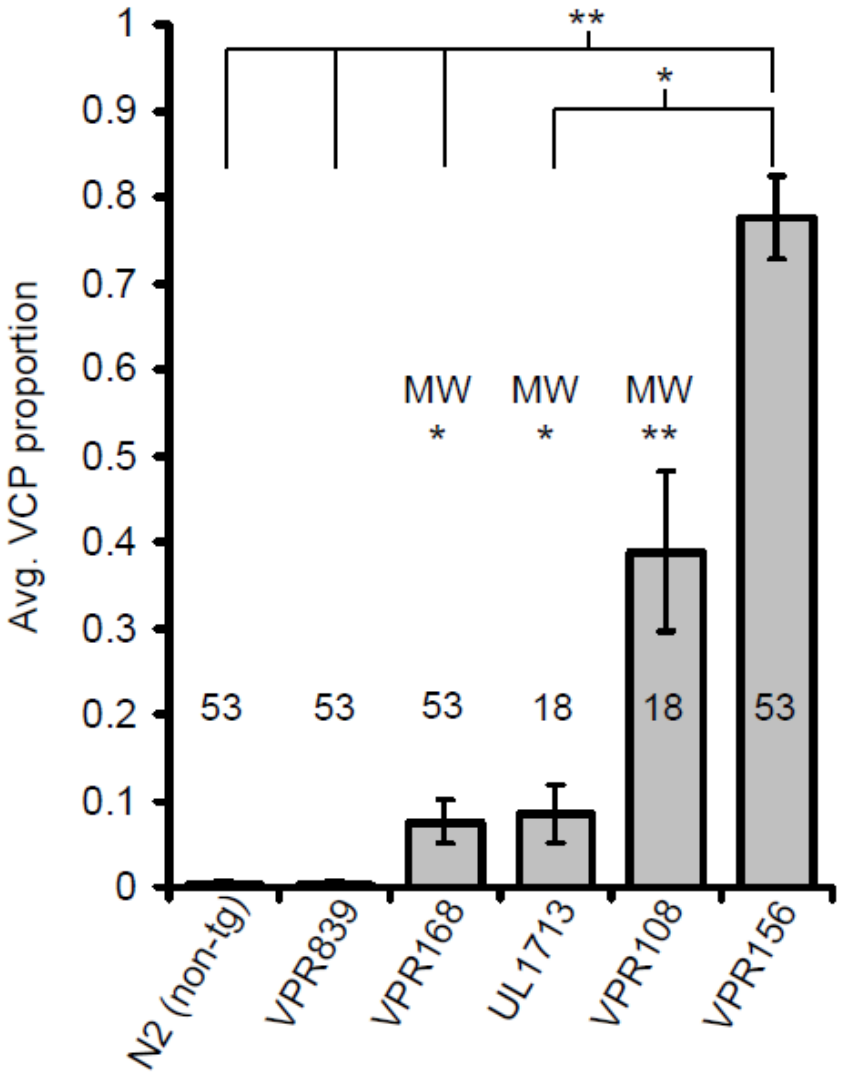

Supplemental Figure 2. Proportion of VCP varies in additional strains.

Supplementary lines expressing fluorescent markers driven by t-*hlh-17* tested were: unpublished VPR168 (*wyEx915 [Phlh-17::mCherry + Punc-122::GFP]);* along with two published *lines,* VPR108 (*vprIs108* [*Phlh-17::GCaMP2.0 + Phlh-17::mCherry*]) and UL1713 *(unc-119(ed3) III, leEx1713[hlh-17::GFP + unc-119(+)].* We compared behavioral test outcomes of these lines with N2 and VPR156 (both sourced from Fig. 1

B) which define the lower and upper limits of VCP dynamic range observed, along with comparison to VPR839 line (sourced from Fig. 1 B), which when tested against N2 alone shows statistical identity (Mann-Whitney U-test; p=1.0). Number of worms tested for each strain is shown aligned within bars. Groups were compared using Kruskal-Wallis one-way ANOVA followed by Dunn's multiple comparisons test. We also tested each supplementary line against N2 alone (and to VPR839 alone; naturally same significance) using Mann-Whitney U-test (MW). **$p< 0.01$, *$p< 0.05$. These data supports the notion that VCP is not fluorescent marker specific. Furthermore, it indicates that above testing can determine experimental applications that are (un)suitable for a strain on an individual strain basis. For instance, VPR108 that has been successfully used for studying intracellular Ca^{2+} dynamics in cell cultured CEPsh glial cells (Stout and Parpura 2011a) would not be a good model for studying freely moving animals that undergo backward locomotion due to high proportion of VCP.

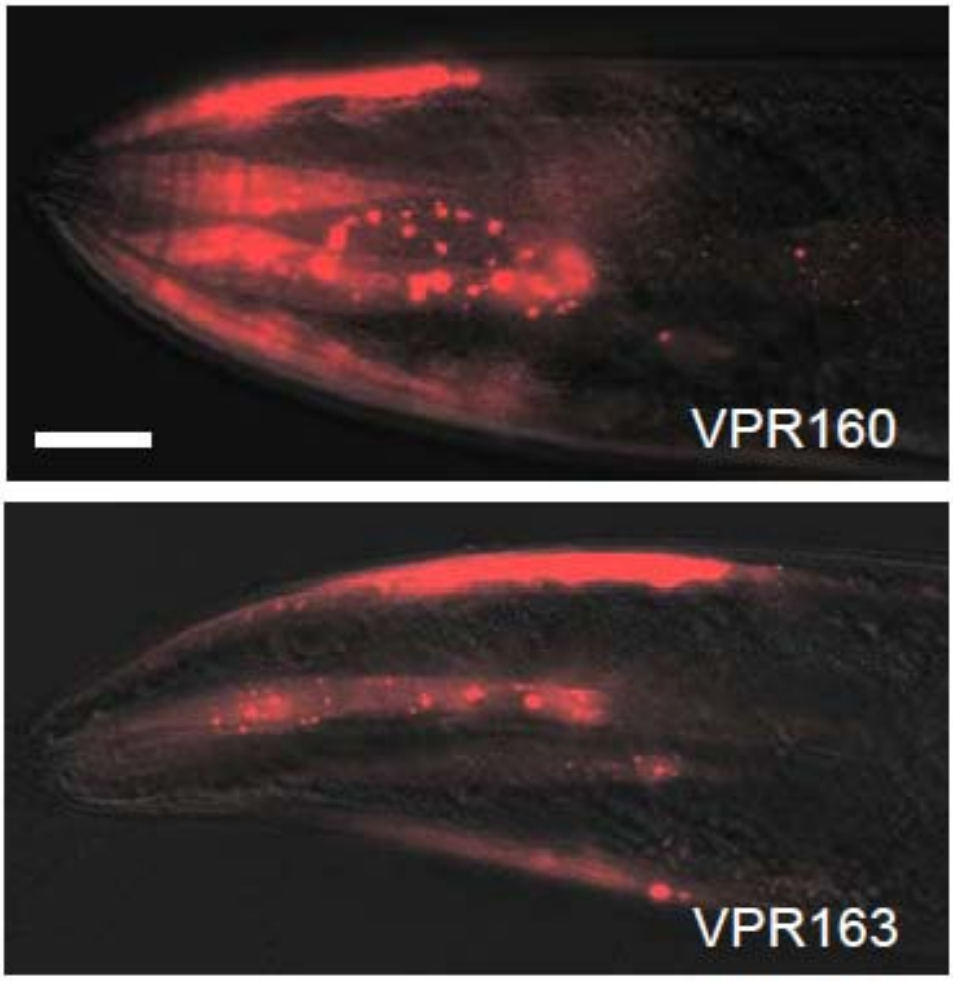

Supplemental Figure 3. Expression pattern of mCherry in VPR160 and VPR163 worms. Wide field fluorescence images of mCherrry overlaid with DIC. Only the anterior portion of each worm is shown. Basic cell morphology of muscle cells in the head region can be observed based on expression of mCherry driven by the *t-Punc-54*. Both lines show mosaicism in mCherry expression among muscle cells due to their extrachromosomal arrays. Note the absence of expression in CEPsh glial cells. Scale bar, 20 μm

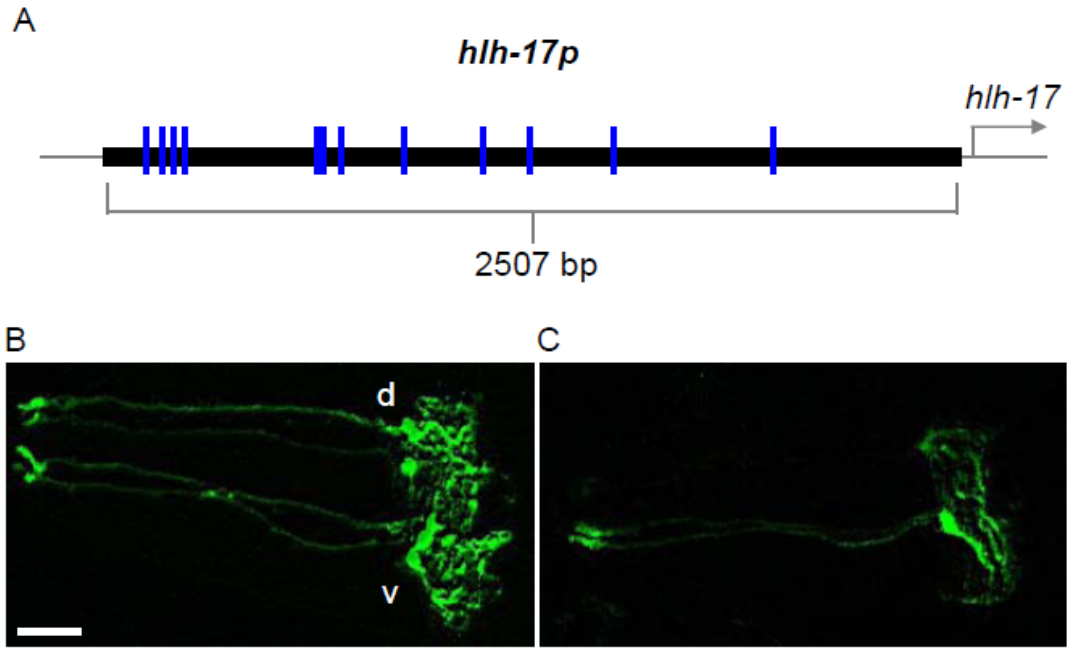

Supplemental Figure 4. Multiple copies of the t-*Phlh-17* may lead to changes in the activity of the t-*Phlh-17*.

(A) Drawing depicting predicted basic Helix-Loop-Helix (bHLH) transcription factor binding sites (blue ticks) based on the recognition sequence CANNTG (Grove et al. 2009). (B, C) Confocal images of two individual VPR169 worms whose *Phlh-17::GFP* expression was imaged with the green channel. While one worm (B) possesses GFP expression that is balanced across the dorsal (d) and ventral (v) CEPsh cells, the other worm (C) has levels of GFP expression that are imbalanced between CEPsh cells of the same worm. This is an example of differential expression levels being driven by the same integrated and homozygous transgenic array (*irIs67[Phlh-17::GFP + unc-119(+)*]), hence with the same insertion site in the genome. Since it is an extrachromosomal, rather

than intrachromosomal, array containing t-*Phlh-17* that displays mosaicism (Colon-Ramos et al. 2007), the imbalance in the expression of GFP driven by the stable, integrated *irIs67* transgenic array indicates stochastic changes in trans-promoter (i.e., t-*hlh-17*) strength, possibly due to disruption of transcription factor network stability. Scale bar, 20 μm.

References

Bacaj T, Shaham S. 2007. Temporal control of cell-specific transgene expression in Caenorhabditis elegans. *Genetics* **176**: 2651-2655.

Brenner M, Kisseberth WC, Su Y, Besnard F, Messing A. 1994. GFAP promoter directs astrocyte-specific expression in transgenic mice. *J Neurosci* **14**: 1030-1037.

Chelur DS, Chalfie M. 2007. Targeted cell killing by reconstituted caspases. *Proc Natl Acad Sci U S A* **104**: 2283-2288.

Colon-Ramos DA, Margeta MA, Shen K. 2007. Glia promote local synaptogenesis through UNC-6 (netrin) signaling in C. elegans. *Science* **318**: 103-106.

Ebralidze A, Wang Y, Petkova V, Ebralidse K, Junghans RP. 2004. RNA leaching of transcription factors disrupts transcription in myotonic dystrophy. *Science* **303**: 383-387.

Feng G, Mellor RH, Bernstein M, Keller-Peck C, Nguyen QT, Wallace M, Nerbonne JM, Lichtman JW, Sanes JR. 2000. Imaging neuronal subsets in transgenic mice expressing multiple spectral variants of GFP. *Neuron* **28**: 41-51.

Gardner-Medwin AR, Coles JA, Tsacopoulos M. 1981. Clearance of extracellular potassium: evidence for spatial buffering by glial cells in the retina of the drone. *Brain Res* **209**: 452-457.

Grove CA, De Masi F, Barrasa MI, Newburger DE, Alkema MJ, Bulyk ML, Walhout AJ. 2009. A multiparameter network reveals extensive divergence between C. elegans bHLH transcription factors. *Cell* **138**: 314-327.

Guo ZV, Hart AC, Ramanathan S. 2009. Optical interrogation of neural circuits in Caenorhabditis elegans. *Nat Methods* **6**: 891-896.

Hedgecock EM, Culotti JG, Hall DH. 1990. The unc-5, unc-6, and unc-40 genes guide circumferential migrations of pioneer axons and mesodermal cells on the epidermis in C. elegans. *Neuron* **4**: 61-85.

Hsieh J, Liu J, Kostas SA, Chang C, Sternberg PW, Fire A. 1999. The RING finger/B-box factor TAM-1 and a retinoblastoma-like protein LIN-35 modulate context-dependent gene silencing in Caenorhabditis elegans. *Genes Dev* **13**: 2958-2970.

Lee SH, Kim WT, Cornell-Bell AH, Sontheimer H. 1994. Astrocytes exhibit regional specificity in gap-junction coupling. *Glia* **11**: 315-325.

Loria PM, Hodgkin J, Hobert O. 2004. A conserved postsynaptic transmembrane protein affecting neuromuscular signaling in Caenorhabditis elegans. *J Neurosci* **24**: 2191-2201.
Maduro M, Pilgrim D. 1995. Identification and cloning of unc-119, a gene expressed in the Caenorhabditis elegans nervous system. *Genetics* **141**: 977-988.
McMiller TL, Johnson CM. 2005. Molecular characterization of HLH-17, a C. elegans bHLH protein required for normal larval development. *Gene* **356**: 1-10.
Mello C, Fire A. 1995. DNA transformation. *Methods Cell Biol* **48**: 451-482.
Mello CC, Kramer JM, Stinchcomb D, Ambros V. 1991. Efficient gene transfer in C.elegans: extrachromosomal maintenance and integration of transforming sequences. *Embo J* **10**: 3959-3970.
Miller DL, Roth MB. 2009. C. elegans are protected from lethal hypoxia by an embryonic diapause. *Curr Biol* **19**: 1233-1237.
Muruve DA, Barnes MJ, Stillman IE, Libermann TA. 1999. Adenoviral gene therapy leads to rapid induction of multiple chemokines and acute neutrophil-dependent hepatic injury in vivo. *Hum Gene Ther* **10**: 965-976.
Nass R, Hall DH, Miller DM, 3rd, Blakely RD. 2002. Neurotoxin-induced degeneration of dopamine neurons in Caenorhabditis elegans. *Proc Natl Acad Sci U S A* **99**: 3264-3269.
Nass R, Miller DM, Blakely RD. 2001. C. elegans: a novel pharmacogenetic model to study Parkinson's disease. *Parkinsonism Relat Disord* **7**: 185-191.
Ortinski PI, Dong J, Mungenast A, Yue C, Takano H, Watson DJ, Haydon PG, Coulter DA. 2010. Selective induction of astrocytic gliosis generates deficits in neuronal inhibition. *Nat Neurosci* **13**: 584-591.
Palmiter RD, Brinster RL. 1986. Germ-line transformation of mice. *Annu Rev Genet* **20**: 465-499.
Raj A, Rifkin SA, Andersen E, van Oudenaarden A. 2010. Variability in gene expression underlies incomplete penetrance. *Nature* **463**: 913-918.
Ruan Q, Harrington AJ, Caldwell KA, Caldwell GA, Standaert DG. 2010. VPS41, a protein involved in lysosomal trafficking, is protective in Caenorhabditis elegans and mammalian cellular models of Parkinson's disease. *Neurobiol Dis* **37**: 330-338.
Sekar RB, Kizana E, Smith RR, Barth AS, Zhang Y, Marban E, Tung L. 2007. Lentiviral vector-mediated expression of GFP or Kir2.1 alters the electrophysiology of neonatal rat ventricular myocytes without inducing cytotoxicity. *Am J Physiol Heart Circ Physiol* **293**: H2757-2770.
Stirman JN, Brauner M, Gottschalk A, Lu H. 2010. High-throughput study of synaptic transmission at the neuromuscular junction enabled by optogenetics and microfluidics. *J Neurosci Methods* **191**: 90-93.
Stout RF, Jr., Parpura V. 2011a. Voltage-gated calcium channel types in cultured C. elegans CEPsh glial cells. *Cell Calcium* **50**: 98-108.
Stout RF, Parpura V. 2011b. Cell culturing of C. elegans glial cells for the assessment of cytosolic Ca2+ dynamics. *Methods Mol Biol* **In Press**.
Towbin BD, Meister P, Pike BL, Gasser SM. 2011. Repetitive Transgenes in C. elegans Accumulate Heterochromatic Marks and Are Sequestered at the Nuclear

Envelope in a Copy-Number- and Lamin-Dependent Manner. *Cold Spring Harb Symp Quant Biol* **75**: 555-565.

Wang LC, Chen KY, Pan H, Wu CC, Chen PH, Liao YT, Li C, Huang ML, Hsiao KM. 2011. Muscleblind participates in RNA toxicity of expanded CAG and CUG repeats in Caenorhabditis elegans. *Cell Mol Life Sci* **68**: 1255-1267.

Yoshimura S, Murray JI, Lu Y, Waterston RH, Shaham S. 2008. mls-2 and vab-3 Control glia development, hlh-17/Olig expression and glia-dependent neurite extension in C. elegans. *Development* **135**: 2263-2275.

CELL CULTURING OF C. ELEGANS GLIAL CELLS FOR ASSESMENT OF CYTOSOLIC CA^{2+} DYNAMICS

RANDY F STOUT JR., VLADIMIR PARPURA

Methods in Molecular Biology, in press

Formatted for dissertation

CHAPTER 2

CELL CULTURING OF C. ELEGANS GLIAL CELLS FOR ASSESSMENT OF CYTOSOLIC CA^{2+} DYNAMICS

Abstract

Cell culture has emerged as an important research method for studying various types of primary cells, including neurons and glial cells. This method has been especially instrumental in assessing intracellular Ca^{2+} dynamics of neural cells. The invertebrate model organism *C. elegans* has been extensively used in neurobiology to study wide-spread issues ranging from gene regulation to behavior. We present some of basic morphological characteristics of four *C. elegans* glial cells residing in cephalic sensilla of the worm followed by a description of cell culturing methods for these glial cells. We describe the combined genetic and fluorescence microscopy approaches for identification of *C. elegans* glial cells in culture and assessment of their cytosolic Ca^{2+} dynamics.

Keywords: *C. elegans*, cell culture, calcium, cephalic sensilla, GCaMP, glia, *hlh-17*

Introduction

Interpreting results from *in vivo* studies is inherently a complex task, since various cell types interact between themselves in a multitude of operations and hence obscure the observed characteristics of an individual cell or a cell type. Consequently, the use of cell culture emerged as a method to isolate and study specific cell types or individual cells and characterize their cellular properties in an attempt to understand how they contribute to the operation of the tissue/organ within which they exist in an organism (see Note 1). In the field of glial biology, cultured cells have provided some of the seminal discoveries regarding glial roles in the mammalian nervous system outside of simple structural support. Examples include striking cytosolic Ca^{2+} excitability in astrocytes and consequential gliotransmitter release from these glial cells (Cornell-Bell et al. 1990; Parpura et al. 1994). Indeed, without a clear understanding and characterization of individual glial cells, we might not be able to fully appreciate their functional contributions when working with other neural cells *in vivo*.

The model organism *C. elegans* has been used to great effect in neurobiology with particularly large contributions on how gene products are expressed and interact in specific cell types to produce the output of the nervous system in the form of various behaviors (Barr 2003). The cell number and identity are invariable between individual adult hermaphrodite wild type *C. elegans*. In the nervous system of this nematode, 302 neurons and 56 glial cells have been categorized (Ward et al. 1975; Thomas 1994). These glial cells are considered orthologous to the mammalian glia (Shaham 2006; Heiman and Shaham 2007). Due to their extensive physical contacts with neurons, and morphological

and gene expression similarities with mammalian glia, here we focused on a subset of the *C. elegans* glial cells located in the cephalic (CEP) sensilla in the anterior part of the worm. These four glial cells associate with CEP neurons and are referred to as CEP sheath (CEPsh) cells (Fig. 1; see Note 2). They play a role in the early development of the nervous system and could contribute to its function in the adult worm (McMiller and Johnson 2005; Bacaj et al. 2008).

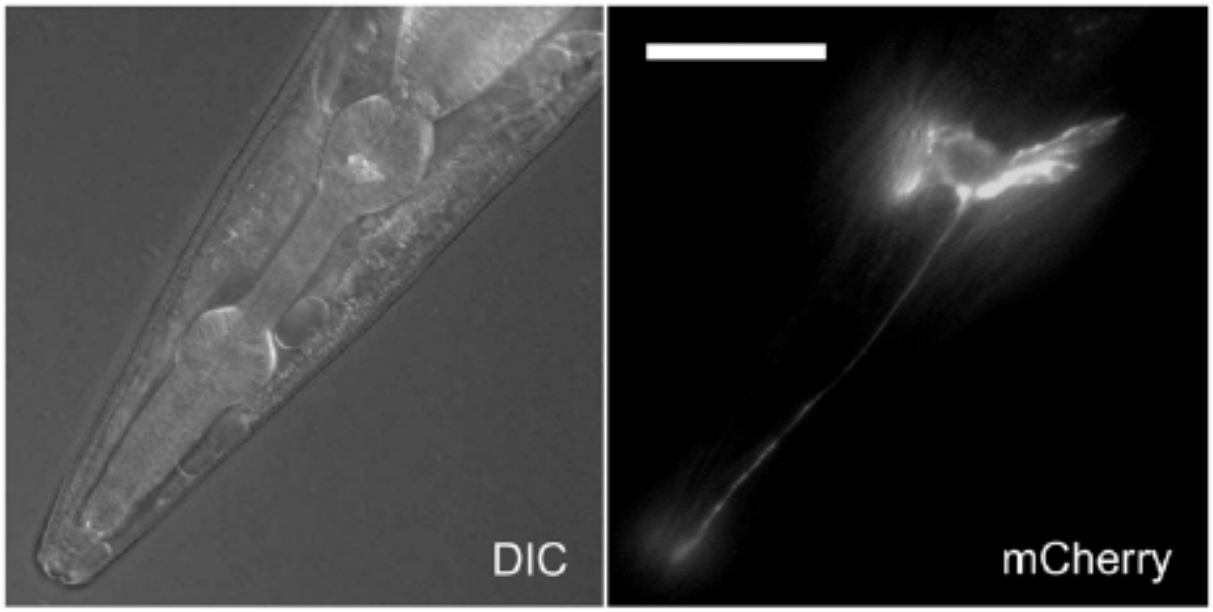

Figure 1. The location and basic cell morphology of cephalic sensilla sheet, CEPsh, glial cells in C. elegans.

Differential interference contrast (DIC) and fluorescence mCherry images obtained from an anterior tip of a worm in which cell specific expression of mCherry is driven by the *hlh-17* promoter with two out of the four CEPsh glial cell bodies visible. The cell bodies are surrounding the central nerve ring and the proximal section of the ventral nerve cord, with their processes, of which one is shown in the focal plane, emanating to the anterior

sensory tip. Texas Red filter set was used for visualization of mCherry. Scale bars, 50 μm. Images were acquired using an inverted microscope (IX71, Olympus) and 40 x oil immersion objective.

We have modified methods for general and neuronal *C. elegans* cell culture (Buechner et al. 1999; Christensen et al. 2002; Bianchi and Driscoll 2006; Strange et al. 2007) to grow and study CEPsh glial cells. We describe the use of the cell specific *hlh-17* promoter driving the expression of the genetically encoded intracellular red fluorescent marker mCherry and the green fluorescent cytosolic Ca^{2+} indicator GCaMP2.0 (Nakai et al. 2001), for identification of CEPsh glial cells in culture and for recording cytosolic Ca^{2+} dynamics. First, we describe the materials and procedures required to grow mixed embryonic cell culture using a transgenic worm strain carrying markers for glial cell identity. Then we provide a primer on recording intracellular Ca^{2+} dynamics in identified individual CEPsh glial cells in culture. The entire preparation of the materials for this procedure takes about four days given that the user already has the transgenic worm strain of interest. The actual cell culture preparation takes about five hours to complete, which includes a three hour incubation period.

Materials

Coverslip Preparation

1. Polyethyleneimine (PEI) 50 mg/mL stock solution. Commercially available 50% w/v PEI (500 mg/mL; cat. no. P-3143, Sigma-Aldrich) solution is diluted 1:10 in sterile water (see Note 3) to yield 50 mg/mL solution, which is sterile filtered through a 0.2 μm Nylon filter. This PEI stock solution can be stored for 4-6 weeks at 4^{o}C. Alternatively, it can be aliquoted in appropriate amounts (100 μL) and stored at -20^{o}C for up to 1 year.

2. Round glass coverslips (see Note 4), plastic Petri dishes (35 mm x 10 mm and 100 x 15mm), circular sterile filter paper (90 mm in diameter, qualitative, cat. no. 1005 090; Whatman), and UV sterilization lamp.

Transgenic C. elegans Propagation

1. A *C. elegans* strain with integrated mCherry and GCaMP2.0 transgenes in CEPsh glial cells driven by the *hlh-17* promoter (see Notes 5 and 6).

2. Nematode Growth Media (NGM) plates. Prepare potassium phosphate buffer by mixing 1 M KH_2PO_4 and 1 M K_2HPO4 until the solution reaches pH=6.0. To prepare NGM media (500 mL) add 10 g agar, 1.5 g $NaCl_2$, 0.72 g $CaCl_2$, 1.25 g peptone, 2 g D-glucose, 5 mL of 2 g/L uracil stock solution in water to 487 mL of water; autoclave, cool to less than 65ºC without solidifying and add sterile 12.5 mL of potassium phosphate buffer, 500 μL of 1 M $MgSO_4$, 500 μL of 5 mg/mL cholesterol stock solution in ethanol, and 500 μL of 200 mg/mL streptomycin sulfate. Mix the resulting melted, complete

NGM medium and pour it into Petri dishes (100 mm x 15 mm) just enough to fill their bottoms (about 2-4 mm thick). Let it cool down to solidify. Cover dishes with their lids. Dishes can be stored in a refrigerator at 4ºC for several weeks.

3. OP50 *E. coli.* Any standard liquid lysogeny broth (LB) media is needed to grow OP50 *E. coli*, which has no antibiotic resistance (see Note 7).

4. M9 buffer. Add 3 g KH_2PO_4, 6.2 g NaH_2PO_4, 5 g NaCl, and 1 mL of 1 M $MgSO_4$ stock in water to a graduated cylinder; dissolve in and top up to 1 L with water. Aliquot into appropriately sized bottles (500 mL) and autoclave. Store at room temperature (20-25ºC).

5. A zoom microscope (see Note 8).

Egg Shell Digestion, Embryo Isolation and Trituration

1. Worm Bleach Solution (WBS) composed of 7.5 mL water, 2 mL household bleach and 500 µL of 10 M NaOH. Make it fresh just before use.

2. Low adhesion 1.5 mL microcentrifuge tubes (Maxymum Recovery™, cat no. MCT-150-L-C; Axygen, Union City, CA).

3. Egg buffer solution (EBS) composed of (in mM): NaCl (118), KCl (48), $CaCl_2$ (2), $MgCl_2$ (2), and HEPES (25) in water; pH=7.3. Autoclave. Store at room temperature.

4. Chitinase (from *Onchocera volvulus)* (10,000 units/mL solution; Cat No. P5206S, New England Biosciences, Ipswich, MA). Store at -20ºC.

5. Zoom and inverted microscopes (see Note 9)

Cell Filtration and Plating

1. Cell culturing media. To make 100 mL of cell culturing medium mix 87 mL of Leibovitz's L-15 media (without phenol red; cat. no. 21083-027, Invitrogen Corp., Carlsbad, CA) with 1mL each of the following supplements: penicillin/streptomycin (stock solution 10,000 U/mL/10,000 µg/mL, cat. no. 25030-081, Invitrogen), D-glucose (2 M stock) and L-glutamine (200 mM stock, cat. no. 15140-122, Invitrogen). Bring this mixture to 335-345 mOsm/kg by adjusting the osmolarity with sucrose and sterile filter through a 0.22 µm pore polyethersulfone filter. Add 10 mL of sterile fetal bovine serum (Hyclone). Store at 4ºC until use.

2. A 5 µm pore size 25 mm in diameter syringe filter (Millex®-SV Low Protein Binding Durapore®, PVDF, cat. no. SLSV025LS, Millipore Corp. Bedford, MA) and a 3 mL syringe.

Intracellular Ca^{2+} Imaging and Cell Stimulation

1. An imaging chamber with a circular recess at its bottom to accommodate for mounting of a coverslip (see Note 10). The coverslip is sealed to the bottom of the chamber using

Dow Corning® High Vacuum Grease (Dow Corning Corporation, Midland, MI; distributed by Fisher Scientific, cat. no. 14-635-5D) (see Note 11).

2. External Solution. Prepare a saline solution containing (in mM): NaCl (145), KCl (5), $MgCl_2$ (1) $CaCl_2$ (2) and HEPES (10) in water, adjust osmolarity to 340 mOsm/kg with sucrose and pH=7.3. Filter through 0.2 μm filter and store at 4ºC. Immediately prior to use warm it to room temperature and add 5 mM D-Glucose (22.5 mg of glucose per 25 mL of solution) to complete the external solution.

3. 4-bromo-A23187 stock solution (20 mM in dry DMSO) (cat. no. B7272; Sigma-Aldrich). Store aliquoted (1-10 μL) at -20ºC (see Note 12).

4. An inverted microscope equipped with differential interference contrast (DIC) and epi-fluorescence illumination, 60 x oil immersion objective and selected filter sets. Standard Texas Red (TXR) and fluorescein isothiocyanate (FITC) filter sets are used for imaging mCherry and GCaMP2.0, respectively. A standard 4'6-diamidino-2-phenylindole (DAPI) filter set is used to assess possible autofluorescence artifacts.

5. A camera for image acquisition and a shutter inserted in the fluorescence light path for time-lapse acquisition; both devices are computer/software interfaced.

Methods

A standard method for culturing *C. elegans* cells developed by Christensen *et al.* (Christensen et al. 2002) uses all cells present in the embryo plated onto glass coverslips. The method described below is modified for ease of identification and culturing of *C. elegans* glial cells. We use the cell-specific expression of fluorescent markers for identification of CEPsh glial cell in culture, which is based on *hlh-17* gene promotor. This gene encodes a basic helix-loop-helix (bHLH) transcription factor with homology to the human *Olig1* and *Olig2* genes expressed in oligodendrocytes. *C. elegans* HLH-17 is most highly expressed in the four CEPsh glial cells along with low level expression in other cell types throughout development (McMiller and Johnson 2005; Yoshimura et al. 2008). The 2 kbp, 2.5 kbp and 2.7 kbp sequences 5' and extending into to the *hlh-17* gene have been shown to drive expression of various fluorescent protein reporters most brightly in the CEPsh glial cells in the embryo (see Notes 5 and 6).

Coverslip Preparation

1. Sterile technique needs to be used for coverslip preparation, which should be done in a laminar flow hood. Nine coverslips are needed for cell culture using worms grown on a single NGM plate (100 mm x 15 mm). Place nine coverslips onto a circular sterile filter paper (90 mm in diameter) inlayed into an inverted lid of the sterile 10 cm Petri dish with maximal spacing between them. Sterilize the coverslips and filter paper using UV lights.

2. Mix 100 µL of 50 mg/mL PEI stock solution with 4.9 mL of sterile water in a 15 mL plastic tube to obtain a 1 mg/mL PEI solution.

3. Apply 100 µL of 1 mg/mL PEI solution to each coverslip with care to avoid spilling the liquid off of the top of the coverslip and onto the filter paper. Cover inverted lids with their bottoms facing up. After the PEI solution has been on the coverslip for three hours, aspirate the solution and wash the top of the coverslip two times with autoclaved/sterile Milli-Q water and allow the water to rest on top of the coverslip for three more hours. Change the water and incubate it on the coverslip for three hours; repeat this step. After completion of two incubation periods, aspirate the water. If any minor residual water is present on coverslips, air dry them.

4. Using a stainless steel instrument such as a 5 mm flat-head screw driver, with the tip heated to glow by a Bunsen burner, emboss the bottom of 35 mm x10 mm Petri dishes to exhibit Y shape, or crossed, grooves to generate three or four segments. Sterilize dishes with UV light. Using tweezers, place 3 to 4 coverslips with the PEI coated surface up into each segment of the dish (see Notes 13 and 14).

Transgenic C. elegans Propagation

1. Grow OP50 *E. coli* strain overnight in a shaker incubator at 37ºC in 15 ml conical tube containing 5 mL of LB media. Apply 100 µL of resulting bacterial suspension onto each NGM plate (at room temperature). The bacterial suspension should be spread over most of the agar surface with a suitable sterile instrument to form a "lawn", but with limited or

no contact with the walls of the plate. The bacterial lawn is allowed to dry on the bench-top for 6-48 hours at room temperature (see Note 15).

2. Grow *C. elegans* on bacterial lawns at room temperature in normal air to expand and split the worm colony. When the OP50 *E. coli* lawn, which has creamy color appearance, is nearly completely consumed (24 to 72 hours at room temperature) on one NGM plate which gets densely populated with worms (see Note 16), it is washed with 500-800 µL of M9 solution (see Note 17). Recovered solution containing worms is placed in a 1.5 mL microcentrifuge tube and spun in a bench-top mini-centrifuge for 5 seconds. The volume of sedimented worms in the bottom of the tube should be between 30 and 100 µL. After removal of all but ~50 µL of the supernatant M9 solution, the worms are re-suspended and placed in equal amounts onto two unused NGM plates containing bacterial lawns (see Note 18).

3. Grow *C. elegans* on bacterial lawns for cell culturing. Once a majority of the worms have reached adulthood, displaying ~ 1mm in length with at least one line of eggs (Fig. 2A) and the bacterial lawn has been almost entirely consumed, the worms are washed with M9 solution into a single 1.5 mL low adhesion microcentrifuge tube as described in the previous step 2 (see Note 17) (Fig. 2B). The worms are spun for 5 seconds on a bench-top mini-centrifuge and at least 100 µL in volume of mostly gravid adults should be visible at the bottom as a beige mass with nearly clear M9 solution supernatant (not cloudy containing bacteria) should be present in the tube at this stage (see Note 19). The

worms are now ready to be lysed to release transgenic embryos growing within the egg shells.

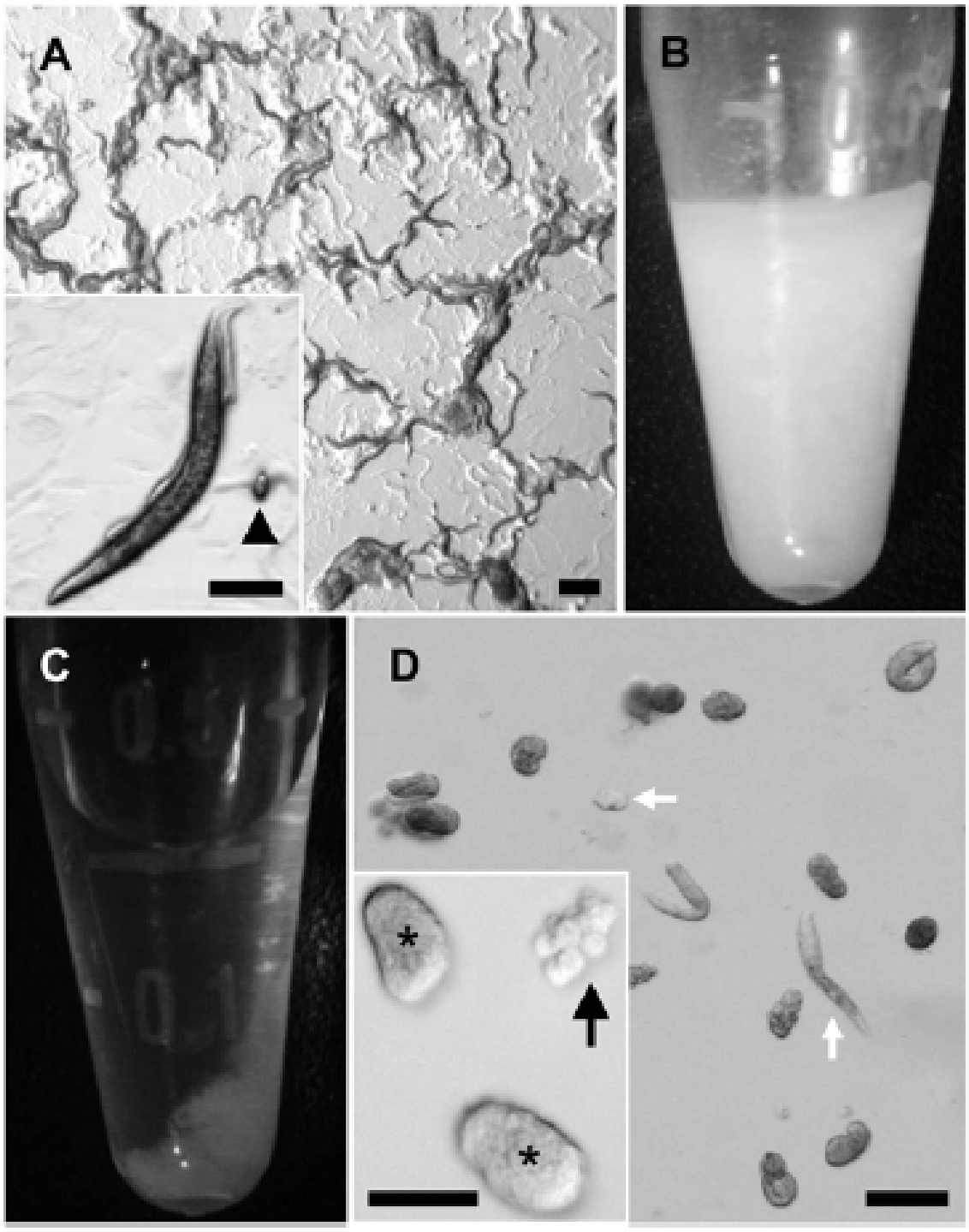

Figure 2. Isolation and digestion of C. elegans eggs.

A) Gravid adult worms grown on an agar plate at the stage/density appropriate for their use in cell culturing. Inset shows a large adult worm with eggs and embryos inside it. Arrowhead indicates a single egg that has already been laid. Scale bars, 500 μm and 250 μm in inset. B) Tube containing concentrated adult worms. C) Tube containing isolated egg mass at the bottom of the tube with clear supernatant. D) Images of a sample from an egg mass dispersion 1 hour after digestion with chitinase. The horizontal white arrow points to debris, while the vertical white arrow points to a hatched larva; they will be removed in the filtration step. Inset, higher magnification phase contrast image of embryos. Black arrow indicates an embryo with its eggshell completely digested. Asterisks mark embryos with partially digested eggshells evident from the fuzzy appearance of the border of the eggs. Scale bars, 100 μm and 50 μm in inset. A zoom microscope (MVX-10, Olympus) was used to acquire all images, except B, inset which was acquired using an inverted microscope (IX71, Olympus) and 20 x air objective.

Egg Shell Digestion, Embryo Isolation and Trituration

1. Remove the M9 solution supernatant above the beige worm mass prepared above. To lyse the worms add 1 mL of WBS and place the 1.5 mL tube on a rotisserie or secure it to an orbital shaker set to about one rotation per second. Check the appearance of the worms after five minutes and for every minute thereafter by briefly spinning down the tube content using the bench-top mini-centrifuge. If the supernatant becomes turbid and/or a tan-orange color then the WBS has lost potency and should be replaced by re-suspending the worms in 1 mL of fresh WBS. The lysis of the adult worms is complete when, upon

centrifugation, the precipitated mass is greatly diminished in volume (10-30 µL) and is uniformly white (not tan or brown) in color (Fig. 2C)(see Note 20). Remove the WBS and re-suspend the white mass in 1 mL of EBS. Inspect the resulting suspension under a zoom microscope. It should now contain almost entirely pure eggs which have a nearly ovoid shape, as seen on NGM plates containing gravid worms (Fig. 2A, inset). At this juncture, a few left over small worm debris will not hamper the success of cell culture.

2. From this point onward it is important to use sterile technique. Wash the egg mass two more times by re-suspending them in 500 µL of (sterile) EBS followed by brief (~5 second) centrifugation on a bench-top mini-centrifuge. After the eggs have been re-suspended and centrifuged twice, remove the supernatant and re-suspend the egg mass in 500 µL of EBS.

3. Add 2 µL (20 units) of chitinase enzyme solution to the suspension of *C. elegans* eggs in EBS, place the 1.5 mL tube on a rotisserie or secure to a slowly rotating orbital shaker at room temperature. Allow the chitinase to weaken the egg shell containing embryos for 1 hour.

4. Take out a small aliquot (~10 µL) and inspect under the zoom and inverted microscopes. The sample should contain mainly eggs, with their eggshells partially or completely digested; some debris and hatched larvae should be observed as well (Fig. 2D).

5. At this juncture, add 500 µL of complete culture media and additional 2 µL (20 units) of the chitinase to the 1.5 mL tube containing the chitinase-treated egg suspension. Incubate the mixture (~ 1 mL) in the 1.5 mL tube on the rotisserie or shaker for additional 30 minutes. During this incubation time you should perform steps 1 and 2 of the next section 3.4.

Cell Filtration and Plating

1. Apply 40 µL of compete complete culture media onto each of PEI-coated coverslip to prime/wet the surface.

2. Place two sterile 1.5 mL tubes in a tube rack. Remove the plunger from a 3 mL syringe, attach it to a 5 µm pore syringe filter, and then place this assembly vertically onto one of the empty 1.5 mL tubes with the filter tip inserted into the tube. Add 500 µL of complete culturing media to the syringe to wet the filter. Do not yet re-insert the plunger.

3. After completion of chitinase treatment, triturate the embryos and the eggs containing embryos 30 times at one stroke per second with a 1 mL sterile plastic barrier filter pipette tip using a 1 mL pipetter set to 500 µL with one edge of the pipette tip resting against the bottom of the tube. This step is necessary to break open the "softened" egg shells that have not been completely digested by chitinase and disperse embryonic cells. After trituration, the resulting suspension is applied into the syringe. Now is the time to re-insert the plunger and slowly apply pressure to it until the suspension has passed through

the filter. The collected liquid in the tube contains the suspension of dissociated embryonic cells, while debris and some embryonic cells are retained at the filter. At this juncture, unlock the filter from syringe, remove the plunger, and place the same filter back on the syringe and mount the assembly on the second 1.5 mL tube. Apply 500 µL of complete culturing medium to the syringe and push it through the filter into the tube. This step serves to recover some of the cells stuck in the filter.

4. Mix the contents of the two tubes containing filtered cells and then use a plastic barrier filter pipette tip to add 100 µL of this media-cell suspension to each wetted coverslip (see Note 21). Place the lids back on the Petri dishes without disrupting the droplets on top of the coverslips. Incubate the cells for 3-6 hours to allow their attachment to the PEI-coated coverslips (see Notes 22 and 23). After incubation, add 2 mL of complete culturing media to each dish to wash out cellular debris, aspirate the media and replace with 2 mL of fresh complete media. Store the dishes containing cells at room temperature in a humidified chamber/box in ambient air atmosphere, shielded from light and air currents (see Note 24). Culture media needs to be replaced every 4 days. Glial cells can be identified immediately upon plating, but we recommend allowing cells to recover for 48 hours before using them in experiments. Although cells can remain viable in culture for over 25 days, we recommend using them in experiments within 14 days of plating (see Note 1).

Intracellular Ca^{2+} Imaging and Cell Stimulation

1. Prepare a clean imaging chamber for the attachment of the coverslip. After placing the chamber up side down, apply a streak of sealing grease at the recess of the chamber. Using sterile forceps, take the coverslip containing cells out of culture media and place it centered onto the chamber recess with the cell-side facing towards the recess and slightly press it by forceps to loosely adhere coverslip to the grease. Flip the chamber so that the open bath faces up, while the coverslip is at the bottom. Press the chamber down against a Kimwipe™ to seal the coverslip (see Note 25). Add ~500 µL of external solution (room temperature) into the chamber. Check for leaks (see Notes 26 and 27). Aspirate the external solution, rinse the chamber with an additional 500 µL of external solution and replace it with 400 µL of external solution.

2. Place the chamber onto the inverted microscope and visualize using a 60 x plan-apochromatic oil immersion objective (see Notes 28 and 29).

3. Focus on cells using DIC (Fig. 3A). Identify CEPsh glial cell based on their mCherry fluorescence using TXR filter set (Fig. 3B). Using DIC observe their morphology. CEPsh glial cells in culture mainly have round morphology with their cells bodies ~ 5-10 µm in diameter (Fig. 3A) (see Note 30). Using the FITC filter set, observe GCaMP2.0 fluorescence (Fig. 3C) (see Note 31). Check autofluorescence of cells using DAPI filter set (Fig. 3D). CEPsh glial cells should have similar autofluorescence as other surrounding cells (see Note 32).

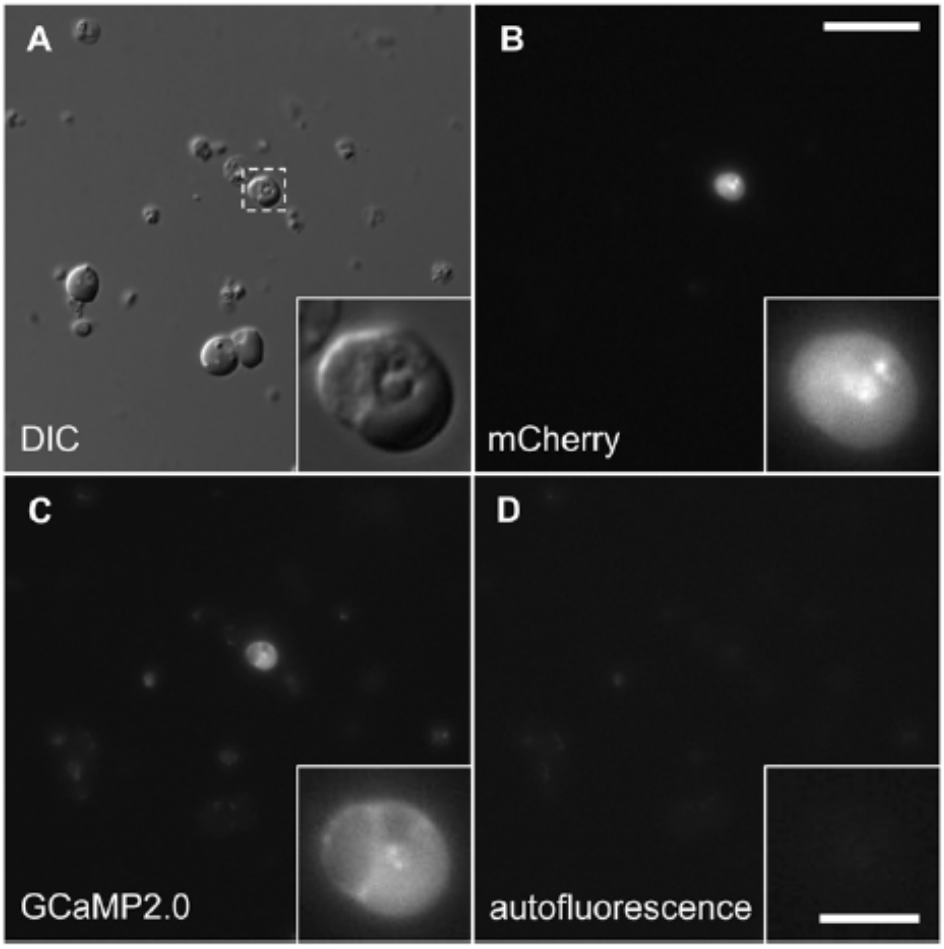

Figure 3. CEPsh glial cell culture.

A) DIC image of mixed embryonic cells in culture isolated from the worm strain VPR108 which has the CEPsh glial cell specific mCherry and GCaMP2.0 expression driven by the *hlh-17* promoter. B) A CEPsh glial cell is identified based on its mCherry (B, TXR filter set) and GCaMP2.0 (C, FITC filter set) fluorescence. D) CEPsh glial cell autofluorescence (DAPI filter set) is similar to other cell types in culture. Dashed boxed area in A, and corresponding unmarked areas in B-D, are shown enlarged in corner insets.

Scale bars, 20 μm and 5μm in insets. Images were acquired using an inverted microscope (IX71, Olympus) and 60 x oil immersion objective.

4. Prepare for the acquisition of intracellular Ca^{2+} dynamics. Bring the CEPsh glial cell of interest approximately into the center of the field of view and take single images in all channels (DIC, TXR, FITC, and DAPI) available. Using neutral density filters and camera integration time adjust the setup to produce images taken through the FITC filter set so that the average intensity in the recorded images from the cells is between 50 and 300 intensity units (i.u.; 14-bit pixel depth) above background before stimulation. Adjust the time interval between images (e.g., 4 seconds) and the duration of experiment/number of images (e.g., total of 21 images acquired for 80 seconds) to suit your experimental needs (Fig. 4A).

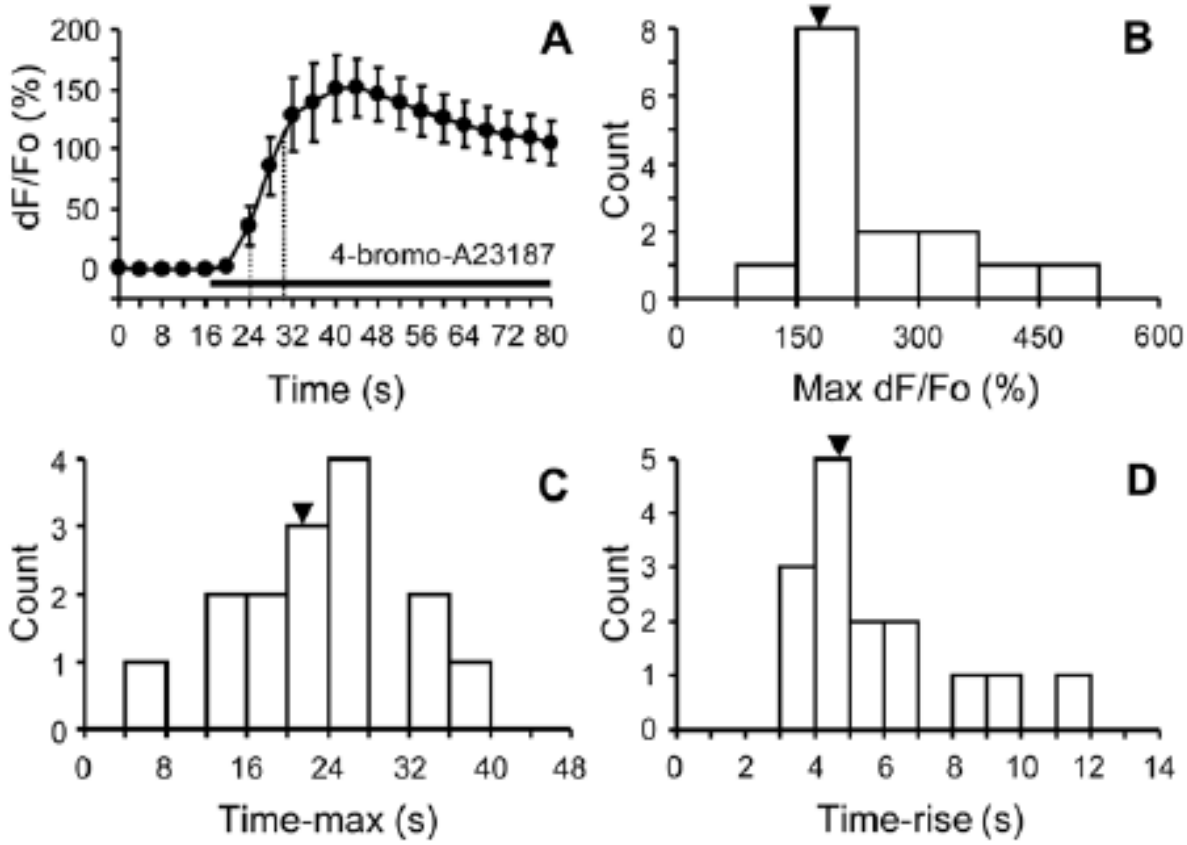

Figure. 4. Intracellular Ca^{2+} dynamics in cultured CEPsh glial cells expressing GCaMP2.0.

A) The bath application of 4-bromo-A23187 (horizontal bar, 20 μM) caused the expected sigmoid time-course of the increase in GCaMP2.0 fluorescence emission expressed as dF/Fo. B-D) Distributions of the maximum dF/Fo (Max dF/Fo; B), the time to reach the Max dF/Fo (Time-max; C) and the time to transition from 0.25 to 0.75 of the Max dF/Fo (Time-rise; D). Vertical dotted lines in A indicate the average times to reach 0.25 (left) and 0.75 (right) of the Max dF/Fo. Arrowheads in B-D indicate the mean values.

5. Initiate imaging sequence. Stimulate cells to increase their intracellular Ca^{2+} level using bath application (e.g., after acquisition of the 5^{th} image) of the Ca^{2+} ionophore 4-bromo-A23187 (20 μM final concentration) (Fig. 4A) (see Notes 33-34).

6. Process and analyze images using Metamorph™ or similar software. Obtain GCaMP2.0 fluorescence intensities from cell bodies of CEPsh glial cells which need to be subtracted by the background fluorescence obtained from regions of coverslips containing no cells (see Note 35-37).

7. Analyze and summarize data using Microsoft Excel XP. Express fluorescence data as dF/Fo (%) with the cell baseline fluorescence (Fo) representing the average of images (e.g., first 5 images) before the ionophore stimulation, while dF represents the change in fluorescence emission. Discard from further analysis data obtained from cells that display high baseline noise defined as dF/Fo which any point of baseline exceeded $\pm$ 15% of the Fo. Also discard the data if the pixel intensity reaches saturation of the camera (see Note 38). Plot the time-course of intracellular Ca^{2+} dynamics (Fig. 4A) and determine parameters, such as, the maximum (Max) dF/Fo, time to reach the Max dF/Fo (Time-max) and the rise time (Time-rise) needed to transition from 0.25 to 0.75 of the Max dF/Fo (Fig. 4B-D) (see Note 39)

Notes

1. One needs to be aware of the possibility that cells, especially with prolonged time, in culture can change their characteristics. For example, glial cells could de-differentiate.

Thus, it is essential that appropriate controls are executed, such as the confirmatory results from cells *in vivo* and freshly isolated cells, as described elsewhere for expression of, e.g., vesicular glutamate transporters in astrocytes (Montana et al. 2004; Ponzio et al. 2006). Another example is the change in morphology of astrocytes, which in culture obtain mainly polygonal shapes as their process-bearing/stellate shape found in tissue depends on the complex signaling mechanisms that involve both humeral factors and adhesion molecules (Cavanaugh et al. 1990; Sasaki and Endo 2000). The majority of neurons retain their polarization in culture, however. Thus, one needs to establish the prospect of using cell culture of each particular cell type when seeking the specific application.

2. For detailed morphology of the cephalic sensilla of *C. elegans* visit http://www.wormatlas.org/ver1/handbook/hypodermis/CEPimage%20gallery.htm web site.

3. Unless specifically indicated otherwise, in all procedures we used water purified by the Milli-Q® Synthesis system (Millipore Corp.; http://www.millipore.com/pressroom/cp3/5khpn7). This ultra-pure water has 18.2 MΩ*cm resistivity, less than 5 parts per billion (ppb) of organics content and pyrogen content less than 0.001 EU/mL.

4. We use borosilicate glass coverslips pre-tested for mammalian neural cell culture. These glass coverslips (thickness #1, 0.13-0.16 mm; D-263 glass, Erie Scientific

Company) can be purchased via Fisher Scientific (cat. no. 12-545-82-12CIR-1D). We clean them by placing the coverslips in 2% v/v RBS 35 (Pierce) detergent dispersion in water and boiling them for 15 min. Coverslips are then washed using running distilled water for 30 min and soaked in water (Milli-Q) overnight. To remove a possible detergent film retained on coverslips we dip them individually three times in water and air dried in a laminar flow hood. Here, the 90 mm in diameter circular filter paper is folded like an accordion into ~1 cm parallel folds and the coverslips are placed at a slanted angle onto the filter paper rested on a 100 mm in diameter Petri dish lid. This assembly serves as a make-shift drying rack for the coverslips, which as subsequently are stored in Petri dishes between sheets of filter paper. They are sterilized under UV light prior to coating. For UV sterilization we use the GS Gene Linker™ UV Chamber (Bio-Rad; Power set at Str, 2 x 90 s). Alternatively, one can use UV lamps in the laminar flow hood, but the duration of exposure needs to be adjusted according to the manufacturer's recommendation.

5. *C. elegans* transgenic strains can be produced using well-established methods described elsewhere (Berkowitz et al. 2008); an excellent compendium of such methods is available in the WormMethods section of the WormBook web site (http://wormbook.org/toc_wormmethods.html). We describe below the production of the VPR108 transgenic strain used throughout this chapter and available upon request. Plasmids used to produce the VPR108 transgenic strain contain the 2.5 kbps 5'of the translation start site of the *hlh-17*gene [as originally described in (McMiller and Johnson 2005)] copied from genomic DNA using a set of primers (forward, *hlh-17* BamHI:

ggccaggatccgaacagcttagctatttcgt; and reverse, *hlh-17* XmaI: ctttggccaatcccccgggtccatgactgg) and then inserted into the *C. elegans* vector pPD95.69 (A. Fire, S. Xu, J. Ahm, and G. Seydoux, personal communication; courtesy of A. Fire, Stanford University, Palo Alto, CA). This cloning plasmid was utilized for subsequent production of two expression plasmids, pRSFX4 and pRSRCRb, used for injection into worms. The construction of expression plasmids involved several intermediate steps. Therefore, the details are not included here; plasmids and their maps and sequences are available upon request. The plasmid pRSFX4 containing *Phlh-17*$_{2.5kbp}$::GCaMP2.0 was constructed using the InFusion2.0™ PCR cloning kit (Clontech, Mountain View, CA) using two sets of primers [GCaMP2.0 primers: *cagtcatggacccgggg*atgcggggttctcatcatcatcat (forward) and *cttgagctcgagat*ctctagagtcgcggccgctcac (reverse); and *hlh-17* primers: *gatctcgagctcaag*cttcgaattccaac (forward) and *ccgggtccatgactg*gggtgtaag (reverse)]. A mammalian expression vector [pN1-GCaMP2.0; kindly provided by J. Nakai, Saitama University Brain Science Institute, Saitama, Japan; (Tallini et al. 2006)] was used as a template for the GCaMP2.0 gene. The plasmid pRSRCRb contains the *Phlh-17*$_{2.5kbp}$ promoter driving transcription of mCherry with synthetic introns optimized for worm codons [the mCherry gene is a gift from K. Oegema, University of California, San Diego; (McNally et al. 2006)]. The plasmids pRSRCRb and pRSFX4 were injected into worms at 40 ng and 75 ng of DNA/µl, respectively, with TE buffer as a vehicle. Transgenes were genome integrated by gamma radiation. Obtained transgenic worms were backcrossed to wild type N2 worms four times.

6. The strain UL1713, available from the *Caenorhabditis* Genetics Center (CGC, University of Minnesota, Minneapolis, MN, www.cbs.umn.edu/CGC), expressing the *Phlh-17*$_{2kbp}$::Green Fluorescent Protein (GFP) (Grove et al. 2009), as well as a strain we made using the *Phlh-17*$_{2.7kbp}$::GFP construct [kindly provided by S. Shaham, Rockefeller University, New York, NY; (Yoshimura et al. 2008)], were also successfully used for culturing of CEPsh glial cells. Both 2 kbp and 2.7 kpb forms of the *hlh-17* promoter drove strong expression in the four CEPsh glial cells of live worms. We observed, as previously reported (McMiller and Johnson 2005), that the *hlh-17* promoter drove comparatively much dimmer expression in some cells in the tail region. This expression varied across and within transgenic strains. Naturally, the worms used for *C. elegans* propagation, and subsequent cell culturing, were selected for their lack of reporter expression in cells other than the CEPsh glial cells.

7. OP50 *E. coli* can be requested from the CGC. Alternatively, it can be isolated from plates containing worms received upon request.

8. A zoom microscope is needed at different stages of *C. elegans* propagation and preparation of cell cultures. We use the MVX-10 (Olympus) model, although more basic models, such as SMZ645 (Nikon) can be satisfactorily used.

9. Besides a zoom microscope (see Note 8), we also use an inverted microscope (IX71, Olympus) with phase contrast and 20x air objective to confirm egg shell digestion (Fig. 2D, inset).

10. We use a custom made open diamond bath imaging chamber with a circular recess at its bottom to accommodate for mounting of a coverslip (12 mm in diameter, thickness #1). Similar imaging chambers are commercially available (e.g., cat. no. RC-25 or RC-25, Warner Instruments).

11. We re-package the vacuum grease into a 3 mL syringe to which we attach a 1 cm long 18 gauge blunt needle. This hand held syringe/needle is used to apply the vacuum grease at the circular recess to the bottom of the chamber in order to attach the coverslip. Note that the grease displays fluorescent properties and should be used parsimoniously without smudging the bottom of the coverslip with it, which would occur if too much grease is applied.

12. To prepare dry dimethyl sulfoxide (DMSO) open an ampoule containing sterile, filtered DMSO (cat. no. D2650, Sigma-Aldrich) and pour it into a 15 mL conical centrifuge tube filled to the 2 ml level with molecular sieve beads (sodium alumino-silicate molecular sieves, 8-12 mesh beads, cat. no. M-2635, Sigma-Aldrich) to absorb water. Keep the tube tightly capped and wrapped in aluminum foil, as DMSO is hygroscopic and light sensitive. Store at room temperature. The beads are reusable. However, note that beads contain 15% of indicator blue beads that turn pink when saturated with water. At that juncture, they need to be replaced.

13. If dishes containing PEI-coated coverslips are not used immediately, their lids can be sealed with Parafilm© and then dishes can be stored in a sterile container for up to one week of PEI coating application. Do not expose these PEI coverslips/dishes to UV light as this polymer is sensitive to UV light.

14. It is cost-effective to have all segments within a Petri dish populated with PEI-coated coverslips as this allows reduced usage of culture media. However, the cell culture is also successful when number of coverslips is reduced from 3-4 to 2-3 coverslips per dish

15. The time that the bacterial lawn takes to dry depends primarily on how long it has been since the agar for NGM plates was poured. The thickness of the bacterial lawn at room temperature will increase over time and this can be accelerated by placing the plates at 37°C. NGM plates with bacterial lawns can be stored in containers at 4°C for several weeks, albeit with much retarded bacterial proliferation. Here, a thick lawn is desirable for *C. elegans* proliferation in order to produce the required volume of adult worms and in turn number of eggs needed for cell culturing.

16. The time that it takes for the worms to consume the bacterial lawn varies with its thickness, the number of worms, and the temperature.

17. More worms can be recovered if the bacterial lawn is completely consumed. To collect the worms into a 1.5 mL tube use 500-800 µL of M9 solution with 1 mL barrier

filter plastic pipette tips. Hold the plate at an ~30 degree angle from the horizontal and expel the M9 solution at an acute angle to the surface of the NGM. Aspirate the solution containing worms from the edge of the plate and pipette it into the 1.5 mL tube. Repeat washing the entire surface of the plate several times to recover as many worms as possible.

18. If the plates containing worms display fungal or non-OP50 *E. coli* bacterial contamination, the latter appears as a yellowish lawn discoloration, it will be difficult to collect enough worms to produce good cell culture. In addition this can be a source of contamination in the final cell culture. The worms can be bleached and the eggs transferred to a new plate (for bleaching see Methods Section 3.3; step 1). If there is an overwhelming fungal contamination nystatin (final concentration of 70 mg/mL) can be added to the NGM agar at the same point as the streptomycin sulfate solution. Nystatin containing NGM plates with bacterial lawns are then used to grow worms.

19. If the supernatant is cloudy, remove it and wash the worm pellet by re-suspending it in M9 solution followed by centrifugation. Repeat this procedure 3 times. If less than the required amount of worms is recovered, simply place all the worms recovered onto two unused 100 mm NGM plates with thick bacterial lawns. Allow the worms to grow for 48 hours or until the bacterial lawn is completely consumed, before using them for the cell culture preparation.

20. The 1.5 mL tube in which the worms are lysed needs to be monitored closely, since the treatment with WBS needs to be just long enough to lyze all of the worms without damaging the eggs. If the worms are not completely lysed during the egg isolation step with WBS, and too much left-over debris or entire worms are present, this can often result in contamination in culture dishes. Excessive incubation times in WBS, however, will damage the eggs and diminish the quality of the cell culture.

21. If a specific cell density is desired, the cells can be counted using a hemocytometer and their count adjusted by dilution or enrichment, the later by spinning them down (10 minutes at 100 x g) and then re-suspending in an appropriate volume.

22. During the incubation time cells should not be disturbed and should not be exposed to excessive vibration such as would occur if the dishes were left in the laminar flow hood with the fan turned on.

23. Coverslip preparation with peanut lectin and poly-L-lysine has been previously used for the culture of other *C. elegans* cell types including neurons (Christensen and Strange 2001; Carvelli et al. 2004; Estevez and Strange 2005; Frokjaer-Jensen et al. 2006). We have successfully grown *C. elegans* neurons on PEI-coated glass coverslips and obtained their morphological characteristics similar to those previously published (Christensen et al. 2002). We used *C. elegans* strain injected with *Pdat-1*::GCaMP2.0 vector [dat-1 promoter kindly provided by R. Blakely, Vanderbilt University, Nashville, TN; (Nass et al. 2002)], to express GCaMP2.0 in a subset of dopaminergic neurons

located in CEP. Neurons in culture were identified based on their GCaMP2.0 fluorescence, which along with DIC revealed that these neurons possess neurites, showing morphological features reminiscent of their appearance in live worms. Consequently, we used PEI-coated coverslips for CEPsh glial cell culture. Indeed, PEI has been used as a standard substrate for rat astrocytic and neuronal cell cultures (Montana et al. 2004; Figueiredo et al. 2011).

24. Evaporation of culture medium should be limited. This can be achieved by placing two 35 mm in diameter Petri dishes within one 100 mm in diameter Petri dish which contains cotton balls wetted with water. Larger Petri dishes can be sealed with Parafilm© and stored in a dark plastic box. The box can be additionally humidified using cotton swabs at the bottom. Alternatively, the bottom of the box can be filled with water, above which an elevated grid is installed that serves for stacking of Petri dishes. One should add some fungicide (e.g., Physan 20) to the water bath or to water used to wet cotton swabs.

25. When pressing the coverslip attached to the imaging chamber against the Kimwipe™ make sure that you place the wipe on a clean flat surface and that you do not apply too much pressure, otherwise the coverslip can crack. If you crack the coverslip, replace it, after cleaning the chamber and re-applying the grease.

26. By initially placing the chamber-coverslip assembly on the Kimwipe™ you will notice some wetting of the wipe, because some of the culturing media will be retained at

the bottom surface of the coverslip. Subsequently, lift up and place the whole assembly onto a different spot of the wipe. Leaks are easily recognized, as the chamber will quickly empty to wet the wipe.

27. Regardless of whether the chamber leaks or not, after pressing the assembly against the wipe, you may also notice a circular grease imprint on the wipe. If any, this should be minimal. If in excess, next time mount the coverslip with somewhat less grease, but not an insufficient amount necessary for sealing. Do not slide the assembly across the wipe at any time as you will cause smudging of the grease onto the coverslip. This will affect the quality of images since: i) the grease does not mix with the oil used on the objective and hence it would generate the distortion of images, and ii) the grease fluoresces and thus increases the background.

28. We place our microscopes on anti-vibration isolation tables. *C. elegans* cells (~ 5-10 μm in diameter) are smaller than mammalian glial cells, and we find this approach necessary in order to prevent possible movement artifacts.

29. The images of cells in culture presented herein were acquired using an inverted microscope (IX71, Olympus) equipped with DIC and epifluorescence illumination (Xenon Arc lamp, 100 W). We visualized cells through a 60x plan-achromatic oil-immersion TIRFM objective (numerical aperture, 1.45; Olympus) and acquired images using a cooled CCD (charged-coupled device) camera (CoolSNAP HQ^2; Photometrics, Tucson, AZ) driven by V++ imaging software (Digital Optics, Auckland, New Zealand)

or MetaMorph™ software (Molecular Devices, Chicago, IL). For time-lapse image acquisition, we inserted into the excitation pathway an electronic shutter (Vincent Associates) controlled by imaging software/camera. The microscope was fitted with a manually operated slider inserted in the excitation pathway that contained a set of neutral density filters. Visualization of GCaMP2.0 fluorescence was done using a standard FITC filter set (Olympus), while a TXR filter set (Olympus) was used to image mCherry. We used a standard DAPI filter set (Olympus) to assess the autofluorescence of *C. elegans* cells. All images displayed in figures represent raw data with their pixel intensities (14-bit depth) within the camera's dynamic range (0-16383 intensity units, i.u.).

30. CEPsh glial cells have long specialized membrane extensions toward the anterior extreme of the intact animal (Fig. 1). In culture, however, they show mainly round shapes (Fig. 3). We have rarely observed CEPsh glial cells to have short membrane processes, less than 15 μm in length, which sometimes branched. However, CEP neurons in our culture readily adopted a polarized morphology similar to that seen *in vivo* (*see* Note 23). CEPsh glial cells and CEP neurons in culture displayed similar cell body size.

31. Although both mCherry and GCaMP2.0 should mainly appear in the cytosol, their intracellular expression slightly differs. GCaMP2.0 appears diffusely in the cytoplasm (Fig. 3C, inset), while mCherry usually displays 2-3 bright puncta around the nucleus, perhaps as some of it might be stuck in the endoplasmic reticulum (Fig. 3B, inset).

32. Some cell types in culture have stronger auto-fluorescence than others. By switching between the TXR, FITC and DAPI filter sets, non-specific fluorescence can be easily distinguished (Fig. 3). Note that images acquired using the FITC filter set show lower signal-noise ratio than those obtained using the TXR filter set (compare Fig. 3 C and B, respectively).

33. We obtained similar results as those reported in Fig. 4A when instead of the bath application we used a pressure ejection of 4-bromo-A23187 (20 μM, 80 s) from a puffer pipette (~70 kPa) onto CEPsh glial cells, as we described elsewhere for drug delivery to cultured astrocytes (Malarkey et al. 2008).

34. The application of a Ca^{2+} ionophore is a non-recovery treatment for the cell. The stand-alone application of a Ca^{2+} ionophore is used for defining the characteristics of the intracellular Ca^{2+} exogenous indicator and endogenous buffers. Consequently, such an approach assesses the appropriateness of the intracellular Ca^{2+} indicator amount. An excess of the intracellular Ca^{2+} indicator can cause buffering and result in spatio-temporal artifacts (Bolsover and Silver 1991). A Ca^{2+} ionophore can also be used as an experimental stimulus that by-passes the activation of ligand-, voltage-, light- or mechanically-gated channels (Hua et al. 2004). Unless used as a stand-alone treatment, an ionophore should be used at the end of experiments measuring intracellular Ca^{2+} dynamics in response to various stimuli, so that, if needed, responses could be normalized to their respective maximal response to the ionophore. The Ca^{2+} ionophore induced Ca^{2+} dynamics can be then used as a criterion for data management (see Note 38).

Furthermore , Ca^{2+} ionophores are used for *in situ* calibration of Ca^{2+} indicators to obtain intracellular Ca^{2+} concentration (in nM) (Thomas and Delaville 1991).

35. Here, we used a single-wavelength imaging of GCaMP2.0 to measure intracellular Ca^{2+} dynamics due to stimulation with a Ca^{2+} ionophore. Since CEPsh glial cells also express mCherry, one can use the dual-wavelength ratiometric approach by expressing the change in GCaMP2.0 fluorescence, reporting on intracellular Ca^{2+} levels and possible other events, to changes in mCherry fluorescence, reporting on Ca^{2+} (un)related biological or technical events. For example, movement artifacts can affect Ca^{2+} imaging in cultured cells. They could be caused by the change in cells shape as a result of the increase in intracellular Ca^{2+} and/or mechanical instability during recordings. Of course, a ratiometric approach would be necessary if recordings of intracellular Ca^{2+} dynamics from cells of freely moving worms are desirable. A detailed description of single-/dual-wavelength approaches in intracellular Ca^{2+} imaging are available elsewhere (Thomas and Delaville 1991).

36. New forms of genetically encoded Ca^{2+}indicators are being developed and may give better results through improved dynamic range, decreased cytotoxicity and/or simply could be better suited for the particular application (Tian et al. 2009).

37. Chemically based Ca^{2+} indicators such as Fluo-4 have been used in other *C. elegans* cell types (Estevez and Strange 2005). They could prove to be useful for studies in CEPsh glial cells, although a fluorescently compatible genetically encoded reporter

(e.g., mCherry) would still need to be used to identify CEPsh glial cells in the mixed culture.

38. Using a 14-bit camera (dynamic range 0-16383 i.u.) and GCaMP2.0, with its initial Fo set at 50-300 i.u. after background subtraction, we have not encountered any pixel saturation. Similarly, using a 12-bit camera (dynamic range 0-4095 i.u.) and same initial Fo, there should be no saturation issue given the recorded Max F/Fo values for GCaMP2.0 expressing CEPsh glial cells (Fig. 4A, and see Note 39). However, for cameras with lower pixel depth, such as an 8-bit depth (dynamic range 0-255 i.u.), the initial Fo should be set at 50-75 i.u. after the background (~10 i.u.) subtraction, and some saturation should be expected.

39. Cultured CEPsh glial cells (n=15) expressing GCaMP2.0, when treated by the bath application of 4-bromo-A23187 (20 μM), displayed the expected sigmoid time-course of the increase in GCaMP2.0 fluorescence emission (Fig. 4A), consistent with previous reports dealing with GCaMP2.0 (Nakai et al. 2001; Chalasani et al. 2010). The maximum response (Max dF/Fo= 179 $\pm$ 102%; mean $\pm$ SD) was reached within the time (Time-max) of 21.1 $\pm$ 8.5 seconds after the addition of the ionophore (Fig. 4 B and C, respectively). A part of the sigmoid time-course response within the range between 0.25 and 0.75 of the Max dF/Fo is considered linear (Fig. 4A, the part between two dotted vertical lines). It can be used to determine the time it takes for GCaMP2.0 fluorescence increase to transition from 0.25 to 0.75 of the Max dF/Fo, referred to as the rise time (Time-rise), which for CEPsh glial cells clocked at 4.7 $\pm$ 2.5 seconds (Fig. 4D). The

above kinetics parameters are useful for characterization of GCaMP2.0 responses within *C. elegans* CEPsh glial cells. We obtained similar intercellular Ca^{2+} dynamics for somata of CEP neurons in culture (n=4), isolated from the *Pdat-1*::GCaMP2.0 worm stain (see Notes 23 and 30), when treated with 4-bromo-A23187. The above kinetics parameters can also be used for data inclusion/exclusion when testing CEP cells intracellular Ca^{2+} response to various stimuli. For example, cells that display Time-rise and/or Time-max values longer than the average times with the addition of their respective 2SDs could be buffering intracellular Ca^{2+} increase due to over-expression of GCaMP2.0. Similarly, buffering could be evidenced as an individual cell Max dF/Fo value being lower than the value for Max dF/Fo subtracted by 2SDs. Given that the stimulus preceding the application of the ionophore caused a transient intracellular Ca^{2+} response that recovered to the baseline, all above parameters can be used for data management. However, if the stimulus caused a sustained elevated response, which is still in effect when the ionophore is subsequently added, then it is highly likely that the only useful parameter for the data management would be the Max dF/Fo.

Acknowledgements

We would like to thank Dr. Morris Maduro for all help with starting up the *C. elegans* research in our laboratory. We thank William Lee for some assistance with imaging and Dr. Gina Broitman-Maduro for practical training on production of transgenic worm strains. Some nematode strains used in this work were provided by the *Caenorhabditis* Genetics Center, which is funded by the NIH National Center for Research Resources

(NCRR). This work was supported by the National Science Foundation (CBET 0943343).

References

Bacaj T, Tevlin M, Lu Y, Shaham S. 2008. Glia are essential for sensory organ function in C. elegans. *Science* **322**: 744-747.

Barr MM. 2003. Super models. *Physiol Genomics* **13**: 15-24.

Berkowitz LA, Knight AL, Caldwell GA, Caldwell KA. 2008. Generation of stable transgenic C. elegans using microinjection. *J Vis Exp*: pii: 833. doi: 810.3791/3833.

Bianchi L, Driscoll M. 2006. Culture of embryonic C. elegans cells for electrophysiological and pharmacological analyses. *WormBook*: 1-15.

Bolsover S, Silver RA. 1991. Artifacts in calcium measurement: recognition and remedies. *Trends Cell Biol* **1**: 71-74.

Buechner M, Hall DH, Bhatt H, Hedgecock EM. 1999. Cystic canal mutants in Caenorhabditis elegans are defective in the apical membrane domain of the renal (excretory) cell. *Dev Biol* **214**: 227-241.

Carvelli L, McDonald PW, Blakely RD, Defelice LJ. 2004. Dopamine transporters depolarize neurons by a channel mechanism. *Proc Natl Acad Sci U S A* **101**: 16046-16051.

Cavanaugh KP, Gurwitz D, Cunningham DD, Bradshaw RA. 1990. Reciprocal modulation of astrocyte stellation by thrombin and protease nexin-1. *J Neurochem* **54**: 1735-1743.

Chalasani SH, Kato S, Albrecht DR, Nakagawa T, Abbott LF, Bargmann CI. 2010. Neuropeptide feedback modifies odor-evoked dynamics in Caenorhabditis elegans olfactory neurons. *Nat Neurosci* **13**: 615-621.

Christensen M, Estevez A, Yin X, Fox R, Morrison R, McDonnell M, Gleason C, Miller DM, 3rd, Strange K. 2002. A primary culture system for functional analysis of C. elegans neurons and muscle cells. *Neuron* **33**: 503-514.

Christensen M, Strange K. 2001. Developmental regulation of a novel outwardly rectifying mechanosensitive anion channel in Caenorhabditis elegans. *J Biol Chem* **276**: 45024-45030.

Cornell-Bell AH, Finkbeiner SM, Cooper MS, Smith SJ. 1990. Glutamate induces calcium waves in cultured astrocytes: long-range glial signaling. *Science* **247**: 470-473.

Estevez AY, Strange K. 2005. Calcium feedback mechanisms regulate oscillatory activity of a TRP-like Ca2+ conductance in C. elegans intestinal cells. *J Physiol* **567**: 239-251.

Figueiredo M, Lane S, Tang F, Liu BH, Hewinson J, Marina N, Kasymov V, Souslova EA, Chudakov DM, Gourine AV et al. 2011. Optogenetic experimentation on astrocytes. *Exp Physiol* **96**: 40-50.

Frokjaer-Jensen C, Kindt KS, Kerr RA, Suzuki H, Melnik-Martinez K, Gerstbreih B, Driscol M, Schafer WR. 2006. Effects of voltage-gated calcium channel subunit genes on calcium influx in cultured C. elegans mechanosensory neurons. *J Neurobiol* **66**: 1125-1139.

Grove CA, De Masi F, Barrasa MI, Newburger DE, Alkema MJ, Bulyk ML, Walhout AJ. 2009. A multiparameter network reveals extensive divergence between C. elegans bHLH transcription factors. *Cell* **138**: 314-327.

Heiman MG, Shaham S. 2007. Ancestral roles of glia suggested by the nervous system of Caenorhabditis elegans. *Neuron Glia Biol* **3**: 55-61.

Hua X, Malarkey EB, Sunjara V, Rosenwald SE, Li WH, Parpura V. 2004. Ca2+-dependent glutamate release involves two classes of endoplasmic reticulum Ca2+ stores in astrocytes. *J Neurosci Res* **76**: 86-97.

Malarkey EB, Ni Y, Parpura V. 2008. Ca2+ entry through TRPC1 channels contributes to intracellular Ca2+ dynamics and consequent glutamate release from rat astrocytes. *Glia* **56**: 821-835.

McMiller TL, Johnson CM. 2005. Molecular characterization of HLH-17, a C. elegans bHLH protein required for normal larval development. *Gene* **356**: 1-10.

McNally K, Audhya A, Oegema K, McNally FJ. 2006. Katanin controls mitotic and meiotic spindle length. *J Cell Biol* **175**: 881-891.

Montana V, Ni Y, Sunjara V, Hua X, Parpura V. 2004. Vesicular glutamate transporter-dependent glutamate release from astrocytes. *J Neurosci* **24**: 2633-2642.

Nakai J, Ohkura M, Imoto K. 2001. A high signal-to-noise Ca2+ probe composed of a single green fluorescent protein. *Nat Biotechnol* **19**: 137-141.

Nass R, Hall DH, Miller DM, 3rd, Blakely RD. 2002. Neurotoxin-induced degeneration of dopamine neurons in Caenorhabditis elegans. *Proc Natl Acad Sci U S A* **99**: 3264-3269.

Parpura V, Basarsky TA, Liu F, Jeftinija K, Jeftinija S, Haydon PG. 1994. Glutamate-mediated astrocyte-neuron signalling. *Nature* **369**: 744-747.

Ponzio TA, Ni Y, Montana V, Parpura V, Hatton GI. 2006. Vesicular glutamate transporter expression in supraoptic neurones suggests a glutamatergic phenotype. *J Neuroendocrinol* **18**: 253-265.

Sasaki T, Endo T. 2000. Both cell-surface carbohydrates and protein tyrosine phosphatase are involved in the differentiation of astrocytes in vitro. *Glia* **32**: 60-70.

Shaham S. 2006. Glia-neuron interactions in the nervous system of Caenorhabditis elegans. *Curr Opin Neurobiol* **16**: 522-528.

Strange K, Christensen M, Morrison R. 2007. Primary culture of Caenorhabditis elegans developing embryo cells for electrophysiological, cell biological and molecular studies. *Nat Protoc* **2**: 1003-1012.

Tallini YN, Ohkura M, Choi BR, Ji G, Imoto K, Doran R, Lee J, Plan P, Wilson J, Xin HB et al. 2006. Imaging cellular signals in the heart in vivo: Cardiac expression of the high-signal Ca2+ indicator GCaMP2. *Proc Natl Acad Sci U S A* **103**: 4753-4758.

Thomas A, Delaville F. 1991. The use of fluorescent indiciators for measurements of cytosolic-free calcium concentration in cell populations and single cells. in

Cellular Calcium (eds. J McCormack, P Cobbold). Oxford University Press, Oxford, UK.

Thomas JH. 1994. The mind of a worm. *Science* **264**: 1698-1699.

Tian L, Hires SA, Mao T, Huber D, Chiappe ME, Chalasani SH, Petreanu L, Akerboom J, McKinney SA, Schreiter ER et al. 2009. Imaging neural activity in worms, flies and mice with improved GCaMP calcium indicators. *Nat Methods* **6**: 875-881.

Ward S, Thomson N, White JG, Brenner S. 1975. Electron microscopical reconstruction of the anterior sensory anatomy of the nematode Caenorhabditis elegans.?2UU. *J Comp Neurol* **160**: 313-337.

Yoshimura S, Murray JI, Lu Y, Waterston RH, Shaham S. 2008. mls-2 and vab-3 Control glia development, hlh-17/Olig expression and glia-dependent neurite extension in C. elegans. *Development* **135**: 2263-2275.

VOLTAGE-GATED CALCIUM CHANNEL TYPES IN CULTURED *C. ELEGANS* CEPSH GLIAL CELLS

RANDY F STOUT JR., VLADIMIR PARPURA

Cell Calcium 50(1):98-108

CHAPTER 3

VOLTAGE-GATED CALCIUM CHANNEL TYPES IN CULTURED *C. ELEGANS* CEP_{SH} GLIAL CELLS

Abstract

The four cephalic sensilla sheath (CEPsh) glial cells are important for development of the nervous system of *C. elegans.* Whether these invertebrate glia can display intracellular Ca^{2+} dynamics, a hallmark of mammalian glial cells excitability, is not known. To address this issue, we developed a transgenic worm with the specific co-expression of genetically encoded red fluorescent protein and green Ca^{2+} sensor in CEPsh glial cell. This allowed us to identify CEPsh cells in culture and monitor their Ca^{2+} dynamics. We show that CEPsh glial cells, in response to depolarization, exhibit variousCa^{2+} dynamics mediated by voltage-gated Ca^{2+} channels (VGCCs). Using a pharmacological approach, we find that the L- type is the preponderant VGCC type mediating Ca^{2+} dynamics. Additionally, using a genetic approach we demonstrate that mutations in three known VGCC α_1-subunit genes, *cca-1, egl-19* and *unc-2*, can affect Ca^{2+} dynamics of CEPsh glial cells. We suggest that VGCC-mediated Ca^{2+} dynamics in the CEPsh glial cells are complex and display heterogeneity. These findings will aid understanding of how CEPsh glial cells contribute to the operation of the *C. elegans* nervous system.

Keywords: *C. elegans*, calcium dynamics, invertebrate glia, voltage-gated calcium channels.

Introduction

With only 302 neurons and 50 glial cells in its nervous system, *C. elegans* has served as a major model organism for neurobiological research. The simplicity of the *C. elegans* nervous system, along with its almost morphologically identical appearance between individual worms, allowed reconstruction at the ultrastructural level with mapping locations of individual synapses (Ward et al. 1975; White et al. 1976; Hall and Russell 1991). Only recently, however, *C. elegans* has emerged as an invertebrate model for studying glial cells [reviewed in (Oikonomou and Shaham 2011)]. A subset of glial cells in *C. elegans*, the sheath glia of the cephalic sensilla (CEPsh glia), display some anatomical and functional characteristics that parallel those of astrocyte and oligodendrocyte lineages in the mammalian nervous system [reviewed in (Oikonomou and Shaham 2011)].

Protoplasmic astrocytes occupy distinct domains within the mammalian central nervous system (CNS), parceling the grey matter, through a process referred to as "tiling", into more or less independent structural units (Bushong et al. 2002; Ogata and Kosaka 2002). Within their individual domains astrocytes have extensive morphological interactions with neurons. In rodents, astrocytes may contact 4 to 8 neurons and surround ~20,000-120,00 synapses (Bushong et al. 2002; Halassa et al. 2009), while a human astrocyte, due to its territorial expansion, integrates over ~2 million synapses. At synapses, astrocytes bi-directionally communicate to neurons leading to the concept of a functional tripartite synapse (Araque et al. 1999). This communication requires increases in astrocytic intracellular Ca^{2+} concentration $[Ca^{2+}]_i$, which can display various

spatiotemporal patterns, including oscillatory, intermediate and sustained temporal changes [reviewed in (Parpura et al. 1994; Hanisch and Kettenmann 2007)].

Oligodendrocytes, the second major class of mammalian neuroglia, are pivotal for the establishment and maintenance of structure and function of white matter. Oligodendrocytes actively and bi-directionally communicate with neurons to achieve a precise information transfer via long axonal processes [reviewed in (Fields 2008)]. Such oligodendroglia-neuron interactions are developmentally regulated. Intracellular Ca^{2+} signaling has been implicated in oligodendrocyte membrane sheet retractions (Benjamins and Nedelkoska 1996), and process extension (Yoo et al. 1999) of these glial cells and their precursor cells (OPC) (Fulton et al. 2010).

Similarly to astrocytes, the four CEPsh glial cells of *C. elegans* engulf the nerve ring with non-overlapping membrane extensions. The nerve ring is density populated with synaptic contacts established between sensory neurons, interneurons and motor neurons. Additionally, CEPsh glial cells send a long anterior process that closely interacts with the dendritic extension of the CEP neuron. Indeed, the ablation of CEPsh glial cells results in axon guidance defects (Yoshimura et al. 2008). CEPsh glial cell development has similarities with some aspects of mammalian oligodendrocyte lineage differentiation. *C. elegans hlh-17* gene which encodes a basic helix-loop-helix transcription factor has homology to the human *Olig1* and *Olig2* genes expressed in oligodendrocytes (McMiller and Johnson 2005; Yoshimura et al. 2008). HLH-17 is most highly expressed in the four CEPsh glial cells. Although CEPsh glial cells possess morphology and functional attributes reminiscent of their mammalian "cousins", whether

CEPsh glial cells can exhibit a hallmark of mammalian glial cells excitability, the intracellular Ca^{2+} dynamics/changes has not been determined, yet.

Astrocytes, oligodendrocytes and OPCs can respond to depolarization with Ca^{2+}-mediated currents that require activity of voltage-gated Ca^{2+} channels (VGCCs) [for reviews see (D'Ascenzo et al. 2004; Seifert and Steinhäuser 2004; Paez et al. 2009; Yaguchi and Nishizaki 2010)]. *C. elegans* possess three known genes encoding VGCC α_1 subunits, *egl-19*, *cca-1*, and *unc-2,* expression of which contributes to VGCC properties corresponding to L- , T-, and N, P/Q, R- type, respectively (Lee et al. 1994; Schafer and Kenyon 1995; Shtonda and Avery 2005). We sought to understand whether the CEPsh glial cells display intracellular Ca^{2+}dynamics due to depolarization. To address this issue, we generated transgenic worms expressing the genetically encoded fluorescent cytosolic Ca^{2+} indicator GCaMP2.0 solely in four CEPsh glial cells, from the embryo through adulthood. We prepared transgenic *C. elegans* cell culture, which allowed us to apply a depolarizing stimulus to CEPsh glial cells apart from the tangle of neurons, and muscle cells in which they exist *in vivo*. Using a combination of acute pharmacological and chronic genetic approaches, we present evidence for a functional role of all three known VGCCs in various aspects of CEPsh glial cell intracellular Ca^{2+} dynamics. The future work will need to investigate whether such intracellular Ca^{2+} dynamics in CEPsh glial cells can affect neuronal activity and exhibit influences on behavior.

Materials and methods

C. elegans Strains

All worms used in this study were derived from the parental transgenic strain VPR108 co-expressing the genetically encoded intracellular red fluorescent marker mCherry and the green fluorescent cytosolic Ca^{2+} indicator GCaMP2.0 solely in four CEPsh glial cells, from the embryo through adulthood. We described the production of this transgenic stain in detail elsewhere (Stout and Parpura 2011a). Briefly, plasmids used to generate the VPR108 strain contained the 2.5 kbps 5'of the translation start site of the *hlh-17*gene [as originally described in (McMiller and Johnson 2005)] copied from genomic DNA. This promoter (*Phlh-17*) was used for construction of *Phlh-17*::mCherry and *Phlh-17*::GCaMP2.0 plasmids and to drive transcription of genes encoding mCherry [gift from K. Oegema, University of California, San Diego; (McNally et al. 2006)] or GCaMP2.0 [kindly provided by J. Nakai, Saitama University Brain Science Institute, Saitama, Japan; (Tallini et al. 2006). We micro-injected the wild-type *C. elegans* variety Bristol, strain N2 worms with these plasmids and the resulting transgene array (*vprEx108*) was integrated with gamma irradiation. Worms with the integrated array (*vprIs108)* were back-crossed to the N2 worms four times producing the VPR108 strain, which was then used as a background line to cross with the following mutant strains received from the Caenorhabditis Genetics Center (University of Minnesota, Minneapolis, MN, www.cbs.umn.edu/CGC): i) L- type voltage-gated Ca^{2+} channel (VGCC) α_1 subunit reduction-of-function (*rf*) mutant DA1006 *egl-19(ad1006) IV*, ii) T- type VGCC α_1 subunit partial deletion knock-out (KO) VC39 *cca-1* (*gk30*) X, and iii) N, P/Q, R- type VGCC α_1 subunit truncation KO CB55 *unc-2 (e55) X*. All worms were grown on

nematode growth medium (NGM) plates (Brenner et al. 1994) at room temperature (~20 ºC) and fed with OP-50 *E. coli* .

Cell Culture

We prepared *C. elegans* cell culture using a modification (Stout and Parpura 2011a) of the originally described procedure (Christensen and Strange 2001). We used the cell-specific expression of fluorescent markers based on the *hlh-17* gene promoter for identification of CEPsh glial cells in culture. Briefly, NGM plates containing mainly gravid adult worms were rinsed with M9 solution containing (in mM): KH_2PO_4 (22 mM), NaH_2PO_4 (40 mM), NaCl (86) and $MgSO_4$ (1) in water. Collected worms were spun (bench-top mini-centrifuge, 5 seconds) and treated with hypochlorite solution (20% v/v household bleach and 80% v/v of 625 mM NaOH in water) on a rotisserie mixer to obtain eggs. Following centrifugation (bench-top mini-centrifuge, 5 s), the resulting egg mass was resuspended in egg buffer solution (EBS) containing (in mM): NaCl (118), KCl (48), $CaCl_2$ (2), $MgCl_2$ (2), and HEPES (25) in water; pH=7.3. The eggs were enzymatically treated with chitinase (40 U/mL; from *Onchocera volvulus*, New England Biosciences, Ipswich, MA) for ~ 1 hour to release the majority of embryos. At this juncture the embryos and the "uncracked" eggs were triturated to obtain a cellular suspension, which was filtered through a 5 μm pore size syringe filter (Millex®-SV Low Protein Binding Durapore®, Millipore Corp. Bedford, MA) to elute cells and remove larger debris. The resulting filtered cells in EBS were diluted with complete culturing media in 1:1 ratio, and plated onto polyethyleneimine (PEI, 1 mg/mL)-coated round (12 mm in diameter) coverslips. The complete culturing media was composed of Leibovitz's L-15 media

(without phenol red; cat. no. 21083-027, Invitrogen Corp., Carlsbad, CA), supplemented with fetal bovine serum (10 % v/v; Thermo Scientific HyClone, Logan, UT), penicillin/streptomycin (100 IU/mL/100 μg/mL), D-glucose (20 mM) and L-glutamine (2 mM); osmolarity was adjusted to 335-345 mOsm/kg with sucrose. After incubation for 3 hours to allow cell attachment to the PEI-coated coverslips, they were rinsed with media, which was aspirated to remove loose cells, and then fresh media was applied. Cells were grown on coverslips in plastic Petri dishes (35 mm in diameter) each receiving 2-3 such coverslips seeded with *C. elegans* cells. Culture was maintained at room temperature in a humidified chamber/box in ambient air atmosphere, shielded from light and air currents. Cultured cells were used for experiments between 4 and 14 days after plating with their media being replaced every 4 days.

Image acquisition and processing

All experiments were done at room temperature (~ 20°C). Individual worms were immobilized using sodium azide solution (20 mM), deposited onto a glass coverslip and imaged. Cultured CEPsh glial cells on glass coverslips were imaged while bathed in external solution containing (in mM): NaCl (145), KCl (5), $MgCl_2$ (1) $CaCl_2$ (2), D-glucose (5) and HEPES (10) in water; osmolarity was adjusted to 340 mOsm/kg with sucrose, pH=7.3. CEPsh cells that were in direct contact with other cultured cells were excluded from experiments. We used an inverted microscope (IX71, Olympus) equipped with wide-field epifluorescence and differential interference contrast (DIC) illumination. Visualization of GCaMP2.0 was accomplished using a standard fluorescein isothiocyanate (FITC) filter set, while a standard Texas Red (TXR) filter set was used for

imaging mCherry. A standard 4'6-diamidino-2-phenylindole (DAPI) filter set was used to assess autofluorescence of cells. In a subset of experiments, we simultaneously visualized GCaMP2.0 and mCherry using a dual EGFP/DsRed filter set in conjunction with the dual-view DV2 emission splitting system (Photometrics, Tucson, AZ) enabling acquisition of two spatially identical but spectrally distinct images routed on its own half of the camera's imaging array. All filter sets were from Chroma Technology Corp., Bellow Falls, VT. We refer to them in the text as blue (DAPI), green (FITC or EGFP) and red (TXR or DsRed) channels, unless specifics are needed. A Xenon arc lamp (100 W) was used as a light source. For time-lapse image acquisition, an electronic shutter (Vincent Associates, Rochester, NY) inserted in the excitation pathway was controlled by software. Images were captured through either a 40 x oil-immersion objective [UAPO40XOI3/340, Olympus; numerical aperture (NA) set at 1.35] when imaging intact worms, or through a 60 x PlanApo oil-immersion objective [PLAPON60XOTIRFM, Olympus; NA, 1.45] when imaging cultured cells, using a CoolSNAP HQ^2 charge-coupled device (CCD) camera (Photometrics, Tucson, AZ) driven by Metamorph™ imaging software ver. 7.0 (Molecular Devices Inc., Chicago, IL). The fluorescent signals were background subtracted using regions of the field containing no cells. Data are expressed as dF/Fo (%) in which dF represents the change in fluorescence, while Fo represents the initial fluorescence of the cell. CEPsh glial cells were considered responsive to a stimulus if dF/Fo GCaMP2.0 values were higher than the Fo + 6SDs. All images shown in the figures represent pseudocolored raw data with their pixel intensities without saturation and within the camera's dynamic range (0-16383; 14-bit pixel depth setting).

Stimulation of CEPsh glial cells and pharmacological blockers

To stimulate CEPsh glial cells and to confirm GCaMP2.0 responsiveness to intracellular Ca^{2+} increases, we bath applied the Ca^{2+} ionophore 4-Br-A23187 (20 μM; 30 s), dissolved in external solution, after acquisition of a baseline sequence as a stand-alone treatment or after various treatments at the end of experiments [for details on kinetics parameters see (Stout and Parpura 2011a)].

Depolarization of CEPsh glial cells was achieved by pressure ejection (70 kPa, 20 s; Picospritzer© III; Parker Hannifin, Inc.), from a puffer pipette (Parpura et al. 1994), of high extracellular potassium (HiK^+) solution containing (in mM): NaCl (50), KCl (100), $MgCl_2$ (1) $CaCl_2$ (2), D-glucose (5) and HEPES (10) in water; osmolarity adjusted to 340 mOsm/kg with sucrose, pH=7.3 . Based on presumed intracellular concentrations of major ions (K^+, Na^+, and Cl^-) in *C. elegans* dopaminergic neurons (Carvelli et al. 2004) and relative plasma membrane ion permabilities (1:0.03:0.1), we calculated, using the Goldman-Hodgkin-Katz equation, a membrane potential to be ~ 45 mV for CEPsh glial cells bathed in our external solution, a value similar to that recorded from *C. elegans* chemosensory neurons (Nickell et al. 2002). Similarly, we calculated, without accounting for change in relative ion permabilities due to opening of various voltage-gated channels, that upon exposure to HiK^+ solution CEPsh glial cells membrane potential would be near -6 mV. This stimulus is expected to cause opening of all VGCC types based on the gating voltages previously determined for these *C. elegans* channels in response to HiK^+ stimulation of neurons in culture and electrophysiological studies on pharynx and body wall muscle (Jospin et al. 2002; Mathews et al. 2003; Shtonda and

Avery 2005; Frokjaer-Jensen et al. 2006). In sham-run experiments we ejected regular external solution.

We also used a "paired-pulse" HiK^+ stimulation protocol. In a subset of experiments, after the first stimulus, we exchanged the bath extracellular solution (20 s), and then repeated this sequence with the second stimulus. Since only a subset of CEPsh glial cells stimulated with the first HiK^+ pulse displayed an increase in intracellular Ca^{2+} levels and GCaMP2.0 emission fluorescence, this approach was necessary when testing the effects of Cd^{2+} or nemadipine-A, pharmacological blockers of Ca^{2+} entry from the extracellular space. In this set of experiments, after completion of the first stimulus sequence, we bathed cells in extracellular solution for an additional 10 minute period before executing the second stimulus. When using blockers, they were added to the extracellular solution during this 10 minute period and then kept in extracellular solution until the end of experiment; for the second pulse, the HiK^+ solution also contained blockers.

Intracellular Ca^{2+} dynamics analysis

We used a set of criteria to categorize CEPsh glial cell Ca^{2+} increase response type due to HiK^+ stimulation. Any responding cell for which the recorded GCaMP2.0 dF/Fo during the HiK^+ stimulation varied by less then 10% of the expected dF/Fo value (normalized to peak response for the trace) at any given time-point, based on the moving bin average of dF/Fo measurements obtained within two consecutive time-points, was categorized as a sustained responder or the Category 1 (Cat.1) cell. CEPsh glial cells

whose responses failed the Cat.1 classification were further sorted into two additional categories. Any non-Cat. 1 responsive cell, displaying Ca^{2+} increases with at least five consecutive dF/Fo values exceeding that of its Fo + 6 SDs value, was classified as an intermediate responder or belonged to the Category 2 (Cat. 2). Cells that failed both Cat.1 and Cat. 2 classifications showed clear oscillatory GCaMP2.0 dF/Fo dynamics and were, thus, termed oscillators or the Category 3 (Cat. 3) cells.

To assess effects of Cd^{2+} or nemadipine-A (NemA) on HiK^{+} -induced Ca^{2+} entry from the extracellular space using a paired-pulse stimulation protocol, we calculated the ratio of the second peak (maximum) response to the first one (P2/P1 ratio).

To estimate the decay time of the recorded GCaMP2.0 dF/Fo increase due to the HiK^{+} stimulation of Cat. 1 cells, we computed time (rounded to the nearest second) required in each experiment/trace for the dF/Fo to lose half of its maximum value.

Statistical analysis

The differences in mCherry and GCaMP2.0 fluorescence signals due to 4-Br-A23187 stimulation were tested using the Wilcoxon signed rank test. The effects of 4-Br-A23187, HiK^{+}, Ca^{2+} entry blocking agents and genetic modification of VGCCs on various intracellular Ca^{2+} dynamics parameters (peak and cumulative GCaMP2.0 dF/Fo, P2/P1 ratio and decay time) were determined using the Mann-Whitney U-test. All statistical tests were performed using GB-STAT software ver. 6.5 (Dynamic Microsystems, Inc., Silver Spring, MD). Data were expressed as mean $\pm$ standard error of mean (SEM).

Results

Basic cell morphology of and intracellular Ca^{2+} dynamics in CEPsh glial cells

We initially visualized *C. elegans* strain VPR108 with integrated mCherry and GCaMP2.0 transgenes in CEPsh glial cells driven by the *hlh-17* promoter to assess the location and basic cell morphology of these glial cells. Differential interference contrast (DIC), and fluorescence mCherry (red channel) and GCaMP2.0 (green channel) images were obtained. Figure 1A shows an anterior tip of an adult VPR108 worm in which cell specific expression of mCherry/GCaMP2.0 is visible within two out of the four CEPsh glial cell bodies in the imaging plane and due to cell "stacking"; although all four cells express both fluorescent proteins. The expression of mCherry was much brighter than that of GCaMP2.0. The cell bodies of CEPsh glial cells, displaying large sheet-like extensions, surrounded the nerve ring and the proximal section of the ventral nerve cord. Additionally their long thin processes emanated from the cell body to the anterior sensory tip. CEPsh glial cell autofluorescence (blue channel) was similar to other cell types within the nerve ring. Thus, inspection at the level of light microscopy indicates that CEPsh glial cells in VPR108 worms display normal location and basic cell morphology.

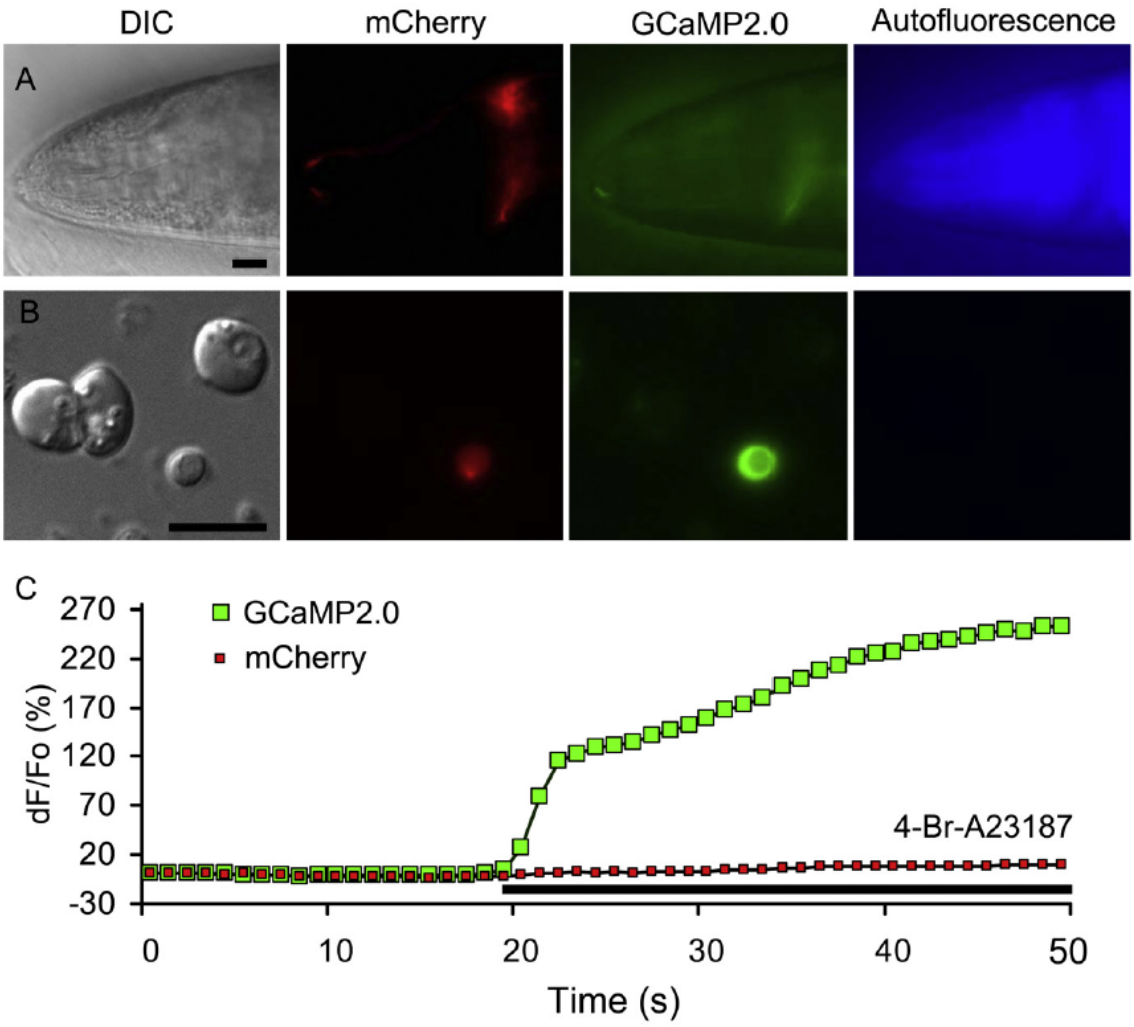

Figure 1. CEPsh glial cells stably co-expressing the genetically-encoded intracellular red fluorescent marker mCherry and the green fluorescent cytosolic Ca^{2+} indicator GCaMP2.0.

A) An anterior portion of an L4 stage VPR108 worm expressing mCherry and GCaMP2.0 in CEPsh glial cells which display normal location and basic morphological features as well as autofluorescence comparable to other cells. B) CEPsh glial cells in mixed culture prepared form VPR108 embryos can be identified based on their mCherry/GCaMP2.0 expression and show low autofluorescence. Images in A and B

were acquired using (left to right): DIC, red (mCherry), green (GCaMP2.0) and blue (autofluorescence) channels; scale bars, 10 μm. C) Time-lapse of simultaneous GCaMP2.0 (green trace) and mCherry (red trace) fluorescence emission from a single representative cell using a dual-view imaging approach. Stimulation with the Ca^{2+} ionophore 4-Br-A23187 reliably raises the intracellular Ca^{2+}, seen as an increase in GCaMP2.0 fluorescence, while mCherry fluorescence displayed stable levels. The time of application of 4-Br-A23187 is indicated by the horizontal bar. Changes in fluorescence are expressed as dF/Fo (percentage).

Using the VPR108 worm strain we prepared mixed embryonic cells in culture. CEPsh glial cells were identified based on their readily detectable mCherry and GCaMP2.0 fluorescence (Fig. 1B). In contrast, their autofluorescence was unremarkable, similar to most other cell types present in whole-worm dissociated culture (Fig. 1B). In our culture conditions, we have not observed long process-bearing CEPsh glial cells with extensive body sheets, as seen in intact worms. Rather, CEPsh cells mainly had round morphology with their cells bodies ~ 5-10 μm in diameter. Some CEPsh cells displayed short processes, less than 15 μm in length, which sometimes branched. The mCherry expression was eminently detectable throughout the entire cell (Fig. 1B, compare DIC and red channel) with a conspicuous peri-nuclear, brighter-red punctum. Unlike its relatively dim appearance in CEPsh glial cells of intact worms, GCaMP2.0 fluorescence in cultured cells was comparable to that of mCherry. The nuclear region of the cell was discernable as a somewhat off-center positioned dimmer circle in GCaMP2.0 images.

Next, we confirmed the responsiveness of the Ca^{2+} indicator GCaMP2.0 to intracellular Ca^{2+} increases in cultured CEPsh glial cells. We bath applied the Ca^{2+}

ionophore 4-Br-A23187 (20 μM, 30 s), allowing Ca^{2+} to enter the cell from the extracellular space, which caused a large increase in GCaMP2.0 fluorescence (n=30, peak dF/Fo = 162 $\pm$ 15 %; Wilcoxon signed rank test, $p<0.01$). However, this stimulus had no significant effect on the fluorescence level of the intracellular marker mCherry (n=5, peak dF/Fo = 1 $\pm$ 4 %; Wilcoxon signed rank test, p= 0.89). This was the case regardless whether: i) we simultaneous acquired GCaMP2.0/mCherry fluorescence using a dual-view approach (Fig. 1C; see materials and methods for details); ii) GCaMP2.0/mCherry fluorescence was recorded by alternating acquisition of individual red and green channels; or iii) mCherry fluorescence was acquired at the beginning and end of recordings, flanking GCaMP2.0 fluorescence time-lapse acquisition. Additionally, based on mCherry fluorescence we have not observed a change in cell shape as a result of the increase in $[Ca^{2+}]_i$. Consequently, even though we could use the dual-wavelength ratiometric approach to express the change of GCaMP2.0 fluorescence, reporting on intracellular Ca^{2+} levels, to mCherry fluorescence, at this juncture we elected, for simplicity, to report on the single-wavelength (green channel) acquisition of GCaMP2.0 fluorescence as a measurement of intracellular Ca^{2+} dynamics in CEPsh glial cells. It should be noted that the application of a Ca^{2+} ionophore is a strong stimulus and a non-recovery treatment for the cell. Consequently, from this point on, we restricted the use of 4-Br-A23187 solely to assess/confirm GCaMP2.0 Ca^{2+} responsiveness under various conditions, at the end of experiments.

Cultured CEPsh glial cells display intracellular Ca^{2+} dynamics in response to a depolarizing stimulus

Having determined GCaMP2.0 responsiveness to intracellular Ca^{2+} increases in cultured CEPsh glial cells, we studied Ca^{2+} excitability of these cells in response to a depolarizing stimulus, the application of high extracellular K^+ (100 mM, HiK^+; pressure injection, 20 s). In the majority of CEPsh glial cells (34 out of 52 tested) we observed heightened GCaMP2.0 fluorescence (dF/Fo= 71 $\pm$ 6 %), reporting on an increase of $[Ca^{2+}]_i$ (Fig. 2A, black squares). The lack of response in a subset of CEPsh glial cells (18 out of 52 tested) upon exposure to Hi K^+ was not due to functionality of GCaMP2.0, as ruled out by a subsequent application of 4-Br-A23187 that caused an increase in $[Ca^{2+}]_i$. Cells that we submitted, in parallel, to a sham-run, by ejecting normal extracellular solution rather than HiK^+, show no responses (10 out of 11 tested; peak dF/Fo= -1 $\pm$ 1 %), indicating that the pressure ejection approach itself did not cause an increase in $[Ca^{2+}]_i$. (Fig. 2A, open circles). The exception was one cell in the sham-run that responded with an increase in GCaMP2.0 fluorescence, a finding consistent with our observation of an occasional spontaneous, brief increase in $[Ca^{2+}]_i$ in CEPsh glial cells (data not shown). Application of 4-Br-A23187 at the end protocol indicates that HiK^+ and sham challenged cells show comparable increase in GCaMP2.0 fluorescence (Mann-Whitney U test, p=0.07).

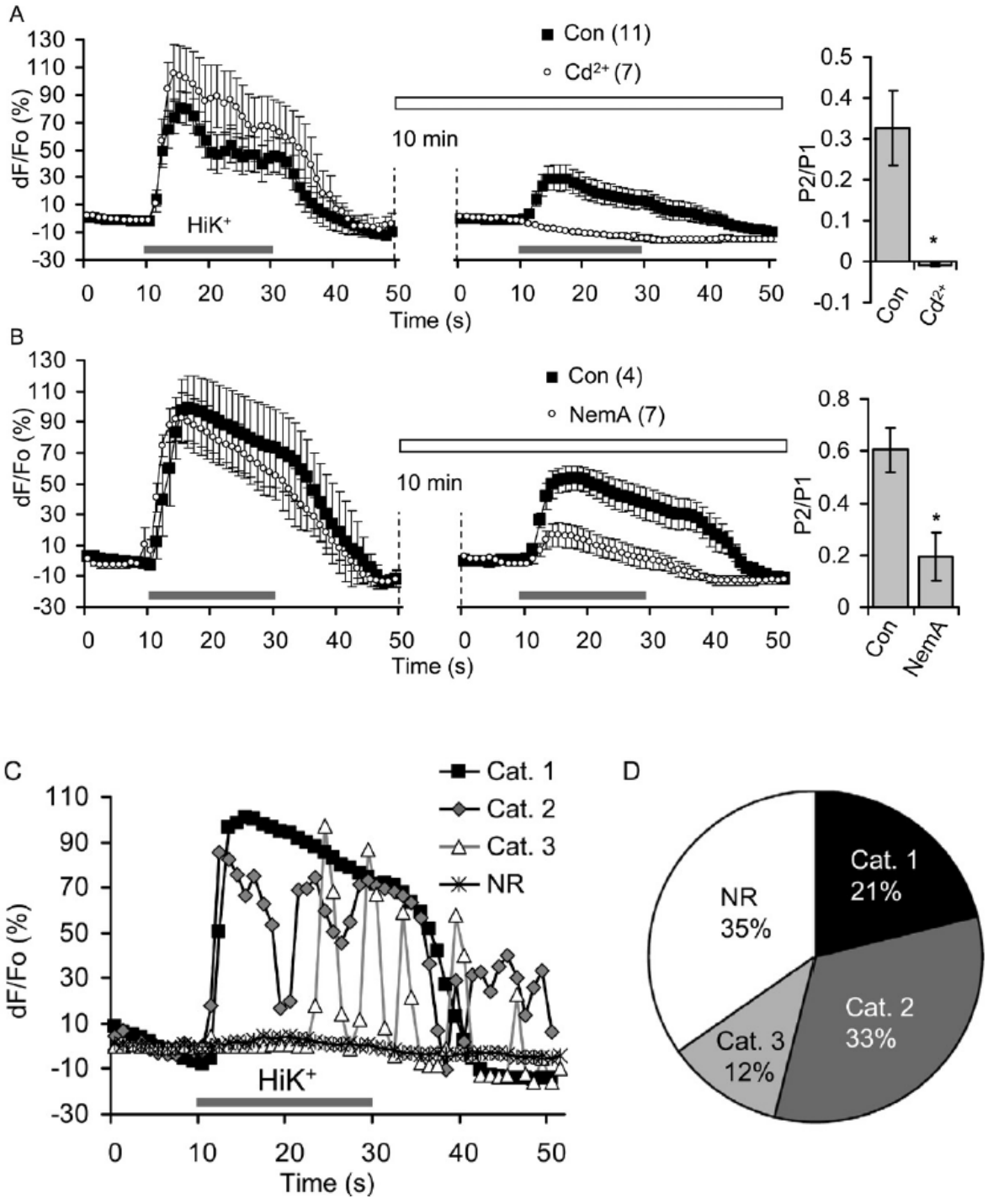

Figure 2. Cultured CEPsh glial cells exhibit intracellular Ca^{2+} dynamics in response to depolarization.

A) Application of a depolarization stimulus, high extracellular potassium (100 mM; HiK^+) to CEPsh glial cells results in an elevation of intracellular Ca^{2+} levels (black squares). Sham treatment of CEPsh glial cells, in which external solution was applied instead of HiK^+, does not affect intracellular Ca^{2+} levels (open circles). Horizontal grey bar indicates the time of stimulus/sham application. At the end of experiment, the application of the Ca^{2+} ionophore 4-Br-A23187 (20 μM, horizontal black bar) confirms the responsiveness of the Ca^{2+} indicator GCaMP2.0 expressed in CEPsh cells. B) Paired-pulse application of HiK^+ (horizontal grey bars). After the first stimulus delivery and a recovery wash as in A, another application of HiK^+ resulted in an elevation of intracellular Ca^{2+} levels, albeit with smaller magnitude. C-D) Classification of CEPsh glial cells Ca^{2+} dynamics in responses to the first HiK^+ stimulus. C) At inspection of GCaMP2.0 time-courses from individual cells, they can be classified as responders or non-responders (NR). Responders can be classified into three distinct categories (Cat.): i) Cat. 1, or sustained responders, ii) Cat. 2, or intermediate responders, and iii) Cat. 3, or oscillators. D) The proportion of cultured CEPsh glial cells from the background strain VPR108 displaying the various categories of responses. The percentage is rounded up in each category and therefore sums to 101%. Traces in A and C represent time courses of GCaMP2.0 fluorescence from single representative cells, while the trace in B shows mean GCaMP2.0 fluorescence $\pm$ SEMs expressed as dF/Fo (percentage).

We tested CEPsh glial cells responses to a paired-pulse stimulation using HiK^+; the resting/intermission period in between two stimuli was initially set equal to the duration of the stimulus (20 s; but see below) and used for a wash-out. In these experiments, we selected the responders to the first HiK^+ stimulus (24 of 35 cells tested; peak dF/Fo= 59 $\pm$ 8 %) and studied their responses to the second stimulus. A subset of cells responded to the second Hi K^+ stimulus (17 out of 24 that responded to the first stimulus) as a result of a stringent criteria we put forward for the cellular response (see material and methods), combined with the decline in the peak response during the second HiK^+ stimulus (peak dF/Fo= 27 $\pm$ 5 %). Normalization of the second peak to the first peak (P2/P1 ratio= 0.58 $\pm$ 0.13) indicates ~ 42 % reduction in the magnitude of the response to the second HiK^+ stimulus.

At close inspection of individual Ca^{2+} traces, we observed that cell responses varied (Fig. 2C), based on which we classified cells (Fig. 2D). As already indicated above, using the response (or lack of it) due to the first HiK^+ stimulus, cells were declared as responders (65 %) or non-responders (35 %). Responders were further classified into three distinct categories (see materials and methods for details): i) Cat. 1, or sustained responders (21 %), ii) Cat. 2, or intermediate responders (33 %), and iii) Cat. 3, or oscillators (12 %). The variable nature of intracellular Ca^{2+} dynamics in response to depolarization may reflect the presence of multiple voltage-gated channels (VGCCs) mediating the Ca^{2+} entry from the extracellular space.

VGCCs Mediate the Ca^{2+} response of cultured CEPsh glial cells to depolarization: an acute pharmacological approach

A prominent pathway for intracellular Ca^{2+} increase in response to HiK^{+} -induced depolarization is the entry of Ca^{2+} from the extracellular space via VGCCs. To start addressing involvement of this pathway, we initially used an acute pharmacological approach with available and limited agents capable of affecting VGCCs of *C. elegans*. Since only a proportion of CEPsh glial cells in our culture responded to HiK^{+} stimulation, we utilized a paired-pulse stimulation protocol. After the first HiK^{+} stimulus and a recovery wash out, we let the cells to recover for a 10 minute period and then repeated the HiK^{+} stimulation, which generated a reduced Ca^{2+} response in the cell (Fig. 3A, trace, black squares). Next, during intermission between the two stimuli, we incubated CEPsh glial cells with Cd^{2+} (100 μM; 10 min), a general blocker of VGCCs across species, including body-wall muscle cells of *C. elegans* (Jospin et al. 2002; Figueiredo et al. 2011). We found that the second Ca^{2+} response was eliminated in the presence of extracellular Cd^{2+} (Fig 3A, trace, open circles) producing a second peak to first peak ratio that was significantly smaller than that in control (P2/P1= 0.01 ± 0.00 and 0.33 ± 0.09, respectively) (Fig. 3A, bar graph).

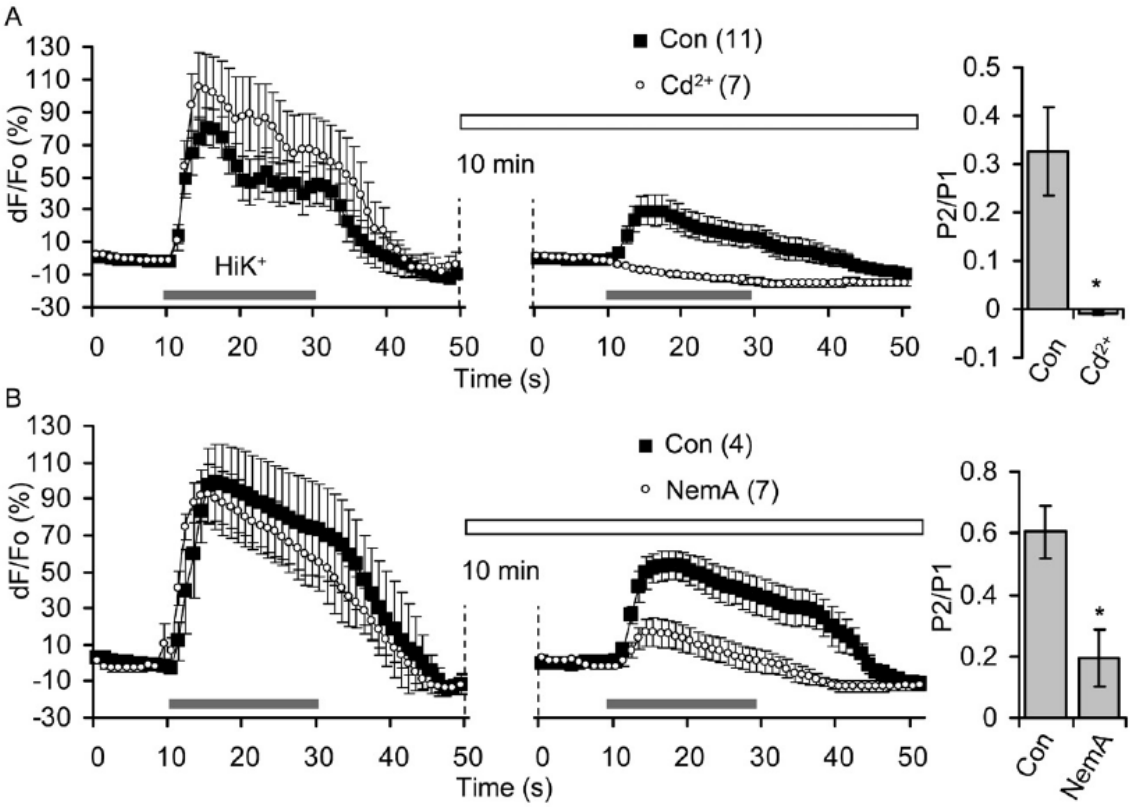

Figure 3. Voltage-gated Ca^{2+} channels (VGCCs) play a role in depolarization-induced intracellular Ca^{2+} elevations in CEPsh glial cells.

A) (left, traces) Application of extracellular HiK^+ (horizontal grey bars below traces) to cause depolarization of CEPsh glial cells results in elevated intracellular Ca^{2+} levels. After an intermission period (10 min, vertical dashed lines), the second application of HiK^+ resulted in a Ca^{2+} elevation of a lesser magnitude [black squares, control (Con)]. Incubating CEPsh glial cells with Cd^{2+}(100 μM, 10 min), a general VGCC blocker, that is applied during the intermission period after the first HiK^+ application and kept until the end of the experiment, causes a reduction of the second Ca^{2+} response (open circle). (right, bar graph) Ratio of the peak Ca^{2+} level in response to the second HiK^+ application

(P2) over the first application (P1). B) (left) A paired-pulse approach as in A. Only CEPsh glial cells that show Cat. 1 responses are tested. (left, traces) Nemadipine-A (NemA, 3 μM, 10 min), an L- type VGCC blocker, is applied during the intermission time and maintained until the end of the experiment. (right, bar graph) P2/P1 ratio shows a decrease when cells were treated with NemA. Traces in A and B represent a mean time course of GCaMP2.0 fluorescence ± SEMs expressed as dF/Fo (percentage). Vertical bars in graphs indicate mean ± SEMs. Notation of HiK^+ stimulation done above the first horizontal grey bar in A is omitted thereafter for clarity. The times of application of Cd^{2+}or NemA are indicated by the open horizontal bars above traces. Numbers in parentheses indicate the number of CEPsh glial cells studied in each condition. Asterisks indicate a significant difference between measurements (Mann-Whitney U test; *$p<0.05$).

To further pharmacologically investigate the involvement of the L- type VGCCs in the response to HiK^+ application, we used the relatively recently identified agent nemadipine-A (NemA), which can block the L- type VGCC-mediated Ca^{2+} influx in *C. elegans* body-wall muscle cells (Kwok et al. 2006; Hui et al. 2009; Figueiredo et al. 2011). These channels have been associated with a large sustained Ca^{2+} entry/responses (Shtonda and Avery 2005; Frokjaer-Jensen et al. 2006), reminiscent of our Cat.1 responses. Thus, in this set of experiments we only utilized CEPsh glial cells displaying a Cat.1 response to the first HiK^+ stimulus. As with the use of Cd^{2+}, during the intermission we applied NemA (3 μM, 10 min). We saw that the subsequent second HiK^+ stimulus in the presence of NemA resulted in a reduced magnitude of Ca^{2+} response (peak 2 dF/Fo= 55 $\pm$ 8 % and 18 $\pm$ 7 % in control or NemA treated cells, respectively; Mann-Whitney U-test; $p< 0.02$), with a second peak to first peak ratio significantly smaller than in matching controls (P2/P1= 0.19 $\pm$ 0.09 and 0.60 $\pm$ 0.09, respectively; Fig. 3B, bar graph). It should be noted that the observed reduction in the P2/P1 ratio caused by the pharmacological agent was not due to their possible interference with GCaMP2.0 responsiveness to the intracellular Ca^{2+} increase, since subsequent to the second HiK^+ stimulus, an application of 4-Br-A23187 caused similar increases in control CEPsh glial cells and those exposed to pharmacological agents (Mann-Whitney U test; $p= 0.465$ and 0.220 for Cd^{2+} and NemA treatments, respectively, when compared to control). Data obtained using an acute pharmacological approach indicate that VGCCs are a major, if not the sole, pathway for the Ca^{2+} entry from the extracellular space following HiK^+-induced depolarization. Additionally, L- type VGCCs contribute ~ 2/3 of the Ca^{2+} source

for sustained Cat.1 peak responses in CEPsh glial cells. Since NemA is a highly effective agent that can lead to a complete block of L- type VGCCs at the concentration we used (Liu et al. 2011), this finding may point to a possible involvement of other VGCC types in depolarization-dependent intracellular Ca^{2+} increases in CEPsh glial cells.

VGCCs mediate the Ca^{2+} response of cultured CEPsh glial cells to depolarization: a chronic genetic approach

As indicated above a pharmacological approach is limited by the lack of agents that have specific effects on various VGCCs types present in *C. elegans*. Thus, to further study the role of various VGCCs in CEPsh glial cells Ca^{2+} dynamics we utilized a genetic approach. We used VPR108 worms as a background strain for crossings with various worm lines carrying mutations for genes encoding α_1-subunits contributing the pore region of L- , T- , and N, P/Q, R- type of *C. elegans* VGCCs. Since knock-out (KO) alleles for the L- type channel α1-subunit gene are homozygous lethal, we used a reduction-of-function (*rf*) *egl-19* allele. Additionally, we used two KOs: a deletion *cca-1* allele for T- type channels, and an *unc-2* allele truncation mutation for N, P/Q, R- type channels. Generated crosses were then used to prepare whole-worm dissociated cell cultures, within which CEPsh glial cells were identified using mCherry/GCaMP2.0 expression.

We studied Ca^{2+} excitability of CEPsh glial cells originating from various VGCCs mutants in response to HiK^+ and compared it to that of background (bkg) strain. CEPsh

glial cells from *egl-19 rf* (L- type) and *cca-1* KO (T- type) worms did not display (within 10% of bkg strain) change in the proportion of non-responders when compared to control cells originating from the bkg strain (Fig. 4 A). This is unlike CEPsh glial cells of *unc-2* KO that had increased number of non-responders, which appears to come at the expense of reducing the proportion of Cat.2 and Cat. 3 responses. Additionally, there was an obvious abrogation of Cat. 2 and Cat. 3 responses in *cca-1* KO CEPsh glial cells that showed only the Cat.1 response. In cells of *egl-19* mutants, the Cat.2 responses had a reduced preponderance when compared to the bkg. Thus, CEPsh glial cells require functional CCA-1 channel to display Cat 2. and 3. responses. In cells expressing CCA-1, however, the proportion of Cat.2 and Cat.3 can be modulated by the presence by EGL-19 and/or UNC-2 VGCCs. The proportion of the Cat. 1 responses appears to be dually regulated by the expression of EGL-19 and UNC-2 channels.

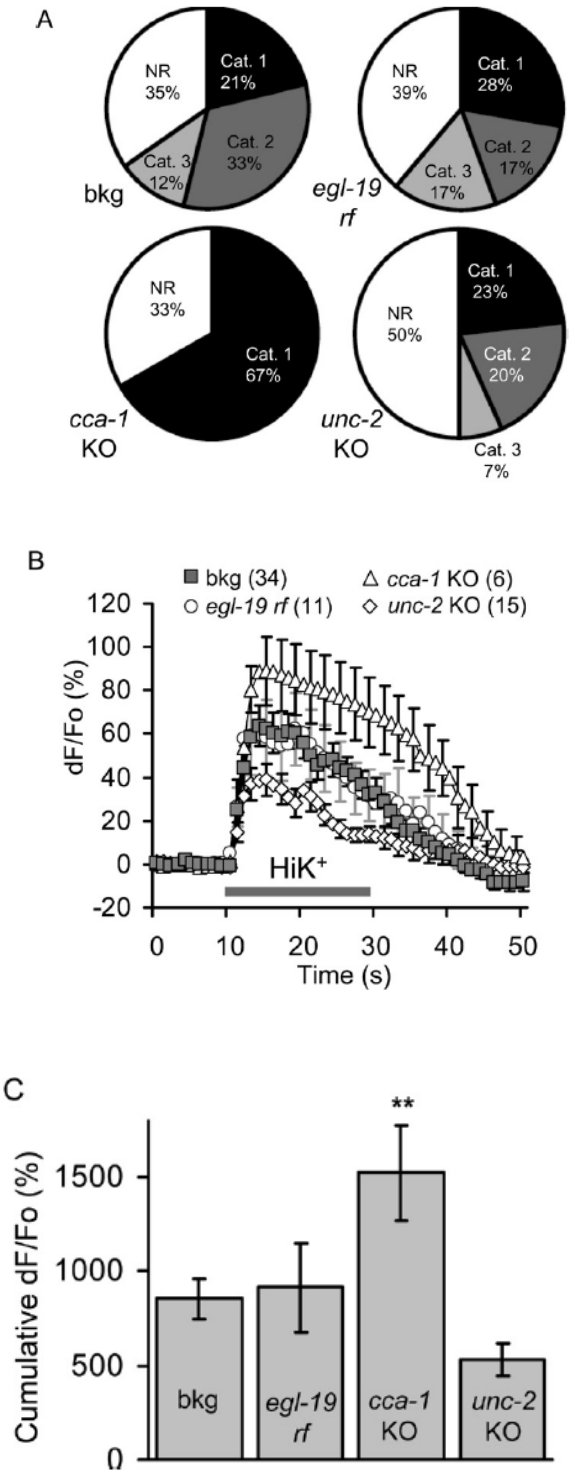

Figure 4. Genetic disruption of VGCC type expression affects depolarization-induced intracellular Ca^{2+} elevations in CEPsh glial cells.

A) Classification of depolarization-induced intracellular Ca^{2+} responses in cultured CEPsh glial cells originating from the background strain VPR108 (bkg, n=52; data/chart from Fig. 2D) and various VGCC α-1 subunits mutants: i) L- type *egl-19* reduction-of-function (*rf*) (n=18), ii) T- type *cca-1* knockout (KO)(n=9), and iii) N, P/Q, R- type *unc-2* KO (n=30). NR, non-responder, Cat., category of response. The percentage contribution for each category in pie charts is rounded, so that the sum may exceed 100%. B) Average GCaMP2.0 fluorescence time-courses recorded from all responders. Horizontal grey bar indicates the time of the extracellular HiK^{+} stimulus. Numbers in parentheses indicate the number of CEPsh glial cells studied in each condition. C) Summary of cumulative intracellular Ca^{2+} load during the stimulus. Points and bars indicate mean of GCaMP2.0 fluorescence shown in dF/Fo ± SEMs. Asterisk indicates a significant change when compared with the bkg group (Mann-Whitney U test; $^{**}p < 0.02$).

We next assessed the effects of various VGCC type expressions on total intracellular Ca^{2+} load in all CEPsh glial cells responding to HiK^{+} stimulus regardless of the category of the response (Fig. 4B-C). The mean time-course of cellular responses points to a possible modulation of the intracellular Ca^{2+} load in CEPsh glial cells cultured from some mutant worms (Fig. 4A). This was quantitatively assessed using cumulative GCaMP2.0 dF/Fo responses during the time of the HiK^{+} stimulus application (Fig. 4C). There was a significant increase in total intracellular Ca^{2+} load in CEPsh glial cells cultured from *cca-1* KO worms. Application of 4-Br-A23187 caused similar increases in GCaMP2.0 fluorescence in CEPsh glial cells from mutant worms when compared to that recorded from bkg worms (Mann-Whitney U test, p= 0.327-0.829 for various mutants)

Since the Cat. 1 response was the only common response occurring in CEPsh glial cells originating from any worm strain, mutants or bkg, we dissected out the contribution of various VGCC types to this category or response. It should be noted that, although Cat.1 responses are reminiscent of large sustained Ca^{2+} entry/responses associated with the L- type channel (Shtonda and Avery 2005; Frokjaer-Jensen et al. 2006), their peak responses were not entirely blocked by NemA (Fig, 3B). This implicates the involvement of more than one VGCCs type contribution to their appearance, as confirmed by the above genetic approach studying the proportion of response categories, and implicating L and T type contribution (Fig. 4A). Consequently, we obtained the time course of Cat. 1 responses (Fig 5A). We assessed possible effects of VGCC type

mutations based on quantification of Cat. 1 intracellular Ca^{2+}load and its decay (Fig. 5B-D). The peak and cumulative GCamp2.0 dF/Fo responses during the HiK^{+} stimulus were analyzed (Fig. 5B, C). The decay of the Cat. 1 response was quantified as the time it took for the dF/Fo signal to drop from its peak value to a half of that ($t_{1/2}$); this analysis included the portion of the trace exceeding the time that HiK^{+} was applied and includes the recovery period as well (Fig. 5D). There was no significant change in the peak (Mann-Whitey U test, p= 0.189-0.481 for various mutants) and cumulative (Mann-Whitney U test, p=0.051-0.533 for various mutants) intracellular Ca^{2+} load in CEPsh glial cells cultured from mutant strains (Fig. 5B-C). The decay time of the Cat. 1 was significantly shorter in CEPsh glial cells cultured from *unc-2* KO (N, P/Q, R- type) mutants, but was increased in cells from cca-1 KO (T- type) mutant (Fig. 5D). Taken together, data obtained using pharmacological and genetic approaches indicate that all known VGCC type contribute to depolarization-dependent intracellular Ca^{2+} load in CEPsh glial cells.

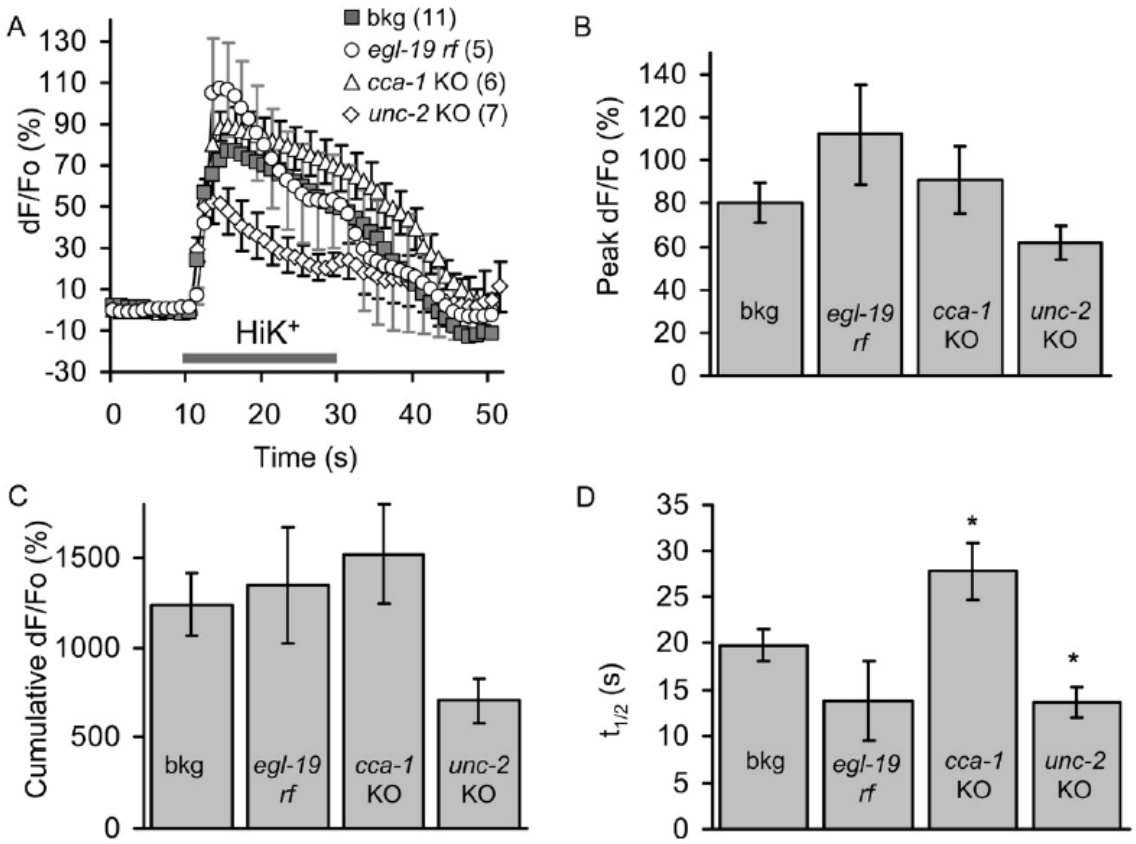

Figure 5. All VGCC types contribute to various characteristics of the sustained category 1 response in CEPsh glial cells

A) Average GCaMP2.0 fluorescence time-courses recorded from CEPsh glial cells displaying the Cat.1 response. Abbreviations for *C. elegans* strain/mutants used to prepare cultured CEPsh glial cells as in Fig. 4. Horizontal grey bar indicates the time of the extracellular HiK^+ stimulus. Numbers in parentheses indicate the number of CEPsh studied in each condition. B-D) Summary of quantitative parameters measured for HiK^+-induced Cat.1 responses. B-C) Peak (B) and cumulative (C) intracellular Ca^{2+} loads during the stimulus. Points and bars in A-C indicate mean GCaMP2.0 fluorescence expressed as dF/Fo $\pm$ SEMs (percentage). D) The decay time ($t_{1/2}$) of the Cat. 1 responses. The time it took for the dF/Fo signal to subside from its peak value to a half of

that ($t_{1/2}$) exceeds the stimulus time. Bars indicate mean ± SEMs (seconds). Asterisks indicate a significant change when compared with the bkg group (Mann-Whitney U test ; *$p<0.05$).

Discussion

Here we report the first examination of intracellular Ca^{2+} dynamics in *C. elegans* glial cells. We used the CEPsh glial cell specific *hlh-17* promoter to drive expression of a genetically encoded Ca^{2+} indicator in these cells, whose Ca^{2+} dynamics were examined in cell culture. The *in vivo* morphology and the suite of genes expressed in the CEPsh glial cells, points to a gross similarity of these invertebrate glial cells to mammalian macroglia: astrocytes, oligodendrocytes and oligodendrocyte precursor cells (OPCs) [reviewed in (Heiman and Shaham 2007; Oikonomou and Shaham 2011)]. Since mammalian macroglia can respond to depolarization with increases in intracellular Ca^{2+} concentrations that are mediated by several differentially expressed VGCC types [reviewed in (Verkhratsky and Steinhauser 2000; Seifert and Steinhäuser 2004; Paez et al. 2009)], we tested the CEPsh glia for depolarization-induced Ca^{2+} excitability. We report that cultured CEPsh glial cells can respond to depolarization with increases in intracellular Ca^{2+} dynamics that display a heterogeneous nature. We used an acute pharmacological approach and a chronic genetic approach to show that this Ca^{2+} excitability in CEPsh glial cells is mediated primarily through VGCCs comprised of multiple core α_1-subunit types.

The total elimination of the depolarization-induced intracellular Ca^{2+} dynamics, using the general VGCC blocker Cd^{2+}, indicates that the cultured CEPsh glial cells express functional VGCCs (Fig. 3). We hypothesized that multiple VGCC types produced the observed variety of Ca^{2+} responses in CEPsh glial cells. To address this hypothesis, we categorized the Ca^{2+} responses to depolarization as: i) sustained, ii) intermediate and iii) oscillatory. We evaluated the contribution of various α_1-subunit

types to the proportion of response categories as well as the effects of VGCC types on quantitative parameters of intracellular Ca^{2+} dynamics, the peak and cumulative intracellular Ca^{2+} load and its decay time (Fig. 4 and 5).

Other than Cd^{2+}, pharmacological agents for the study of VGCCs in *C. elegans* are limited, since they differ from mammalian VGCCs in the respect to their sensitivity to commonly used pharmacological blockers (Kwok et al. 2006). However, NemA likely provides a complete and specific block of L- type channel activity in *C. elegans* cells (Kwok et al. 2006; Hui et al. 2009; Figueiredo et al. 2011). We found that the application of NemA blocked about two thirds of the sustained Cat. 1 type of Ca^{2+} response (Fig. 3B). This provided us not only with evidence that L- type VGCCs are active in cultured CEPsh glial cells, but also that other VGCC types are involved. Consequently, we went on to use the available *C. elegans* strains carrying mutations in the genes encoding the three α_1 subunits of this animal: CCA-1, EGL-19 and UNC-2, corresponding to T-, L- and N, P/Q, R- type of VGCCs, respectively (Lee et al. 1994; Schafer and Kenyon 1995; Shtonda and Avery 2005).

The elimination of responses that fall into the intermediate and oscillator categories (Cat. 2 and Cat. 3, respectively) in CEPsh glial cells lacking CCA-1 clearly points to an important role for T- type VGCCs in Ca^{2+} dynamics of these cells (Fig. 4A); more specifically these channels are required for oscillatory Ca^{2+} dynamics of CEPsh glial cells. When all response categories were pooled together and quantitatively examined, an increase in cumulative responses were seen in the *cca-1* KO glial cells (Fig. 4C). One would expect such an effect based on the elimination of oscillatory and intermediate responses, with the remaining presence of only sustained responses, which

inherently can contribute more extensively to cumulative Ca^{2+} load. This explanation might be, however, an overly simplified scenario, since the observed increase in cumulative Ca^{2+} response in *cca-1* KO CEPsh glial cells might be, to some extent, mediated by a possible increased number of L- type channels due to compensatory increases in EGL-19 expression. Indeed, such homeostatic regulation of *egl-19* expression has been suggested in studies on VGCCs in other *C. elegans* cell types (Shtonda and Avery 2005; Frokjaer-Jensen et al. 2006; Saheki and Bargmann 2009).

The observation of oscillatory calcium responses during a persistently depolarized plasma membrane that requires T-type VGCCs indicates an interaction between VGCC mediated calcium responses and other components of the complex calcium signaling network that is present in cells such as the smooth ER and mitochondria. This interdependent network of calcium stores, release mechanisms and buffers is important for mammalian glia calcium dynamics, albeit primary external sources of calcium do not readily include VGCCs in mature mammalian macroglia [(Hua et al. 2004; Malarkey et al. 2008; Reyes and Parpura 2008) and reviewed in (Reyes and Parpura 2009)]. The depolarizing stimulus we applied to the cultured CEPsh cells would be expected to activate all VGCC types present and also quickly inactivate T-type channels. This fast inactivation of T-type channels may work together with other calcium sources to generate the oscillatory Category 3 responses we observed in cultured CEPsh cells. The specialized interaction that L-type channels have with the smooth ER may also be necessary for the sustained responses (Tsien 1983; Bers 2002). It is currently unknown if ryanodine and IP_3 receptors of the ER modulate calcium dynamics in *C. elegans* glia but

that question and if there is an interaction with VGCCs could be answered with similar experimental approaches in future studies.

Because deletion of the L- type channel encoding *egl-19* gene is lethal, we were limited to the use of a reduction-of-function mutant of the channel. This means that L-type channels could be still present and functional in the plasma membrane of the CEPsh glial cells from the *egl-19* mutant strain. This could explain the lack of significant effect on depolarization-induced Ca^{2+} dynamics (Fig. 4C, and 5B-D). These findings using a chronic genetic approach should not distract from those obtained using an acute pharmacology, the NemA treatment (Fig. 3B), which selects the L- type channels as a major contributor to VGCC activity in CEPsh glial cells.

Faster decay time in the *unc-2* (N, P/Q, R- type) KO CEPsh glial cells implicates some role for this VGCC in depolarization-mediated Ca^{2+} dynamics of glial cells. A possible explanation for such an effect could be that UNC-2 and EGL-19 interact. Namely, an accessory subunit to VGCCs UNC-36 may have a negative regulatory action on EGL-19 that is enhanced when *unc-2* is ablated (Saheki and Bargmann 2009). Since, based on pharmacology, EGL-19 is the primary mediator of depolarization-induced Ca^{2+} increases in CEPsh glial cells, a decrease in negative regulation by an accessory protein in the *unc-2* KO would be expected to cut across all response category measures. While we observed a trend toward reduction in the peak and cumulative responses (Fig. 5B-C), the later barely missing its statistical significance ($p=0.051$), there was a significant reduction in the decay time in *unc-2* KO CEPsh glial cells (Fig. 5D). Altogether, we present evidence of heterogeneity in VGCC activity, in cultured CEPsh glial cells. It is

then tempting to speculate on what function VGCCs might have in the CEPsh glial cells *in vivo*.

If we combine the knowledge that presently exists regarding CEPsh glial cells, VGCC functions in other cell types of *C. elegans*, and the related oligodendrocyte lineage of mammalian nervous systems, two possible functions for VGCCs in CEPsh glial cells are apparent: i) regulation of CEPsh cell gene expression and morphology and ii) modulation of neuronal/synaptic morphology and signaling via putative release of growth factors and/or transmitters from CEPsh glial cells.

Ca^{2+} entry through L- type VGCCs in particular is an important regulator of gene expression in the nervous system (Bading et al. 1993). VGCCs are required for normal axon extension and branching in *C. elegans* (Tam et al. 2000). Similarly, L- type VGCCs play a role in OPCs process extension (Yoo et al. 1999; Fulton et al. 2010). Consequently, it is feasible that VGCCs could play similar roles in CEPsh glial cells.

Ca^{2+}-dependent exocytosis in astrocytes can lead to gliotransmission [reviewed in (Parpura et al. 1994; Montana et al. 2006)], whereby vesicular release of transmitters and/or growth factors can lead to modulation of synaptic transmission (Araque et al. 1999; Hanisch and Kettenmann 2007) and presumably synapse development and maintenance (Slezak and Pfrieger 2004). Netrin (UNC-6) expression in the ventral CEPsh glial cells is required for normal neuronal axon development and formation of specific synapses (Hedgecock et al. 1990; Wadsworth et al. 1996; Lim et al. 1999; Colon-Ramos et al. 2007; Yoshimura et al. 2008). Interestingly, in mammalian neurons, netrin signaling is regulated by L- type VGCC-mediated Ca^{2+} signaling at the level of netrin gene transcription through a fragment of the L- type α_1-channel subunit (Gomez-Ospina

et al. 2006). Distribution of UNC-6 in *C. elegans* has been shown to require elements of the vesicular transport and release machinery (Asakura et al. 2010). Furthermore, vesicle-like structures have been identified in adult worms in the region where the glial cells ensheath the ciliated sensory structure of neurons at the anterior tip of the worm indicating that vesicular fusion might be an important process in the CEPsh cells throughout the life of the animal (Ward et al. 1975). Thus, it is plausible that VGCCs and Ca^{2+} dynamics in CEPsh glial cells could play a role in the regulation of synaptic development and transmission. It should be noted, however, that unlike neurons in mammalian model systems, *C. elegans* neurons do not need glial trophic support to survive [reviewed in (Oikonomou and Shaham 2011)]

C. elegans has been extensively utilized to study neuronal function and communication. Only recently, it has emerged as an invertebrate model to study glial cells [reviewed in (Oikonomou and Shaham 2011)]. Our demonstration of VGCC-mediated Ca^{2+} dynamics in cultured CEPsh glial cells is a major advance in our understanding of glial cells and the nervous system of *C. elegans.*

Acknowledgments

This work was supported by the National Science Foundation (CBET 0943343). Some nematode strains used in this work were provided by the Caenorhabditis Genetics Center, which is funded by the NIH National Center for Research Resources (NCRR). We would like to thank Dr. Morris Maduro for help with starting up the *C. elegans* research in our laboratory. We thank William Lee for some assistance with imaging and Dr. Gina Broitman-Maduro for practical training on production of transgenic worm

strains. We thank Dr. Michael Miller for help with strain crosses and genotyping. The Heflin Center Genomics Core at UAB provided sequencing information for the DNA plasmids used in this work.

References

Araque A, Parpura V, Sanzgiri RP, Haydon PG. 1999. Tripartite synapses: glia, the unacknowledged partner. *Trends Neurosci* **22**: 208-215.

Asakura T, Waga N, Ogura K, Goshima Y. 2010. Genes required for cellular UNC-6/netrin localization in Caenorhabditis elegans. *Genetics* **185**: 573-585.

Bading H, Ginty DD, Greenberg ME. 1993. Regulation of gene expression in hippocampal neurons by distinct calcium signaling pathways. *Science* **260**: 181-186.

Benjamins JA, Nedelkoska L. 1996. Release of intracellular calcium stores leads to retraction of membrane sheets and cell death in mature mouse oligodendrocytes. *Neurochem Res* **21**: 471-479.

Bers DM. 2002. Cardiac excitation-contraction coupling. *Nature* **415**: 198-205.

Brenner M, Kisseberth WC, Su Y, Besnard F, Messing A. 1994. GFAP promoter directs astrocyte-specific expression in transgenic mice. *J Neurosci* **14**: 1030-1037.

Bushong EA, Martone ME, Jones YZ, Ellisman MH. 2002. Protoplasmic astrocytes in CA1 stratum radiatum occupy separate anatomical domains. *J Neurosci* **22**: 183-192.

Carvelli L, McDonald PW, Blakely RD, Defelice LJ. 2004. Dopamine transporters depolarize neurons by a channel mechanism. *Proc Natl Acad Sci U S A* **101**: 16046-16051.

Christensen M, Strange K. 2001. Developmental regulation of a novel outwardly rectifying mechanosensitive anion channel in Caenorhabditis elegans. *J Biol Chem* **276**: 45024-45030.

Colon-Ramos DA, Margeta MA, Shen K. 2007. Glia promote local synaptogenesis through UNC-6 (netrin) signaling in C. elegans. *Science* **318**: 103-106.

D'Ascenzo M, Vairano M, Andreassi C, Navarra P, Azzena GB, Grassi C. 2004. Electrophysiological and molecular evidence of L-(Cav1), N- (Cav2.2), and R-(Cav2.3) type Ca2+ channels in rat cortical astrocytes. *Glia* **45**: 354-363.

Fields RD. 2008. Oligodendrocytes changing the rules: action potentials in glia and oligodendrocytes controlling action potentials. *Neuroscientist* **14**: 540-543.

Figueiredo M, Lane S, Tang F, Liu BH, Hewinson J, Marina N, Kasymov V, Souslova EA, Chudakov DM, Gourine AV et al. 2011. Optogenetic experimentation on astrocytes. *Exp Physiol* **96**: 40-50.

Frokjaer-Jensen C, Kindt KS, Kerr RA, Suzuki H, Melnik-Martinez K, Gerstbreih B, Driscol M, Schafer WR. 2006. Effects of voltage-gated calcium channel subunit genes on calcium influx in cultured C. elegans mechanosensory neurons. *J Neurobiol* **66**: 1125-1139.

Fulton D, Paez PM, Fisher R, Handley V, Colwell CS, Campagnoni AT. 2010. Regulation of L-type Ca++ currents and process morphology in white matter oligodendrocyte precursor cells by golli-myelin proteins. *Glia* **58**: 1292-1303.

Gomez-Ospina N, Tsuruta F, Barreto-Chang O, Hu L, Dolmetsch R. 2006. The C terminus of the L-type voltage-gated calcium channel Ca(V)1.2 encodes a transcription factor. *Cell* **127**: 591-606.

Halassa MM, Florian C, Fellin T, Munoz JR, Lee SY, Abel T, Haydon PG, Frank MG. 2009. Astrocytic modulation of sleep homeostasis and cognitive consequences of sleep loss. *Neuron* **61**: 213-219.

Hall DH, Russell RL. 1991. The posterior nervous system of the nematode Caenorhabditis elegans: serial reconstruction of identified neurons and complete pattern of synaptic interactions. *J Neurosci* **11**: 1-22.

Hanisch UK, Kettenmann H. 2007. Microglia: active sensor and versatile effector cells in the normal and pathologic brain. *Nat Neurosci* **10**: 1387-1394.

Hedgecock EM, Culotti JG, Hall DH. 1990. The unc-5, unc-6, and unc-40 genes guide circumferential migrations of pioneer axons and mesodermal cells on the epidermis in C. elegans. *Neuron* **4**: 61-85.

Heiman MG, Shaham S. 2007. Ancestral roles of glia suggested by the nervous system of Caenorhabditis elegans. *Neuron Glia Biol* **3**: 55-61.

Hua X, Malarkey EB, Sunjara V, Rosenwald SE, Li WH, Parpura V. 2004. Ca2+-dependent glutamate release involves two classes of endoplasmic reticulum Ca2+ stores in astrocytes. *J Neurosci Res* **76**: 86-97.

Hui K, Kwok TC, Kostelecki W, Leen J, Roy PJ, Feng ZP. 2009. Differential sensitivities of CaV1.2 IIS5-S6 mutants to 1,4-dihydropyridine analogs. *Eur J Pharmacol* **602**: 255-261.

Jospin M, Jacquemond V, Mariol MC, Segalat L, Allard B. 2002. The L-type voltage-dependent Ca2+ channel EGL-19 controls body wall muscle function in Caenorhabditis elegans. *J Cell Biol* **159**: 337-348.

Kwok TC, Ricker N, Fraser R, Chan AW, Burns A, Stanley EF, McCourt P, Cutler SR, Roy PJ. 2006. A small-molecule screen in C. elegans yields a new calcium channel antagonist. *Nature* **441**: 91-95.

Lee SH, Kim WT, Cornell-Bell AH, Sontheimer H. 1994. Astrocytes exhibit regional specificity in gap-junction coupling. *Glia* **11**: 315-325.

Lim YS, Mallapur S, Kao G, Ren XC, Wadsworth WG. 1999. Netrin UNC-6 and the regulation of branching and extension of motoneuron axons from the ventral nerve cord of Caenorhabditis elegans. *J Neurosci* **19**: 7048-7056.

Liu P, Ge Q, Chen B, Salkoff L, Kotlikoff MI, Wang ZW. 2011. Genetic dissection of ion currents underlying all-or-none action potentials in C. elegans body-wall muscle cells. *J Physiol* **589**: 101-117.

Malarkey EB, Ni Y, Parpura V. 2008. Ca2+ entry through TRPC1 channels contributes to intracellular Ca2+ dynamics and consequent glutamate release from rat astrocytes. *Glia* **56**: 821-835.

Mathews, E.A., Garcia, E., Santi, C.M., Mullen, G.P., Thacker, C., Moerman, D.G., and Snutch, T.P. 2003. Critical residues of the Caenorhabditis elegans unc-2 voltage-gated calcium channel that affect behavioral and physiological properties. *J Neurosci* **23**(16): 6537-6545.

McMiller TL, Johnson CM. 2005. Molecular characterization of HLH-17, a C. elegans bHLH protein required for normal larval development. *Gene* **356**: 1-10.
McNally K, Audhya A, Oegema K, McNally FJ. 2006. Katanin controls mitotic and meiotic spindle length. *J Cell Biol* **175**: 881-891.
Montana V, Malarkey EB, Verderio C, Matteoli M, Parpura V. 2006. Vesicular transmitter release from astrocytes. *Glia* **54**: 700-715.
Nickell WT, Pun RY, Bargmann CI, Kleene SJ. 2002. Single ionic channels of two Caenorhabditis elegans chemosensory neurons in native membrane. *J Membr Biol* **189**: 55-66.
Ogata K, Kosaka T. 2002. Structural and quantitative analysis of astrocytes in the mouse hippocampus. *Neuroscience* **113**: 221-233.
Oikonomou G, Shaham S. 2011. The Glia of Caenorhabditis elegans. *Glia* **In Press**.
Paez PM, Fulton D, Colwell CS, Campagnoni AT. 2009. Voltage-operated Ca2+ and Na+ channels in the oligodendrocyte lineage. *J Neurosci Res* **87**: 3259-3266.
Parpura V, Basarsky TA, Liu F, Jeftinija K, Jeftinija S, Haydon PG. 1994. Glutamate-mediated astrocyte-neuron signalling. *Nature* **369**: 744-747.
Reyes RC, Parpura V. 2008. Mitochondria modulate Ca2+-dependent glutamate release from rat cortical astrocytes. *J Neurosci* **28**: 9682-9691.
Reyes RC, Parpura V. 2009. The trinity of Ca2+ sources for the exocytotic glutamate release from astrocytes. *Neurochem Int* **55**: 2-8.
Saheki Y, Bargmann CI. 2009. Presynaptic CaV2 calcium channel traffic requires CALF-1 and the alpha2delta subunit UNC-36. *Nat Neurosci* **12**: 1257-1265.
Schafer WR, Kenyon CJ. 1995. A calcium-channel homologue required for adaptation to dopamine and serotonin in Caenorhabditis elegans. *Nature* **375**: 73-78.
Seifert G, Steinhäuser C. 2004. Ion channels in astrocytes. in *Glial óNeuronal Signaling* (eds. GI Hatton, V Parpura), pp. 187-213. Kluwer Academic Publishers, Boston, MA.
Shtonda B, Avery L. 2005. CCA-1, EGL-19 and EXP-2 currents shape action potentials in the Caenorhabditis elegans pharynx. *J Exp Biol* **208**: 2177-2190.
Slezak M, Pfrieger FW. 2004. Role of astrocytes in the formation, maturation andmaintenance of synapses. in *Glial óNeuronal Signaling* (eds. GI Hatton, V Parpura). Kluwer Academic Publishers, Boston, MA.
Stout RF, Jr., Parpura V. 2011a. Voltage-gated calcium channel types in cultured C. elegans CEPsh glial cells. *Cell Calcium* **50**: 98-108.
Tallini YN, Ohkura M, Choi BR, Ji G, Imoto K, Doran R, Lee J, Plan P, Wilson J, Xin HB et al. 2006. Imaging cellular signals in the heart in vivo: Cardiac expression of the high-signal Ca2+ indicator GCaMP2. *Proc Natl Acad Sci U S A* **103**: 4753-4758.
Tam T, Mathews E, Snutch TP, Schafer WR. 2000. Voltage-gated calcium channels direct neuronal migration in Caenorhabditis elegans. *Dev Biol* **226**: 104-117.
Tsien RW. 1983. Calcium channels in excitable cell membranes. *Annu Rev Physiol* **45**: 341-358.
Verkhratsky A, Steinhauser C. 2000. Ion channels in glial cells. *Brain Res Brain Res Rev* **32**: 380-412.

Wadsworth WG, Bhatt H, Hedgecock EM. 1996. Neuroglia and pioneer neurons express UNC-6 to provide global and local netrin cues for guiding migrations in C. elegans. *Neuron* **16**: 35-46.

Ward S, Thomson N, White JG, Brenner S. 1975. Electron microscopical reconstruction of the anterior sensory anatomy of the nematode Caenorhabditis elegans.?2UU. *J Comp Neurol* **160**: 313-337.

White JG, Southgate E, Thomson JN, Brenner S. 1976. The structure of the ventral nerve cord of Caenorhabditis elegans. *Philos Trans R Soc Lond B Biol Sci* **275**: 327-348.

Yaguchi T, Nishizaki T. 2010. Extracellular high K+ stimulates vesicular glutamate release from astrocytes by activating voltage-dependent calcium channels. *J Cell Physiol* **225**: 512-518.

Yoo AS, Krieger C, Kim SU. 1999. Process extension and intracellular Ca2+ in cultured murine oligodendrocytes. *Brain Res* **827**: 19-27.

Yoshimura S, Murray JI, Lu Y, Waterston RH, Shaham S. 2008. mls-2 and vab-3 Control glia development, hlh-17/Olig expression and glia-dependent neurite extension in C. elegans. *Development* **135**: 2263-2275.

DISCUSSION

Summary

This dissertation encompasses studies on how *C. elegans* can be used as a model organism to better understand the scope of functions of the glial cell type. I present the first experimental information about *C. elegans* glial functions with temporal resolution in the range of seconds and go on to explore the underlying genetic components. I described the use of transgenic technology with classic mutant strains and breeding to analyze *C. elegans* glial calcium fluctuations. In this section I discuss what my findings on worm glia mean for research on the nervous system of this nematode species and glial research in general. I will also describe how this basic research serendipitously led to the first strong evidence for trans-promoter induced behavior changes that, in combination with aspects of *C. elegans* biology, can be used in investigations of human diseases and has potential as a novel therapy in human diseases.

Comparison between C. elegans and Drosophila melanogaster glia

Because there are four general categories of glia in the fly compared to only two in worms (the sheath and socket, three if the CEPsh cells are considered a separate group from other sheath cells based on their morphology), the glia of Drosophila may be able to take on more specialized roles within the central nervous system [see (Parker and Auld

2006) and (Freeman and Doherty 2006) for reviews on *Drosophila* glia]. My research also indicates that neuron-glia signaling in the worm nervous system may be less advanced, in the sense that the CEPsh glia respond more readily to a generalized indicator of neuron activity (membrane depolarization) than to the more specialized signaling through neurotransmitter receptors. However, I have not completely ruled out *in vivo* expression and function of these receptors in worm glia, which could be addressed in the future through similar genetic and pharmacological approaches as those I used in my studies as discussed in later sub-sections of this dissertation.

Using the Phlh-17 to mark CEPsh glia in future studies

I have used the trans-*Phlh-17* throughout my research, as others have for publications examining neuronal development and behavior (Colon-Ramos et al. 2007; Felton and Johnson 2011). I defined effects that this genetic tool have on the worm at the level of behavior and then preformed experiments designed to circumvent confounding issues created by such effects through the use of cell culture. Some aspects of cell culture limit the conclusions that can be drawn from experiments in which it is used, but as a first step in finding roles that CEPsh glia have in the development and function of the nervous system, cell culture was a logical starting point when our findings on trans-*Phlh-17* effects are considered. These findings should be used when designing future experiments that will extend research on *C. elegans* glia to other functions and to test for forms of cellular signaling, such as for the presence of G-protein coupled receptors in the CEPsh glia.

How the glia of C. elegans compare with those of mammals

The purpose for using *C. elegans* as a model to study glia is to overcome obstacles that have been encountered in mammalian glial research. The full scope of functions that the macroglia: astrocytes, oligodendrocytes perform in development and in adulthood in the human brain is far from complete. Working with the information we do have, though, I put the findings of my work into context. A major influence on development of oligodendrocytes and a cornerstone in the current model of how astrocytes modulate synaptic activity is changes in calcium levels. The activity of neurons in the vicinity of these macroglia is sensed by VGCCs in the case of oligodendrocyte precursors and by neurotransmitter receptors in the case of astrocytes (Paez et al. 2009; Verkhratsky et al. 2009). One major way mammalian macroglia respond to neuronal activity is through increases in cytosolic calcium levels (Di Garbo et al. 2007; Deitmer et al. 2009). Therefore, the demonstration by my research that CEPsh cells in culture express channels that would allow them to undertake this function points to similarity between the roles of glia in mammals and nematodes, however, there are caveats raised by the use of cell culture that should be considered.

Do CEPsh cells undergo calcium level changes in vivo?

Gene expression and cell function changes from those of *in vivo* conditions have been reported in cultured astrocytes (Passaquin et al. 1994). This raises the question of if the depolarization induced calcium increases that I find in cultured *C. elegans* glia are due to culture conditions since large and rapid increases in GCaMP2.0 fluorescence were

not observed in the intact worm, even in the rare cases when expression was easily observable. In my experiments in culture conditions the stimulus in the form of 100 mM K^+ external solution contacted most of the glial cell membrane nearly simultaneously. There is almost no way that a large portion of the CEPsh cell membrane could be exposed to 100 mM K^+ extracellular solution in the intact worm where, instead, isolated subdomains of the CEPsh cell membrane may be depolarized by potassium release from axons or the cell body of neurons during intense activity (*C.* elegans neurons and muscle have been shown to express and use inwardly rectifying potassium channels to re-polarize following excitation) (Bargmann 1998; Davis et al. 1999; Fleischhauer et al. 2000; Shtonda and Avery 2005). In order to test if this scenario actually occurs in reality, a combination of a glial membrane localized genetically encoded calcium sensor and a restrained worm preparation might be necessary (Chronis et al. 2007; Shigetomi et al. 2010).

This idea of subdivisions of the CEPsh cell being exposed to different extracellular environments highlights may explain why the CEPsh glia express multiple VGCC types. In the intact worm the expression and trafficking of each type may be directed to areas of the CEPsh cell or developmental stages where the low or high voltage gating of the channels fits the requirements needed for proper CEPsh cell function. The unexpected increase in total calcium influx with the deletion of the T-type encoding gene may reflect dis-regulation of voltage gated responses due to a missing component of a system genetically setup to perform multiple fine-tuned responses across separate areas of each glial cell. Since the thin membrane processes extend to many specific parts of the

worm central nerve ring, if subdomains of the CEPsh cells can respond differentially, this might allow synapse specific control over development or neuron activity.

Possible functional outcomes of CEPsh cell calcium dynamics

The ventral pair of CEPsh cells expresses netrin (UNC-6) and its expression is required for normal synapse development (Wadsworth et al. 1996; Colon-Ramos et al. 2007). Netrin is a secreted protein and its normal trafficking in *C. elegans* requires SNARE proteins (Asakura et al. 2010). Voltage-Gated Calcium Channels in mammals have been shown to regulate netrin expression (Gomez-Ospina et al. 2006). While indirect, the information above along with the results of my research point to a role for depolarization induced calcium dynamics in the expression and release of netrin to help guide development of the *C. elegans* nervous system. This could be an exciting area for future studies on nematode glia. Netrin fusions to fluorescent reporters have been used by Colon-Ramos et. al. 2007 and others, and examination of their expression and trafficking in *in vitro* with membrane depolarization and *in vivo* with the VGCC mutants used in my research would be very interesting research directions (Colon-Ramos et al. 2007; Ziel et al. 2009). Another way calcium dynamics might affect the nervous system is through modulating glial morphology. There is variability, even within integrated lines, in the pattern disclosed by *Phlh-17::GFP* disclosed CEPsh cell extensions around the nerve ring. In future studies the lines expressing light gated channels such as channelrhodopsin-2 in the CEPsh cells could be subjected to chronic stimulation to tests for effects on glial or neuronal development. Controls based on the parameters I established in CHAPTER 1 of this manuscript would need to be employed.

What CEPsh cell calcium changes in culture reveal about mammalian astrocytes and glia in general

First my results showing that membrane depolarization induced calcium changes in cultured CEPsh glia indicate that while the signal may be more generalized (sensing general activity through K^+ elevation instead of a specific neurotransmitter) in this evolutionarily earlier "proto-astrocytes" worm glial cell, neuron glial signaling seems to have appeared early in the evolution of glia. Earlier forms of glia compared to mammalian astrocytes also respond to K^+ elevation with Ca^{2+}, which supports a move toward more complex, specialized calcium signaling with the evolution of more complex nervous systems. Although they do not express the specialized protein found in the myelin of mammalian oligodendrocytes, the CEPsh glia of *C. elegans* also seem to have a similar function of both oligodendrocytes and astrocyte whereby they form membrane structures that surround neuronal processes and separate the neuropil form the rest of the body. The CEPsh cells of *C. elegans* may have taken on a dual role as both a sheath cells and a proto-astrocyte while co-opting this less specialized method for responding to neuron activity to begin to take on some of the roles astrocytes perform through calcium signaling in vertebrates. Therefore I propose they represent a unique "snapshot" of the evolution of macroglia that can be studied to better understand human astrocyte function.

This highlights an interesting comparison since just as some connexin subunits of gap junctions are expressed in only glia within the nervous system, some innexin genes seem to be expressed predominantly in the sheath and socket cells of *C. elegans*. This is particularly striking since the innexins of invertebrates and connexins of vertebrates

perform very similar, specialized cellular functions but do not have significant sequence homology (Scemes et al. 2009).

The CEPsh glia form a tiling arrangement and express innexins but do not appear to form gap junctions with each other (White et al. 1986; Altun et al. 2009; Oikonomou and Shaham 2011). The expression pattern for one of the innexin genes has led some researchers to speculate that glia use innexins to form both a junction with the worm version of the excretory system and, at the same time, a barrier between the rest of the body and the nervous system (Altun et al. 2009). It is tempting to speculate further that the CEPsh glia of the worm form four domains similar to the domains/divisions of the nervous system that are formed by mammalian astrocytes (Bushong et al. 2002). In this same vein of thinking, learning more about the purposes of glial calcium signaling in the worm and its functional roles in the nervous system may provide explanations as to why the number and size of astrocytes (and thereby domain complexity) seems to increase with nervous system complexity (Oberheim et al. 2006; Heiman and Shaham 2007; Oberheim et al. 2009; Hartline 2011).

Calcium responses to receptor signaling in C. elegans glia

Astrocytes and oligodendrocytes in mammalian glia can sense neuronal activity directly though ionotropic and metabotropic purinergic and glutamate receptors, as reviewed in (Verkhratsky et al. 2009). Therefore I initiated a pilot study to test if the cultured CEPsh glia respond to neurotransmitters that are known to be released by neurons near the CEPsh cells in the intact worm. The data was not included in the published findings that make up earlier sections of this text but do indicate that further

tests using other neurotransmitters might give positive results. Neurons within the nerve ring of the worm are known to release glutamate, γ-Aminobutyric acid, dopamine, serotonin, acetylcholine, and some more obscure compounds such as octopamine and a wide array of neuropeptides. I did not see robust calcium level changes in cells cultured from VPR108 *vprIs108[Phlh-17::mCherry + Phlh-17::GCaMP2.0]* worms when I applied the neurotransmitters listed in Table 3. All tests were conducted with the same methods as those for the 100 mM K^+ external membrane depolarization experiments, only instead normal external solution (5 mM K^+) and the pharmacological agent was applied to the cells. We only saw one response in all of the tests with neurotransmitter application to cultured cells (1/28 tests for all neurotransmitters, see Table 3). The lone significant increase in calcium was likely an example of the spontaneous events that rarely occur in the CEPsh cells as in noted in the controls of CHAPTER 3. It would be worthwhile, though, to test for responses to application of other neurotransmitters but the list of possible stimuli that CEPsh cells might be exposed to is quite extensive. Since the neurons of *C. elegans* are known to respond to a wide range of peptides that signal through G-coupled protein receptors (GPCRs), I decided to take a more general, inclusive approach to testing experimental stimuli. The Gi stimulator/ Go inhibitor melittin was applied to cultured CEPsh cells from VPR108 worms (Fukushima et al. 1998). Melittin was applied at a concentration of 500 nM in normal external solution as a bath application.

Table 3.

A Selection of Neurotransmitters and Pharmacological Compounds Tested on Cultured CEPsh Cells.

Stimulus	Concentration in External Soln.	Number of Responding Cells/ Number Tested
Glutamate	100 μM	1/21
ATP	100 μM	0/4
Dopamine	100 μM	0/3
Melittin	500 nM	2/15*

* 5/15 cells tested showed a large decrease in dF/Fo after 500 nM melittin application while 2/15 displayed an increase in dF/Fo immediately after melittin application that was 6 standard deviations over Fo. Both responses would have been labeled oscillators (Category 3) based on the parameters established in CHAPTER 3 of this text.

The low occurrence of calcium responses to neurotransmitter receptor stimulation in cultured CEPsh glial cells could be due to several factors other than their absences from glia in the intact nervous system. Expression or trafficking of receptors for neurotransmitters in the CEPsh glia may be dependent on other signals from neurons or other cell types. Additionally, we observe a different morphology in culture than what has been observed *in vivo* (as discussed in CHAPTER 2). Cultured primary mammalian astrocytes also display different morphology in culture compared to their *in vivo* appearance. It is conceivable that these neurotransmitter receptors are displayed on the membrane at specific structures of the CEPsh glia in the intact nervous system. Since

cultured *C. elegans* cells have also been found to be somewhat locked into a differentiated state, we would not expect to see responses to neurotransmitters that are only transiently and developmentally regulated (Strange et al. 2007). Along these same lines astrocytes have slightly altered gene expression but do not show characteristics of de-differentiation *in vitro* (Montana et al. 2004). Therefore, it is possible but unlikely that there is a loss of expression for receptors that are expressed in the early embryonic development of the intact worm. The expression of receptors for the set of neurotransmitters tested here (or others such as serotonin, GABA, acetylcholine, or octopamine) should be included in the list of stimuli applied in future studies using the next generation of genetically encoded indicators.

The test results of this small pilot study indicate that, in culture, the CEPsh cells may express GPCRs that are activated by signals that we have not yet tested. This could be an area for future study that would include both pharmacological and genetic based tests using the methods and worm lines I developed in my graduate research. By crossing worm strains carrying mutations for components of the GPCR signaling system with line VPR108 (see Table 1 of CHAPTER 1 for strain descriptions) carrying the genetically encoded calcium indicator it would be possible to further define the roles that various neuropeptides have on glial calcium levels. Since *C. elegans* glia share some similar characteristics as mammals at the gene expression and functional levels, information about neuron-glia signaling through GPCRs might be informative to human diseases or pharmacological therapies.

Neurotransmitter reuptake

In a study by Spencer et al, the trans-*Phlh-17* was used to drive expression of a general RNA binding protein with an epitope tag that allow the transcript levels for all genes expressed in the CEPsh cells to be compared to gene expression in the rest of the cells of the worm (Spencer et al. 2011). Two of the many interesting genes that were found to be preferentially expressed in the CEPsh glia are the worm homolog for glutamine synthetase and the plasma membrane glutamate transporter glt-1 (see supplemental data in (Spencer et al. 2011)). As glutamate transport from the extracellular space into glia is important for synaptic signaling and cell survival, this would be a fascinating macroglial function to study in the worm. If the CEPsh glia are eventually shown to have the ability to take up glutamate then it will be important to consider calcium dynamics data that I have produced in my dissertation research. For instance, in mice expression of the glutamate transporter GLAST has been shown to be influenced by calcium levels (Liu et al. 2010). It will be important to determine if glutamate transporters and calcium signaling interact in worm glia as this would show that fine-tuned expression of neurotransmitter re-uptake genes is an early derived and fundamental function of glia. Altogether the findings of my research indicate that glia of *C. elegans* retain many of the functions of macroglia of mammals but in a less complex form.

Extending tests for CEPsh calcium dynamics to the intact worm

As noted in CHAPTERs 2 and 3 of this manuscript the level of GCaMP2 fluorescence is very low in the transgenic line I used throughout this work: strain VPR108. I made four separate lines and obtained integrated lines carrying the *Phlh-17::GCaMP2* transgene but none of the attempts produced lines with higher *in vivo* GCaMP2 signals. Since GCaMP2 has been shown to buffer calcium (all genetically encoded calcium sensors do this to some degree), this may indicate that calcium levels are normally low in the CEPsh cells or that high expression and buffering is not tolerated by the CEPsh cells. Alternatively, if high copy numbers of the trans-*Phlh-17* cause disruption of glial function, as is indicated in CHAPTER 1, then the use of multiple CEPsh specific promoters might be a way to boost the expression and signal from genetically encoded calcium sensors. No other CEPsh specific promoters are known but some candidates have been identified that are only expressed in cells in other parts of the worm body such the promoters for *nhr-57* or *ptr-10* (Yoshimura et al. 2008; Shao et al. 2009). My work in identifying and quantifying effects of the t-*Phlh-17* will allow better experimental design in future research on *C. elegans* glia.

Transcription factor networks

Diseases caused by expansion or duplication of sections of genetic code with highly repetitive nature are common, particularly in dysfunction of the nervous system. The reasons why repetitive genetic sequences are more susceptible are obvious if anyone who has tried to copy information considers that chromosomal replication and segregation involve similar actions by the machinery of the cell. The reasons why repetitive sequence mutations seem to be over-represented by neurological disorders instead of evenly distributed across the list of possible human maladies are likely to be the same as why genetic mutations in general seem to affect the nervous system preferentially. The nervous system itself, its protein constitution, its cellular interactions during development, and its transcriptional regulatory system for gene expression are all multi-level networks. Comparisons of mathematical and biological models of network (in)stability show that the gene-protein system that forms a network that functions to build a living organism such as a *C. elegans* worm is finely tuned and that alterations in the level of one component can have surprisingly large effects on the network as a whole (Vermeirssen et al. 2007; Grove et al. 2009). Since behavior is the output of a "layer-cake" of networks, it is not surprising that small changes in the base layer (the genetic code) so often lead to variable and unpredictable effects at the level of system output (behavior) (Oltvai and Barabasi 2002). The t-*Phlh-17* induced VCP that I discovered is variable and shows a threshold nature that I suggest is a reflection of it being a change to the genetic base network of the worm that has non-digital effects on the next, higher-level network: transcription factor interactions and gene regulation.

There has been some recent research using *C. elegans* to study genetic factors that confer flexibility or robustness to the gene regulatory network. Knowledge gained during my dissertation research will provide an important background for future studies in this area and may be useful as a research tool.

Human repeat expansion diseases

The primary causes of nervous system dysfunction in some human repeat expansion diseases are known. Expansion of trinucleotide repeats within the protein coding region of the Huntingtin and CACNA1 genes leads to Huntington's disease and Spinocerebellar ataxia type 6, respectively, among a long list of other trinucleotide expansion-caused neurological diseases (Zhuchenko et al. 1997; Nance et al. 1999). However, not all repeat expansion diseases are caused by changes in protein coding regions. Fragile X syndrome is mainly caused by the loss of FMR1 protein expression induced by disruption of the regulatory region in its encoding gene by repeat expansion (Verkerk et al. 1991). Other diseases caused by repetitive sequence mutations occurring in non-regulatory regions are not as well understood and do not involve loss of transcription of the gene. Many mechanisms by which repetitive sequences in non-coding regions could lead to behavioral phenotypes have been put forward; often these mechanisms are supported by tests with transgenic model organisms. Fragile X-associated tremor/ataxia syndrome (FXTAS) is thought to be caused by repeat expansion through the elongation of an untranslated region of the transcript through accumulation toxic levels of RNA within the nucleus (Hessl et al. 2005; Tassone et al. 2007; Garcia-Arocena and Hagerman 2010). How this lengthened transcript leads to cellular

dysfunction is not fully understood but the sequestration of RNA binding proteins is one proposed possibility (Ebralidze et al. 2004; Lin et al. 2006). There is substantial evidence based on human studies and work with model organisms such as *Drosophila* and *C. elegans* that some of the main aspects of cellular pathology in myotonic dystrophy type 1 (DM1) are caused by sequestration of the RNA binding protein Muscleblind and its homologues (Miller et al. 2000; Jiang et al. 2004; Wang et al. 2011) but see (Houseley et al. 2005). As transcripts that contain DNA or RNA binding sequences, these expanded transcripts and DNA sequences would be expected to be able to bind more of the protein species that it normally binds or possibly even leads to aberrant binding to new DNA/RNA binding proteins since transcription factors have been shown to sometimes work in concert. I propose that this aberrant binding and removal of protein factors from the active pool within neurons causes some symptoms of human repetitive sequence based diseases, possibly even in diseases that do have a primary cause induced by loss of expression of a particular protein.

Trans-promoters in C. elegans to model transcription factor sequestration in human repeat expansion diseases

A better system than *C. elegans* for studying these effects of repetitive sequences and/or stochastic changes in DNA binding proteins is hard to imagine. Worms are easily made to contain and transmit foreign DNA sequences and the sequences can be introduced in the form of a single copy or automatically made repetitive depending on the desired applications (Mello et al. 1991; Frokjaer-Jensen et al. 2008; Meister et al. 2010). The worm has one of the most well studied developmental transcriptional regulatory

networks of all organisms with a nervous system (Reece-Hoyes et al. 2005). The effects of DNA binding factor sequestration on the nervous system can be easily measured at the cellular or behavioral level in this model organism.

Trans-DNA binding sequences as therapy

Since the VCP that we found to be caused by the trans-*Phlh-17* is likely produced by improper excitation and contraction control of the worm body muscles by the nervous system, it can be viewed as a phenotype due to imbalance of neuron or glial activity. Many human neurological diseases are manifestations of imbalances of cellular activity in the brain. Human nervous system disorders often have a multigenic pathology and a spectrum of severities. In this context an effective corrective measure should be able to have genetic specificity while being able to target multiple genes and also have tune-ability. It is conceivable that the introduction of properly designed trans-DNA binding sequences could have all of these properties once gene-therapy technologies are further developed. For instance a specific set of genes could be up-regulated by introducing repeats of a DNA sequence that binds repressor transcription factors for those genes. The degree of up-regulation could be tuned to the desired level through the number of binding sites (repeats) introduced. This use of trans-DNA binding sequences is unproven at this time but could be tested for feasibility in the worm using the *Phlh-17* through testing if, as a trans-promoter, it could alleviate locomotor defects in worms with a dorsal coiling phenotype caused by transgenes containing a gene linked to locomotor dysfunction in humans (Ash et al. 2010).

GENERAL REFERENCES

Agulhon, C., Petravicz, J., McMullen, A.B., Sweger, E.J., Minton, S.K., Taves, S.R., Casper, K.B., Fiacco, T.A., and McCarthy, K.D. 2008. What is the role of astrocyte calcium in neurophysiology? *Neuron* **59**(6): 932-946.

Altun, Z.F., Chen, B., Wang, Z.W., and Hall, D.H. 2009. High resolution map of Caenorhabditis elegans gap junction proteins. *Dev Dyn* **238**(8): 1936-1950.

Araque, A., Parpura, V., Sanzgiri, R.P., and Haydon, P.G. 1999. Tripartite synapses: glia, the unacknowledged partner. *Trends Neurosci* **22**(5): 208-215.

Asakura, T., Waga, N., Ogura, K., and Goshima, Y. 2010. Genes required for cellular UNC-6/netrin localization in Caenorhabditis elegans. *Genetics* **185**(2): 573-585.

Ash, P.E., Zhang, Y.J., Roberts, C.M., Saldi, T., Hutter, H., Buratti, E., Petrucelli, L., and Link, C.D. 2010. Neurotoxic effects of TDP-43 overexpression in C. elegans. *Hum Mol Genet* **19**(16): 3206-3218.

Bacaj, T. and Shaham, S. 2007. Temporal control of cell-specific transgene expression in Caenorhabditis elegans. *Genetics* **176**(4): 2651-2655.

Bacaj, T., Tevlin, M., Lu, Y., and Shaham, S. 2008. Glia are essential for sensory organ function in C. elegans. *Science* **322**(5902): 744-747.

Bading, H., Ginty, D.D., and Greenberg, M.E. 1993. Regulation of gene expression in hippocampal neurons by distinct calcium signaling pathways. *Science* **260**(5105): 181-186.

Bargmann, C.I. 1998. Neurobiology of the Caenorhabditis elegans Genome. *Science* **282**(5396): 2028-2033.

Barr, M.M. 2003. Super models. *Physiol Genomics* **13**(1): 15-24.

Bauer Huang, S.L., Saheki, Y., VanHoven, M.K., Torayama, I., Ishihara, T., Katsura, I., van der Linden, A., Sengupta, P., and Bargmann, C.I. 2007. Left-right olfactory asymmetry results from antagonistic functions of voltage-activated calcium channels and the Raw repeat protein OLRN-1 in C. elegans. *Neural Dev* **2**: 24.

Benjamins, J.A. and Nedelkoska, L. 1996. Release of intracellular calcium stores leads to retraction of membrane sheets and cell death in mature mouse oligodendrocytes. *Neurochem Res* **21**(4): 471-479.

Berkowitz, L.A., Knight, A.L., Caldwell, G.A., and Caldwell, K.A. 2008. Generation of stable transgenic C. elegans using microinjection. *J Vis Exp*(18): pii: 833. doi: 810.3791/3833.

Bers, D.M. 2002. Cardiac excitation-contraction coupling. *Nature* **415**(6868): 198-205.

Bianchi, L. and Driscoll, M. 2006. Culture of embryonic C. elegans cells for electrophysiological and pharmacological analyses. *WormBook*: 1-15.

Bolsover, S. and Silver, R.A. 1991. Artifacts in calcium measurement: recognition and remedies. *Trends Cell Biol* **1**(2-3): 71-74.
Brenner, M., Kisseberth, W.C., Su, Y., Besnard, F., and Messing, A. 1994. GFAP promoter directs astrocyte-specific expression in transgenic mice. *J Neurosci* **14**(3 Pt 1): 1030-1037.
Brenner, S. 1974. The genetics of Caenorhabditis elegans. *Genetics* **77**(1): 71-94.
Brightman, M.W. and Reese, T.S. 1969. Junctions between intimately apposed cell membranes in the vertebrate brain. *J Cell Biol* **40**(3): 648-677.
Buechner, M., Hall, D.H., Bhatt, H., and Hedgecock, E.M. 1999. Cystic canal mutants in Caenorhabditis elegans are defective in the apical membrane domain of the renal (excretory) cell. *Dev Biol* **214**(1): 227-241.
Bunge, M.B., Bunge, R.P., and Pappas, G.D. 1962. Electron microscopic demonstration of connections between glia and myelin sheaths in the developing mammalian central nervous system. *J Cell Biol* **12**: 448-453.
Bushong, E.A., Martone, M.E., Jones, Y.Z., and Ellisman, M.H. 2002. Protoplasmic astrocytes in CA1 stratum radiatum occupy separate anatomical domains. *J Neurosci* **22**(1): 183-192.
Cai, J., Chen, Y., Cai, W.H., Hurlock, E.C., Wu, H., Kernie, S.G., Parada, L.F., and Lu, Q.R. 2007. A crucial role for Olig2 in white matter astrocyte development. *Development* **134**(10): 1887-1899.
Carvelli, L., McDonald, P.W., Blakely, R.D., and Defelice, L.J. 2004. Dopamine transporters depolarize neurons by a channel mechanism. *Proc Natl Acad Sci U S A* **101**(45): 16046-16051.
Casper, K.B., Jones, K., and McCarthy, K.D. 2007. Characterization of astrocyte-specific conditional knockouts. *Genesis* **45**(5): 292-299.
Catterall, W.A. 2011. Voltage-gated calcium channels. *Cold Spring Harb Perspect Biol* **3**(8).
Cavanaugh, K.P., Gurwitz, D., Cunningham, D.D., and Bradshaw, R.A. 1990. Reciprocal modulation of astrocyte stellation by thrombin and protease nexin-1. *J Neurochem* **54**(5): 1735-1743.
Chalasani, S.H., Kato, S., Albrecht, D.R., Nakagawa, T., Abbott, L.F., and Bargmann, C.I. 2010. Neuropeptide feedback modifies odor-evoked dynamics in Caenorhabditis elegans olfactory neurons. *Nat Neurosci* **13**(5): 615-621.
Chanal, P. and Labouesse, M. 1997. A screen for genetic loci required for hypodermal cell and glial-like cell development during Caenorhabditis elegans embryogenesis. *Genetics* **146**(1): 207-226.
Chelur, D.S. and Chalfie, M. 2007. Targeted cell killing by reconstituted caspases. *Proc Natl Acad Sci U S A* **104**(7): 2283-2288.
Chen, H., McCarty, D.M., Bruce, A.T., and Suzuki, K. 1999. Oligodendrocyte-specific gene expression in mouse brain: use of a myelin-forming cell type-specific promoter in an adeno-associated virus. *J Neurosci Res* **55**(4): 504-513.
Chen, H., McCarty, D.M., Bruce, A.T., Suzuki, K., and Suzuki, K. 1998. Gene transfer and expression in oligodendrocytes under the control of myelin basic protein transcriptional control region mediated by adeno-associated virus. *Gene Ther* **5**(1): 50-58.

Chen, L., Chetkovich, D.M., Petralia, R.S., Sweeney, N.T., Kawasaki, Y., Wenthold, R.J., Bredt, D.S., and Nicoll, R.A. 2000. Stargazin regulates synaptic targeting of AMPA receptors by two distinct mechanisms. *Nature* **408**(6815): 936-943.

Christensen, M., Estevez, A., Yin, X., Fox, R., Morrison, R., McDonnell, M., Gleason, C., Miller, D.M., 3rd, and Strange, K. 2002. A primary culture system for functional analysis of C. elegans neurons and muscle cells. *Neuron* **33**(4): 503-514.

Christensen, M. and Strange, K. 2001. Developmental regulation of a novel outwardly rectifying mechanosensitive anion channel in Caenorhabditis elegans. *J Biol Chem* **276**(48): 45024-45030.

Chronis, N., Zimmer, M., and Bargmann, C.I. 2007. Microfluidics for in vivo imaging of neuronal and behavioral activity in Caenorhabditis elegans. *Nat Methods* **4**(9): 727-731.

Colon-Ramos, D.A., Margeta, M.A., and Shen, K. 2007. Glia promote local synaptogenesis through UNC-6 (netrin) signaling in C. elegans. *Science* **318**(5847): 103-106.

Condorelli, D.F., Conti, F., Gallo, V., Kirchhoff, F., Seifert, G., Steinhauser, C., Verkhratsky, A., and Yuan, X. 1999. Expression and functional analysis of glutamate receptors in glial cells. *Adv Exp Med Biol* **468**: 49-67.

Cornell-Bell, A.H., Finkbeiner, S.M., Cooper, M.S., and Smith, S.J. 1990. Glutamate induces calcium waves in cultured astrocytes: long-range glial signaling. *Science* **247**(4941): 470-473.

Curtis, B.M. and Catterall, W.A. 1984. Purification of the calcium antagonist receptor of the voltage-sensitive calcium channel from skeletal muscle transverse tubules. *Biochemistry* **23**(10): 2113-2118.

D'Ascenzo, M., Vairano, M., Andreassi, C., Navarra, P., Azzena, G.B., and Grassi, C. 2004. Electrophysiological and molecular evidence of L-(Cav1), N- (Cav2.2), and R- (Cav2.3) type Ca2+ channels in rat cortical astrocytes. *Glia* **45**(4): 354-363.

Davis, M.W., Fleischhauer, R., Dent, J.A., Joho, R.H., and Avery, L. 1999. A mutation in the C. elegans EXP-2 potassium channel that alters feeding behavior. *Science* **286**(5449): 2501-2504.

de Vivo, L., Melone, M., Rothstein, J.D., and Conti, F. 2010. GLT-1 Promoter Activity in Astrocytes and Neurons of Mouse Hippocampus and Somatic Sensory Cortex. *Front Neuroanat* **3**: 31.

Deitmer, J.W., Singaravelu, K., Lohr, C., Parpura, V., and Haydon, P.G. 2009. Calcium ion signaling in astrocytes

Astrocytes in (Patho)Physiology of the Nervous System. pp. 201-224. Springer US.

Dhaunchak, A.S. and Nave, K.A. 2007. A common mechanism of PLP/DM20 misfolding causes cysteine-mediated endoplasmic reticulum retention in oligodendrocytes and Pelizaeus-Merzbacher disease. *Proc Natl Acad Sci U S A* **104**(45): 17813-17818.

Di Garbo, A., Barbi, M., Chillemi, S., Alloisio, S., and Nobile, M. 2007. Calcium signalling in astrocytes and modulation of neural activity. *Biosystems* **89**(1-3): 74-83.

Ebralidze, A., Wang, Y., Petkova, V., Ebralidse, K., and Junghans, R.P. 2004. RNA leaching of transcription factors disrupts transcription in myotonic dystrophy. *Science* **303**(5656): 383-387.

Estevez, A.Y. and Strange, K. 2005. Calcium feedback mechanisms regulate oscillatory activity of a TRP-like Ca2+ conductance in C. elegans intestinal cells. *J Physiol* **567**(Pt 1): 239-251.

Felton, C.M. and Johnson, C.M. 2011. Modulation of dopamine-dependent behaviors by the Caenorhabditis elegans Olig homolog HLH-17. *J Neurosci Res* **89**(10): 1627-1636.

Feng, G., Mellor, R.H., Bernstein, M., Keller-Peck, C., Nguyen, Q.T., Wallace, M., Nerbonne, J.M., Lichtman, J.W., and Sanes, J.R. 2000. Imaging neuronal subsets in transgenic mice expressing multiple spectral variants of GFP. *Neuron* **28**(1): 41-51.

Fiacco, T.A., Agulhon, C., Taves, S.R., Petravicz, J., Casper, K.B., Dong, X., Chen, J., and McCarthy, K.D. 2007. Selective stimulation of astrocyte calcium in situ does not affect neuronal excitatory synaptic activity. *Neuron* **54**(4): 611-626.

Fields, R.D. 2008. Oligodendrocytes changing the rules: action potentials in glia and oligodendrocytes controlling action potentials. *Neuroscientist* **14**(6): 540-543.

Figueiredo, M., Lane, S., Tang, F., Liu, B.H., Hewinson, J., Marina, N., Kasymov, V., Souslova, E.A., Chudakov, D.M., Gourine, A.V., Teschemacher, A.G., and Kasparov, S. 2011. Optogenetic experimentation on astrocytes. *Exp Physiol* **96**(1): 40-50.

Fire, A., Xu, S., Montgomery, M.K., Kostas, S.A., Driver, S.E., and Mello, C.C. 1998. Potent and specific genetic interference by double-stranded RNA in Caenorhabditis elegans. *Nature* **391**(6669): 806-811.

Fitzner, D., Schneider, A., Kippert, A., Mobius, W., Willig, K.I., Hell, S.W., Bunt, G., Gaus, K., and Simons, M. 2006. Myelin basic protein-dependent plasma membrane reorganization in the formation of myelin. *Embo J* **25**(21): 5037-5048.

Fleischhauer, R., Davis, M.W., Dzhura, I., Neely, A., Avery, L., and Joho, R.H. 2000. Ultrafast inactivation causes inward rectification in a voltage-gated K(+) channel from Caenorhabditis elegans. *J Neurosci* **20**(2): 511-520.

Fossat, P., Turpin, F.R., Sacchi, S., Dulong, J., Shi, T., Rivet, J.M., Sweedler, J.V., Pollegioni, L., Millan, M.J., Oliet, S.H., and Mothet, J.P. 2011. Glial D-Serine Gates NMDA Receptors at Excitatory Synapses in Prefrontal Cortex. *Cereb Cortex*.

Freeman, M.R. and Doherty, J. 2006. Glial cell biology in Drosophila and vertebrates. *Trends Neurosci* **29**(2): 82-90.

Frokjaer-Jensen, C., Davis, M.W., Hopkins, C.E., Newman, B.J., Thummel, J.M., Olesen, S.P., Grunnet, M., and Jorgensen, E.M. 2008. Single-copy insertion of transgenes in Caenorhabditis elegans. *Nat Genet* **40**(11): 1375-1383.

Frokjaer-Jensen, C., Kindt, K.S., Kerr, R.A., Suzuki, H., Melnik-Martinez, K., Gerstbreih, B., Driscol, M., and Schafer, W.R. 2006. Effects of voltage-gated calcium channel subunit genes on calcium influx in cultured C. elegans mechanosensory neurons. *J Neurobiol* **66**(10): 1125-1139.

Fukushima, N., Kohno, M., Kato, T., Kawamoto, S., Okuda, K., Misu, Y., and Ueda, H. 1998. Melittin, a metabostatic peptide inhibiting Gs activity. *Peptides* **19**(5): 811-819.

Fulton, D., Paez, P.M., Fisher, R., Handley, V., Colwell, C.S., and Campagnoni, A.T. 2010. Regulation of L-type Ca++ currents and process morphology in white

matter oligodendrocyte precursor cells by golli-myelin proteins. *Glia* **58**(11): 1292-1303.
Garcia-Arocena, D. and Hagerman, P.J. 2010. Advances in understanding the molecular basis of FXTAS. *Hum Mol Genet* **19**(R1): R83-89.
Gardner-Medwin, A.R., Coles, J.A., and Tsacopoulos, M. 1981. Clearance of extracellular potassium: evidence for spatial buffering by glial cells in the retina of the drone. *Brain Res* **209**(2): 452-457.
Gomez-Ospina, N., Tsuruta, F., Barreto-Chang, O., Hu, L., and Dolmetsch, R. 2006. The C terminus of the L-type voltage-gated calcium channel Ca(V)1.2 encodes a transcription factor. *Cell* **127**(3): 591-606.
Gordon, G.R.J., Mulligan, S.J., MacVicar, B.A., Parpura, V., and Haydon, P.G. 2009. Astrocyte control of blood flow
Astrocytes in (Patho)Physiology of the Nervous System. pp. 461-486. Springer US.
Gourine, A.V., Kasymov, V., Marina, N., Tang, F., Figueiredo, M.F., Lane, S., Teschemacher, A.G., Spyer, K.M., Deisseroth, K., and Kasparov, S. 2010. Astrocytes control breathing through pH-dependent release of ATP. *Science* **329**(5991): 571-575.
Grove, C.A., De Masi, F., Barrasa, M.I., Newburger, D.E., Alkema, M.J., Bulyk, M.L., and Walhout, A.J. 2009. A multiparameter network reveals extensive divergence between C. elegans bHLH transcription factors. *Cell* **138**(2): 314-327.
Guo, Z.V., Hart, A.C., and Ramanathan, S. 2009. Optical interrogation of neural circuits in Caenorhabditis elegans. *Nat Methods* **6**(12): 891-896.
Gutnick, M.J., Connors, B.W., and Ransom, B.R. 1981. Dye-coupling between glial cells in the guinea pig neocortical slice. *Brain Res* **213**(2): 486-492.
Halassa, M.M., Florian, C., Fellin, T., Munoz, J.R., Lee, S.Y., Abel, T., Haydon, P.G., and Frank, M.G. 2009. Astrocytic modulation of sleep homeostasis and cognitive consequences of sleep loss. *Neuron* **61**(2): 213-219.
Hall, D.H. and Russell, R.L. 1991. The posterior nervous system of the nematode Caenorhabditis elegans: serial reconstruction of identified neurons and complete pattern of synaptic interactions. *J Neurosci* **11**(1): 1-22.
Hanisch, U.K. and Kettenmann, H. 2007. Microglia: active sensor and versatile effector cells in the normal and pathologic brain. *Nat Neurosci* **10**(11): 1387-1394.
Hartline, D.K. 2011. The evolutionary origins of glia. *Glia* **59**(9): 1215-1236.
Hedgecock, E.M., Culotti, J.G., and Hall, D.H. 1990. The unc-5, unc-6, and unc-40 genes guide circumferential migrations of pioneer axons and mesodermal cells on the epidermis in C. elegans. *Neuron* **4**(1): 61-85.
Heiman, M.G. and Shaham, S. 2007. Ancestral roles of glia suggested by the nervous system of Caenorhabditis elegans. *Neuron Glia Biol* **3**(1): 55-61.
Henneberger, C., Papouin, T., Oliet, S.H., and Rusakov, D.A. 2010. Long-term potentiation depends on release of D-serine from astrocytes. *Nature* **463**(7278): 232-236.
Hessl, D., Tassone, F., Loesch, D.Z., Berry-Kravis, E., Leehey, M.A., Gane, L.W., Barbato, I., Rice, C., Gould, E., Hall, D.A., Grigsby, J., Wegelin, J.A., Harris, S., Lewin, F., Weinberg, D., Hagerman, P.J., and Hagerman, R.J. 2005. Abnormal elevation of FMR1 mRNA is associated with psychological symptoms in

individuals with the fragile X premutation. *Am J Med Genet B Neuropsychiatr Genet* **139B**(1): 115-121.
Houseley, J.M., Wang, Z., Brock, G.J., Soloway, J., Artero, R., Perez-Alonso, M., O'Dell, K.M., and Monckton, D.G. 2005. Myotonic dystrophy associated expanded CUG repeat muscleblind positive ribonuclear foci are not toxic to Drosophila. *Hum Mol Genet* **14**(6): 873-883.
Hsieh, J., Liu, J., Kostas, S.A., Chang, C., Sternberg, P.W., and Fire, A. 1999. The RING finger/B-box factor TAM-1 and a retinoblastoma-like protein LIN-35 modulate context-dependent gene silencing in Caenorhabditis elegans. *Genes Dev* **13**(22): 2958-2970.
Hua, X., Malarkey, E.B., Sunjara, V., Rosenwald, S.E., Li, W.H., and Parpura, V. 2004. Ca2+-dependent glutamate release involves two classes of endoplasmic reticulum Ca2+ stores in astrocytes. *J Neurosci Res* **76**(1): 86-97.
Hui, K., Kwok, T.C., Kostelecki, W., Leen, J., Roy, P.J., and Feng, Z.P. 2009. Differential sensitivities of CaV1.2 IIS5-S6 mutants to 1,4-dihydropyridine analogs. *Eur J Pharmacol* **602**(2-3): 255-261.
Jay, S.D., Sharp, A.H., Kahl, S.D., Vedvick, T.S., Harpold, M.M., and Campbell, K.P. 1991. Structural characterization of the dihydropyridine-sensitive calcium channel alpha 2-subunit and the associated delta peptides. *J Biol Chem* **266**(5): 3287-3293.
Jeziorski, M.C., Greenberg, R.M., and Anderson, P.A. 2000. The molecular biology of invertebrate voltage-gated Ca(2+) channels. *J Exp Biol* **203**(Pt 5): 841-856.
Jiang, H., Mankodi, A., Swanson, M.S., Moxley, R.T., and Thornton, C.A. 2004. Myotonic dystrophy type 1 is associated with nuclear foci of mutant RNA, sequestration of muscleblind proteins and deregulated alternative splicing in neurons. *Hum Mol Genet* **13**(24): 3079-3088.
Jospin, M., Jacquemond, V., Mariol, M.C., Segalat, L., and Allard, B. 2002. The L-type voltage-dependent Ca2+ channel EGL-19 controls body wall muscle function in Caenorhabditis elegans. *J Cell Biol* **159**(2): 337-348.
Kerr, R.A. 2006. Imaging the activity of neurons and muscles. *WormBook*: 1-13.
Kettenmann, H., Backus, K.H., and Schachner, M. 1984. Aspartate, glutamate and gamma-aminobutyric acid depolarize cultured astrocytes. *Neurosci Lett* **52**(1-2): 25-29.
Kirchhoff, F. 2010. Neuroscience. Questionable calcium. *Science* **327**(5970): 1212-1213.
Kolodziej, P.A. 1997. DCC's function takes shape in the nervous system. *Curr Opin Genet Dev* **7**(1): 87-92.
Krause, M., Harrison, S.W., Xu, S.Q., Chen, L., and Fire, A. 1994. Elements regulating cell- and stage-specific expression of the C. elegans MyoD family homolog hlh-1. *Dev Biol* **166**(1): 133-148.
Kuffler, S.W. 1967. Neuroglial cells: physiological properties and a potassium mediated effect of neuronal activity on the glial membrane potential. *Proc R Soc Lond B Biol Sci* **168**(10): 1-21.
Kwok, T.C., Ricker, N., Fraser, R., Chan, A.W., Burns, A., Stanley, E.F., McCourt, P., Cutler, S.R., and Roy, P.J. 2006. A small-molecule screen in C. elegans yields a new calcium channel antagonist. *Nature* **441**(7089): 91-95.

Labouesse, M., Hartwieg, E., and Horvitz, H.R. 1996. The Caenorhabditis elegans LIN-26 protein is required to specify and/or maintain all non-neuronal ectodermal cell fates. *Development* **122**(9): 2579-2588.

Labouesse, M., Sookhareea, S., and Horvitz, H.R. 1994. The Caenorhabditis elegans gene lin-26 is required to specify the fates of hypodermal cells and encodes a presumptive zinc-finger transcription factor. *Development* **120**(9): 2359-2368.

Lee, S.H., Kim, W.T., Cornell-Bell, A.H., and Sontheimer, H. 1994. Astrocytes exhibit regional specificity in gap-junction coupling. *Glia* **11**(4): 315-325.

Lehre, K.P., Levy, L.M., Ottersen, O.P., Storm-Mathisen, J., and Danbolt, N.C. 1995. Differential expression of two glial glutamate transporters in the rat brain: quantitative and immunocytochemical observations. *J Neurosci* **15**(3 Pt 1): 1835-1853.

Lim, Y.S., Mallapur, S., Kao, G., Ren, X.C., and Wadsworth, W.G. 1999. Netrin UNC-6 and the regulation of branching and extension of motoneuron axons from the ventral nerve cord of Caenorhabditis elegans. *J Neurosci* **19**(16): 7048-7056.

Lin, X., Miller, J.W., Mankodi, A., Kanadia, R.N., Yuan, Y., Moxley, R.T., Swanson, M.S., and Thornton, C.A. 2006. Failure of MBNL1-dependent post-natal splicing transitions in myotonic dystrophy. *Hum Mol Genet* **15**(13): 2087-2097.

Liu, P., Ge, Q., Chen, B., Salkoff, L., Kotlikoff, M.I., and Wang, Z.W. 2011. Genetic dissection of ion currents underlying all-or-none action potentials in C. elegans body-wall muscle cells. *J Physiol* **589**(Pt 1): 101-117.

Liu, Y.P., Yang, C.S., Chen, M.C., Sun, S.H., and Tzeng, S.F. 2010. Ca(2+)-dependent reduction of glutamate aspartate transporter GLAST expression in astrocytes by P2X(7) receptor-mediated phosphoinositide 3-kinase signaling. *J Neurochem* **113**(1): 213-227.

Llinas, R. and Yarom, Y. 1981. Properties and distribution of ionic conductances generating electroresponsiveness of mammalian inferior olivary neurones in vitro. *J Physiol* **315**: 569-584.

Llinas, R.R., Sugimori, M., and Cherksey, B. 1989. Voltage-dependent calcium conductances in mammalian neurons. The P channel. *Ann N Y Acad Sci* **560**: 103-111.

Loria, P.M., Hodgkin, J., and Hobert, O. 2004. A conserved postsynaptic transmembrane protein affecting neuromuscular signaling in Caenorhabditis elegans. *J Neurosci* **24**(9): 2191-2201.

Lu, Q.R., Sun, T., Zhu, Z., Ma, N., Garcia, M., Stiles, C.D., and Rowitch, D.H. 2002. Common developmental requirement for Olig function indicates a motor neuron/oligodendrocyte connection. *Cell* **109**(1): 75-86.

Maduro, M. and Pilgrim, D. 1995. Identification and cloning of unc-119, a gene expressed in the Caenorhabditis elegans nervous system. *Genetics* **141**(3): 977-988.

Magistretti, P.J. and Pellerin, L. 1996. Cellular bases of brain energy metabolism and their relevance to functional brain imaging: evidence for a prominent role of astrocytes. *Cereb Cortex* **6**(1): 50-61.

Malarkey, E.B., Ni, Y., and Parpura, V. 2008. Ca2+ entry through TRPC1 channels contributes to intracellular Ca2+ dynamics and consequent glutamate release from rat astrocytes. *Glia* **56**(8): 821-835.

Mathews, E.A., Garcia, E., Santi, C.M., Mullen, G.P., Thacker, C., Moerman, D.G., and Snutch, T.P. 2003. Critical residues of the Caenorhabditis elegans unc-2 voltage-gated calcium channel that affect behavioral and physiological properties. *J Neurosci* **23**(16): 6537-6545.

McMiller, T.L. and Johnson, C.M. 2005. Molecular characterization of HLH-17, a C. elegans bHLH protein required for normal larval development. *Gene* **356**: 1-10.

McNally, K., Audhya, A., Oegema, K., and McNally, F.J. 2006. Katanin controls mitotic and meiotic spindle length. *J Cell Biol* **175**(6): 881-891.

Meister, P., Towbin, B.D., Pike, B.L., Ponti, A., and Gasser, S.M. 2010. The spatial dynamics of tissue-specific promoters during C. elegans development. *Genes Dev* **24**(8): 766-782.

Mello, C. and Fire, A. 1995. DNA transformation. *Methods Cell Biol* **48**: 451-482.

Mello, C.C., Kramer, J.M., Stinchcomb, D., and Ambros, V. 1991. Efficient gene transfer in C.elegans: extrachromosomal maintenance and integration of transforming sequences. *Embo J* **10**(12): 3959-3970.

Miller, D.L. and Roth, M.B. 2009. C. elegans are protected from lethal hypoxia by an embryonic diapause. *Curr Biol* **19**(14): 1233-1237.

Miller, J.W., Urbinati, C.R., Teng-Umnuay, P., Stenberg, M.G., Byrne, B.J., Thornton, C.A., and Swanson, M.S. 2000. Recruitment of human muscleblind proteins to (CUG)(n) expansions associated with myotonic dystrophy. *Embo J* **19**(17): 4439-4448.

Mintz, I.M., Adams, M.E., and Bean, B.P. 1992. P-type calcium channels in rat central and peripheral neurons. *Neuron* **9**(1): 85-95.

Montana, V., Malarkey, E.B., Verderio, C., Matteoli, M., and Parpura, V. 2006. Vesicular transmitter release from astrocytes. *Glia* **54**(7): 700-715.

Montana, V., Ni, Y., Sunjara, V., Hua, X., and Parpura, V. 2004. Vesicular glutamate transporter-dependent glutamate release from astrocytes. *J Neurosci* **24**(11): 2633-2642.

Mothet, J.P., Parent, A.T., Wolosker, H., Brady, R.O., Jr., Linden, D.J., Ferris, C.D., Rogawski, M.A., and Snyder, S.H. 2000. D-serine is an endogenous ligand for the glycine site of the N-methyl-D-aspartate receptor. *Proc Natl Acad Sci U S A* **97**(9): 4926-4931.

Mothet, J.P., Pollegioni, L., Ouanounou, G., Martineau, M., Fossier, P., and Baux, G. 2005. Glutamate receptor activation triggers a calcium-dependent and SNARE protein-dependent release of the gliotransmitter D-serine. *Proc Natl Acad Sci U S A* **102**(15): 5606-5611.

Muller, M., Jabs, N., Lorke, D.E., Fritzsch, B., and Sander, M. 2003. Nkx6.1 controls migration and axon pathfinding of cranial branchio-motoneurons. *Development* **130**(23): 5815-5826.

Muruve, D.A., Barnes, M.J., Stillman, I.E., and Libermann, T.A. 1999. Adenoviral gene therapy leads to rapid induction of multiple chemokines and acute neutrophil-dependent hepatic injury in vivo. *Hum Gene Ther* **10**(6): 965-976.

Nakai, J., Ohkura, M., and Imoto, K. 2001. A high signal-to-noise Ca2+ probe composed of a single green fluorescent protein. *Nat Biotechnol* **19**(2): 137-141.

Nance, M.A., Mathias-Hagen, V., Breningstall, G., Wick, M.J., and McGlennen, R.C. 1999. Analysis of a very large trinucleotide repeat in a patient with juvenile Huntington's disease. *Neurology* **52**(2): 392-394.

Nass, R., Hall, D.H., Miller, D.M., 3rd, and Blakely, R.D. 2002. Neurotoxin-induced degeneration of dopamine neurons in Caenorhabditis elegans. *Proc Natl Acad Sci U S A* **99**(5): 3264-3269.

Nass, R., Miller, D.M., and Blakely, R.D. 2001. C. elegans: a novel pharmacogenetic model to study Parkinson's disease. *Parkinsonism Relat Disord* **7**(3): 185-191.

Nickell, W.T., Pun, R.Y., Bargmann, C.I., and Kleene, S.J. 2002. Single ionic channels of two Caenorhabditis elegans chemosensory neurons in native membrane. *J Membr Biol* **189**(1): 55-66.

Nowycky, M.C., Fox, A.P., and Tsien, R.W. 1985. Three types of neuronal calcium channel with different calcium agonist sensitivity. *Nature* **316**(6027): 440-443.

Oberheim, N.A., Takano, T., Han, X., He, W., Lin, J.H., Wang, F., Xu, Q., Wyatt, J.D., Pilcher, W., Ojemann, J.G., Ransom, B.R., Goldman, S.A., and Nedergaard, M. 2009. Uniquely hominid features of adult human astrocytes. *J Neurosci* **29**(10): 3276-3287.

Oberheim, N.A., Wang, X., Goldman, S., and Nedergaard, M. 2006. Astrocytic complexity distinguishes the human brain. *Trends Neurosci* **29**(10): 547-553.

Ogata, K. and Kosaka, T. 2002. Structural and quantitative analysis of astrocytes in the mouse hippocampus. *Neuroscience* **113**(1): 221-233.

Oikonomou, G. and Shaham, S. 2011. The Glia of Caenorhabditis elegans. *Glia* **In Press**.

Oltvai, Z.N. and Barabasi, A.L. 2002. Systems biology. Life's complexity pyramid. *Science* **298**(5594): 763-764.

Orkand, R.K., Nicholls, J.G., and Kuffler, S.W. 1966. Effect of nerve impulses on the membrane potential of glial cells in the central nervous system of amphibia. *J Neurophysiol* **29**(4): 788-806.

Ortinski, P.I., Dong, J., Mungenast, A., Yue, C., Takano, H., Watson, D.J., Haydon, P.G., and Coulter, D.A. 2010. Selective induction of astrocytic gliosis generates deficits in neuronal inhibition. *Nat Neurosci* **13**(5): 584-591.

Paez, P.M., Fulton, D., Colwell, C.S., and Campagnoni, A.T. 2009. Voltage-operated Ca2+ and Na+ channels in the oligodendrocyte lineage. *J Neurosci Res* **87**(15): 3259-3266.

Palmiter, R.D. and Brinster, R.L. 1986. Germ-line transformation of mice. *Annu Rev Genet* **20**: 465-499.

Parker, R.J. and Auld, V.J. 2006. Roles of glia in the Drosophila nervous system. *Semin Cell Dev Biol* **17**(1): 66-77.

Parpura, V., Basarsky, T.A., Liu, F., Jeftinija, K., Jeftinija, S., and Haydon, P.G. 1994. Glutamate-mediated astrocyte-neuron signalling. *Nature* **369**(6483): 744-747.

Passaquin, A.C., Schreier, W.A., and de Vellis, J. 1994. Gene expression in astrocytes is affected by subculture. *Int J Dev Neurosci* **12**(4): 363-372.

Patneau, D.K., Wright, P.W., Winters, C., Mayer, M.L., and Gallo, V. 1994. Glial cells of the oligodendrocyte lineage express both kainate- and AMPA-preferring subtypes of glutamate receptor. *Neuron* **12**(2): 357-371.

Pellerin, L. and Magistretti, P.J. 1994. Glutamate uptake into astrocytes stimulates aerobic glycolysis: a mechanism coupling neuronal activity to glucose utilization. *Proc Natl Acad Sci U S A* **91**(22): 10625-10629.

Petravicz, J., Fiacco, T.A., and McCarthy, K.D. 2008. Loss of IP3 receptor-dependent Ca2+ increases in hippocampal astrocytes does not affect baseline CA1 pyramidal neuron synaptic activity. *J Neurosci* **28**(19): 4967-4973.

Ponzio, T.A., Ni, Y., Montana, V., Parpura, V., and Hatton, G.I. 2006. Vesicular glutamate transporter expression in supraoptic neurones suggests a glutamatergic phenotype. *J Neuroendocrinol* **18**(4): 253-265.

Raj, A., Rifkin, S.A., Andersen, E., and van Oudenaarden, A. 2010. Variability in gene expression underlies incomplete penetrance. *Nature* **463**(7283): 913-918.

Randall, A. and Tsien, R.W. 1995. Pharmacological dissection of multiple types of Ca2+ channel currents in rat cerebellar granule neurons. *J Neurosci* **15**(4): 2995-3012.

Reece-Hoyes, J.S., Deplancke, B., Shingles, J., Grove, C.A., Hope, I.A., and Walhout, A.J. 2005. A compendium of Caenorhabditis elegans regulatory transcription factors: a resource for mapping transcription regulatory networks. *Genome Biol* **6**(13): R110.

Regan, M.R., Huang, Y.H., Kim, Y.S., Dykes-Hoberg, M.I., Jin, L., Watkins, A.M., Bergles, D.E., and Rothstein, J.D. 2007. Variations in promoter activity reveal a differential expression and physiology of glutamate transporters by glia in the developing and mature CNS. *J Neurosci* **27**(25): 6607-6619.

Reuter, H. 1976. Properties of Two Inward Membrane Currents in the Heart. *Annual Reviews in Physiology* **41**: 413-424.

Reyes, R.C. and Parpura, V. 2008. Mitochondria modulate Ca2+-dependent glutamate release from rat cortical astrocytes. *J Neurosci* **28**(39): 9682-9691.

-. 2009. The trinity of Ca2+ sources for the exocytotic glutamate release from astrocytes. *Neurochem Int* **55**(1-3): 2-8.

Rouach, N., Koulakoff, A., Abudara, V., Willecke, K., and Giaume, C. 2008. Astroglial metabolic networks sustain hippocampal synaptic transmission. *Science* **322**(5907): 1551-1555.

Ruan, Q., Harrington, A.J., Caldwell, K.A., Caldwell, G.A., and Standaert, D.G. 2010. VPS41, a protein involved in lysosomal trafficking, is protective in Caenorhabditis elegans and mammalian cellular models of Parkinson's disease. *Neurobiol Dis* **37**(2): 330-338.

Saheki, Y. and Bargmann, C.I. 2009. Presynaptic CaV2 calcium channel traffic requires CALF-1 and the alpha2delta subunit UNC-36. *Nat Neurosci* **12**(10): 1257-1265.

Santello, M. and Volterra, A. 2009. Synaptic modulation by astrocytes via Ca2+-dependent glutamate release. *Neuroscience* **158**(1): 253-259.

Sasaki, T. and Endo, T. 2000. Both cell-surface carbohydrates and protein tyrosine phosphatase are involved in the differentiation of astrocytes in vitro. *Glia* **32**(1): 60-70.

Scemes, E., Spray, D.C., Parpura, V., and Haydon, P.G. 2009. Connexin Expression (Gap Junctions and Hemichannels) in Astrocytes

Astrocytes in (Patho)Physiology of the Nervous System. pp. 107-150. Springer US.

Schafer, W.R. and Kenyon, C.J. 1995. A calcium-channel homologue required for adaptation to dopamine and serotonin in Caenorhabditis elegans. *Nature* **375**(6526): 73-78.

Seifert, G. and Steinhäuser, C. 2004. Ion channels in astrocytes. in *Glial ⇔Neuronal Signaling* (ed. G.I. Hatton and V. Parpura), pp. 187-213. Kluwer Academic Publishers, Boston, MA.

Sekar, R.B., Kizana, E., Smith, R.R., Barth, A.S., Zhang, Y., Marban, E., and Tung, L. 2007. Lentiviral vector-mediated expression of GFP or Kir2.1 alters the electrophysiology of neonatal rat ventricular myocytes without inducing cytotoxicity. *Am J Physiol Heart Circ Physiol* **293**(5): H2757-2770.

Shaham, S. 2006. Glia-neuron interactions in the nervous system of Caenorhabditis elegans. *Curr Opin Neurobiol* **16**(5): 522-528.

Shao, Z., Zhang, Y., and Powell-Coffman, J.A. 2009. Two distinct roles for EGL-9 in the regulation of HIF-1-mediated gene expression in Caenorhabditis elegans. *Genetics* **183**(3): 821-829.

Shigetomi, E., Kracun, S., and Khakh, B.S. 2010. Monitoring astrocyte calcium microdomains with improved membrane targeted GCaMP reporters. *Neuron Glia Biol*: 1-9.

Shtonda, B. and Avery, L. 2005. CCA-1, EGL-19 and EXP-2 currents shape action potentials in the Caenorhabditis elegans pharynx. *J Exp Biol* **208**(Pt 11): 2177-2190.

Slezak, M. and Pfrieger, F.W. 2004. Role of astrocytes in the formation, maturation andmaintenance of synapses. in *Glial ⇔Neuronal Signaling* (ed. G.I. Hatton and V. Parpura). Kluwer Academic Publishers, Boston, MA.

Spencer, W.C., Zeller, G., Watson, J.D., Henz, S.R., Watkins, K.L., McWhirter, R.D., Petersen, S., Sreedharan, V.T., Widmer, C., Jo, J., Reinke, V., Petrella, L., Strome, S., Von Stetina, S.E., Katz, M., Shaham, S., Ratsch, G., and Miller, D.M., 3rd. 2011. A spatial and temporal map of C. elegans gene expression. *Genome Res* **21**(2): 325-341.

Steger, K.A., Shtonda, B.B., Thacker, C., Snutch, T.P., and Avery, L. 2005. The C. elegans T-type calcium channel CCA-1 boosts neuromuscular transmission. *J Exp Biol* **208**(Pt 11): 2191-2203.

Steinhauser, C. and Gallo, V. 1996. News on glutamate receptors in glial cells. *Trends Neurosci* **19**(8): 339-345.

Stirman, J.N., Brauner, M., Gottschalk, A., and Lu, H. 2010. High-throughput study of synaptic transmission at the neuromuscular junction enabled by optogenetics and microfluidics. *J Neurosci Methods* **191**(1): 90-93.

Stout, R.F., Jr. and Parpura, V. 2011a. Voltage-gated calcium channel types in cultured C. elegans CEPsh glial cells. *Cell Calcium* **50**(1): 98-108.

Stout, R.F. and Parpura, V. 2011b. Cell culturing of C. elegans glial cells for the assessment of cytosolic Ca2+ dynamics. *Methods Mol Biol* **In Press**.

Strange, K., Christensen, M., and Morrison, R. 2007. Primary culture of Caenorhabditis elegans developing embryo cells for electrophysiological, cell biological and molecular studies. *Nat Protoc* **2**(4): 1003-1012.

Sulston, J.E. and Horvitz, H.R. 1977. Post-embryonic cell lineages of the nematode, Caenorhabditis elegans. *Dev Biol* **56**(1): 110-156.

Takahashi, M., Seagar, M.J., Jones, J.F., Reber, B.F., and Catterall, W.A. 1987. Subunit structure of dihydropyridine-sensitive calcium channels from skeletal muscle. *Proc Natl Acad Sci U S A* **84**(15): 5478-5482.

Tallini, Y.N., Ohkura, M., Choi, B.R., Ji, G., Imoto, K., Doran, R., Lee, J., Plan, P., Wilson, J., Xin, H.B., Sanbe, A., Gulick, J., Mathai, J., Robbins, J., Salama, G., Nakai, J., and Kotlikoff, M.I. 2006. Imaging cellular signals in the heart in vivo: Cardiac expression of the high-signal Ca2+ indicator GCaMP2. *Proc Natl Acad Sci U S A* **103**(12): 4753-4758.

Tam, T., Mathews, E., Snutch, T.P., and Schafer, W.R. 2000. Voltage-gated calcium channels direct neuronal migration in Caenorhabditis elegans. *Dev Biol* **226**(1): 104-117.

Tassone, F., Adams, J., Berry-Kravis, E.M., Cohen, S.S., Brusco, A., Leehey, M.A., Li, L., Hagerman, R.J., and Hagerman, P.J. 2007. CGG repeat length correlates with age of onset of motor signs of the fragile X-associated tremor/ataxia syndrome (FXTAS). *Am J Med Genet B Neuropsychiatr Genet* **144B**(4): 566-569.

Thomas, A. and Delaville, F. 1991. The use of fluorescent indiciators for measurements of cytosolic-free calcium concentration in cell populations and single cells. in *Cellular Calcium* (ed. J. McCormack and P. Cobbold). Oxford University Press, Oxford, UK.

Thomas, J.H. 1994. The mind of a worm. *Science* **264**(5166): 1698-1699.

Tian, L., Hires, S.A., Mao, T., Huber, D., Chiappe, M.E., Chalasani, S.H., Petreanu, L., Akerboom, J., McKinney, S.A., Schreiter, E.R., Bargmann, C.I., Jayaraman, V., Svoboda, K., and Looger, L.L. 2009. Imaging neural activity in worms, flies and mice with improved GCaMP calcium indicators. *Nat Methods* **6**(12): 875-881.

Towbin, B.D., Meister, P., Pike, B.L., and Gasser, S.M. 2011. Repetitive Transgenes in C. elegans Accumulate Heterochromatic Marks and Are Sequestered at the Nuclear Envelope in a Copy-Number- and Lamin-Dependent Manner. *Cold Spring Harb Symp Quant Biol* **75**: 555-565.

Tsien, R.W. 1983. Calcium channels in excitable cell membranes. *Annu Rev Physiol* **45**: 341-358.

Tsien, R.W., Lipscombe, D., Madison, D.V., Bley, K.R., and Fox, A.P. 1988. Multiple types of neuronal calcium channels and their selective modulation. *Trends Neurosci* **11**(10): 431-438.

Verkerk, A.J., Pieretti, M., Sutcliffe, J.S., Fu, Y.H., Kuhl, D.P., Pizzuti, A., Reiner, O., Richards, S., Victoria, M.F., Zhang, F.P., and et al. 1991. Identification of a gene (FMR-1) containing a CGG repeat coincident with a breakpoint cluster region exhibiting length variation in fragile X syndrome. *Cell* **65**(5): 905-914.

Verkhratsky, A., Lalo, U., Pankratov, Y., and Parpura, V. 2011. Ionotropic receptors in neuronal-astroglial signalling: What is the role of "excitable" molecules in non-excitable cells. *Biochimica Et Biophysica Acta-Molecular Cell Research* **1813**(5): 992-1002.

Verkhratsky, A., Parpura, V., and Haydon, P.G. 2009. Neurotransmitter Receptors in Astrocytes

Astrocytes in (Patho)Physiology of the Nervous System. pp. 49-67. Springer US.

Verkhratsky, A. and Steinhauser, C. 2000. Ion channels in glial cells. *Brain Res Brain Res Rev* **32**(2-3): 380-412.

Vermeirssen, V., Barrasa, M.I., Hidalgo, C.A., Babon, J.A., Sequerra, R., Doucette-Stamm, L., Barabasi, A.L., and Walhout, A.J. 2007. Transcription factor modularity in a gene-centered C. elegans core neuronal protein-DNA interaction network. *Genome Res* **17**(7): 1061-1071.

Vives, V., Alonso, G., Solal, A.C., Joubert, D., and Legraverend, C. 2003. Visualization of S100B-positive neurons and glia in the central nervous system of EGFP transgenic mice. *J Comp Neurol* **457**(4): 404-419.

Wadsworth, W.G., Bhatt, H., and Hedgecock, E.M. 1996. Neuroglia and pioneer neurons express UNC-6 to provide global and local netrin cues for guiding migrations in C. elegans. *Neuron* **16**(1): 35-46.

Wang, L.C., Chen, K.Y., Pan, H., Wu, C.C., Chen, P.H., Liao, Y.T., Li, C., Huang, M.L., and Hsiao, K.M. 2011. Muscleblind participates in RNA toxicity of expanded CAG and CUG repeats in Caenorhabditis elegans. *Cell Mol Life Sci* **68**(7): 1255-1267.

Ward, S., Thomson, N., White, J.G., and Brenner, S. 1975. Electron microscopical reconstruction of the anterior sensory anatomy of the nematode Caenorhabditis elegans.?2UU. *J Comp Neurol* **160**(3): 313-337.

White, J.G., Southgate, E., Thomson, J.N., and Brenner, S. 1976. The structure of the ventral nerve cord of Caenorhabditis elegans. *Philos Trans R Soc Lond B Biol Sci* **275**(938): 327-348.

-. 1986. The structure of the nervous system of the nematode Caenorhabditis elegans. *Philos Trans R Soc Lond B Biol Sci* **314**(1165): 1-340.

Yaguchi, T. and Nishizaki, T. 2010. Extracellular high K+ stimulates vesicular glutamate release from astrocytes by activating voltage-dependent calcium channels. *J Cell Physiol* **225**(2): 512-518.

Yamamoto, T., Ochalski, A., Hertzberg, E.L., and Nagy, J.I. 1990a. LM and EM immunolocalization of the gap junctional protein connexin 43 in rat brain. *Brain Res* **508**(2): 313-319.

-. 1990b. On the organization of astrocytic gap junctions in rat brain as suggested by LM and EM immunohistochemistry of connexin43 expression. *J Comp Neurol* **302**(4): 853-883.

Yamazaki, Y. and Kato, H. 2007. [Modulatory effects of peri-interneuronal glial cells on neuronal activities]. *Brain Nerve* **59**(7): 689-695.

Yang, Y., Vidensky, S., Jin, L., Jie, C., Lorenzini, I., Frankl, M., and Rothstein, J.D. 2011. Molecular comparison of GLT1+ and ALDH1L1+ astrocytes in vivo in astroglial reporter mice. *Glia* **59**(2): 200-207.

Yoo, A.S., Krieger, C., and Kim, S.U. 1999. Process extension and intracellular Ca2+ in cultured murine oligodendrocytes. *Brain Res* **827**(1-2): 19-27.

Yoshida, M. and Macklin, W.B. 2005. Oligodendrocyte development and myelination in GFP-transgenic zebrafish. *J Neurosci Res* **81**(1): 1-8.

Yoshimura, S., Murray, J.I., Lu, Y., Waterston, R.H., and Shaham, S. 2008. mls-2 and vab-3 Control glia development, hlh-17/Olig expression and glia-dependent neurite extension in C. elegans. *Development* **135**(13): 2263-2275.

Zhuchenko, O., Bailey, J., Bonnen, P., Ashizawa, T., Stockton, D.W., Amos, C., Dobyns, W.B., Subramony, S.H., Zoghbi, H.Y., and Lee, C.C. 1997. Autosomal dominant

cerebellar ataxia (SCA6) associated with small polyglutamine expansions in the alpha 1A-voltage-dependent calcium channel. *Nat Genet* **15**(1): 62-69.

Ziel, J.W., Hagedorn, E.J., Audhya, A., and Sherwood, D.R. 2009. UNC-6 (netrin) orients the invasive membrane of the anchor cell in C. elegans. *Nat Cell Biol* **11**(2): 183-189.